

https://dspace.org/

Development of GIS based composite drought monitoring model for spatio-temporal drought vulnerability assessment at Intsika Yethu, South Africa

Majeke, Bongani

2023

University of the Witwatersrand, Johannesburg

https://hdl.handle.net/10539/50322

Majeke, Bongani. (2023). Development of GIS based composite drought monitoring model for spatio-temporal drought vulnerability assessment at Intsika Yethu, South Africa. [Master's dissertation, University of the Witwatersrand, Johannesburg]. WIReDSpace. https://hdl.handle.net/10539/50322

Downloaded from a DSpace repository. https://dspace.org/



DEVELOPMENT OF GIS BASED COMPOSITE DROUGHT MONITORING MODEL FOR SPATIO-TEMPORAL DROUGHT VULNERABILITY ASSESSMENT AT INTSIKA YETHU, SOUTH AFRICA

Master's Research Report

By
Bongani Majeke
740615

Supervisor: Dr Iqra Atif
Co-supervisor: Prof Elhadi Adam

Submitted in partial fulfilment of the requirements for the degree of Master of Science in Geographic Information Systems and Remote Sensing in the School of Geography, Archaeology and Environmental Studies, Faculty of Science, University of the Witwatersrand

2023

ABSTRACT

The aim of the study was to develop the Composite Drought Monitoring Model (CDMM) for Spatio-temporal drought vulnerability assessment at Intsika Yethu municipality, South Africa.The study utilized multi spectral indices using multi source satellite remote sensing data from January to May of the years 2017 to 2021.

Sentinel-2 data was processed for Normalized Difference Vegetation Index (NDVI) and Normalized Difference Water Index (NDWI) in order to map spatio-temporal variability of agricultural drought.

Hydrometeorological data was gathered from meteorological stations, complemented by satellite based precipitation and soil moisture measurements. This comprehensive dataset was then employed to compute indices, including the Standardized Precipitation Index (SPI), Precipitation Condition Index (PCI), and Soil Moisture Condition Index (SMCI). Ultimately, CDMM was developed by Multi Criteria Decision Analysis (MCDA) approach which combined different datasets including Landover data. The NDVI and NDWI, found to be effective to map the spatio-temporal agricultural drought variations. Both indices accurately identified January of 2019 as the driest month during the study period followed by January 2020 while January and February 2021 were by far the wettest months followed by March 2018 and April 2020. Additionally, satellite based precipitation mapping confirmed that 2019 stood out as the driest year among the observed years.

The CDMM effectively identified areas vulnerable to agricultural drought, with 2019 emerging as the driest year in Intsika Yethu hence negatively affecting over 58% of the households who are dependent on agricultural activities. This study underscore the effectiveness of geospatial techniques in mapping drought variations both spatially and temporally while identifying and predicting drought-prone areas. The model accuracy can be improved by utilizing the high resolution satellite data. Future research should focus on increasing data accessibility and undertaking comprehensive validation to improve the usefulness and accuracy of the Composite Drought Monitoring Model (CDMM) for a wider range of applications.

Keywords: Composite Drought Monitoring Model; Multi-Criteria Decision Analysis; Sentinel-2; Spatio-temporal

DECLARATION

I declare that this report titled "Development of GIS based composite drought monitoring model for spatio-temporal drought vulnerability assessment at Intsika Yethu, South Africa" has been carried out at University of the Witwatersrand by me. The work properly acknowledges the material drawn from the literature and includes references. This report was not submitted before for another degree or certificate at this university or any other.

Name : Bongani Majeke

Signature : 

Place : Pretoria, South Africa

Date : 04 December 2023

DEDICATION

I dedicate the study to my partner Zee for all the support, love and patience. To my lovely kids, Lathi, Usi, Gosi and Liya, thank you for understanding why daddy spent less time with you.

ACKNOWLEDGEMENT

I would like to express my sincere gratitude to Dr. Atif for her guidance, commitment, patience and continued support in my Wits journey. There were times when I felt like giving up but through her guidance and patience I continued. I am indebted to her.

Special acknowledgement to Mr Joe Matsapola from South African Weather Services for the prompt assistance he provided me whenever I needed data. Also, I would like to acknowledge United States Geological Survey (USGS) Earth Explorer for the free images it provided for this research.

My parents, siblings, nephews and nieces for inspiring me.

My colleagues especially Tar X, Ndiyabulela Grootman for all your assistance.

CONTENTS

ABSTRACT ..... **i**

DECLARATION ..... **ii**

DEDICATION ..... **iii**

ACKNOWLEDGEMENT ..... **iv**

LIST OF TABLES ..... **viii**

LIST OF FIGURES ..... **ix**

LIST OF ACRONYMS ..... **xii**

1. INTRODUCTION **1**

1.1. BACKGROUND **1**

1.2. RESEARCH PROBLEM STATEMENT **2**

1.3. AIM AND OBJECTIVES **3**

1.3.1. AIM **3**

1.3.2. OBJECTIVES **3**

2. LITERATURE REVIEW **4**

2.1. AGRICULTURAL AND METERIOLOGICAL DROUGHT **4**

2.2. IMPACTS OF DROUGHT IN SOUTHERN AFRICA **5**

2.3. MAPPING AND MONITORING OF DROUGHT **5**

2.3.1. TRADITIONAL METHODS **5**

2.3.2. GIS AND REMOTE SENSING METHODS **5**

2.4. CLIMATE CHANGE AND DROUGHT **11**

2.5. LIMITATIONS OF REMOTE SENSING **12**

2.6. OPPORTUNITIES FOR IMPROVEMENT **12**

2.7. SUMMARY **12**

3. MATERIALS AND METHODS **14**

3.1. STUDY AREA **14**

3.2. RESEARCH DESIGN **16**

3.3. DATA REQUIREMENTS **17**

3.3.1. SENTINEL-2 DATA **18**

3.3.2. FIELD BASED METEOROLOGICAL STATIONS DATA **19**

3.3.3. SATELLITE BASED GLOBAL PRECIPITATION MEASURING MISSION DATA....20
3.3.4. ADVANCED MICROWAVE SCANNING RADIOMETER SOIL MOISTURE DATA....20
3.4. METHODOLOGY....21
3.4.1. LANDCOVER DATA OF STUDY AREA....21
3.4.2. PRE-PROCESSING OF SENTINEL 2 IMAGERY USED....21
3.4.3. PROCESSING OF THE VEGETATION INDICES....21
3.4.4. PROCESSING OF METEOROLOGICAL STATIONS DATA....23
3.4.5. STANDARDISED PRECIPITATION INDEX (SPI)....24
3.4.6. PROCESSING OF GLOBAL PRECIPITATION MISSION (GPM) SATELLITE DATA....25
3.4.7. PROCESSING OF ADVANCED MICROWAVE SCANNING RADIOMETER (AMSR-2) SOIL MOISTURE....25
3.4.8. MANN-KENDALL TREND ANALYSIS....26
3.4.9. DEVELOPING A COMPOSITE DROUGHT MONITORING MODEL (CDMM) FOR DROUGHT VULNERABILITY MAPPING....27
4. RESULTS AND DISCUSSION....29
4.1. GENERAL STATISTICS OF THE STUDY AREA....29
4.2. ANALYSIS OF AGRICULTURAL DROUGHT USING VEGETATION INDICES AT INTSIKA YETHU....30
4.2.1. ANALYSIS OF NDVI....30
4.2.2. ANALYSIS OF SPATIO-TEMPORAL VARIATION OF NDVI AT INTSIKA YETHU....32
4.2.3. SPATIAL PATTERN OF NORMALIZE DIFFERENCE WATER INDEX 39
4.3. DATA FROM METEOROLOGICAL STATIONS....46
4.3.1. STANDARDIZED PRECIPITATION INDEX DERIVED FROM FOUR WEATHER STATIONS....46
4.3.2. MANN-KENDALL TREND OF METERIOLOGICAL VARIABLES....48
4.4. GPM SATELLITE PRECIPITATION DATA....50
4.4.1. SPATIO-TEMPORAL VARIABILITY OF GPM SATELLITE PRECIPITATION DATA....50
4.4.2. PRECIPITATION CONDITION INDEX (PCI)....52
4.5. AVERAGE SEASONAL AMSR-2 SOIL MOISTURE PATTERN....53

4.5.1. SPATIO_TEMPORAL VARIABILITY OF AMSR-2 SOIL MOISTURE53
4.5.2. SOIL MOISTURE CONDITION INDEX (SMCI).....55
4.6. MANN-KENDALL TREND TEST FOR ALL THE DROUGHT VARIABLES 56
4.7. DEVELOPING A COMPOSITE DROUGHT MONITORING MODEL (CDMM) FOR DROUGHT VULNERABILITY MAPPING.....58
5. CONCLUSION.....68
REFERENCES.....70
6. APPENDICES.....81

LIST OF TABLES

Table 2.1: Various drought indices used to monitor and assess agricultural drought 6
Table 3.1: Summary of data required for the research.....17
Table 3.2: Different spectral bands of Sentinel-2 (Source: Wessel et al., (2018)) 19
Table 3.3: Pixel classification range of NDVI (Source: Altunet al., (2020)) 22
Table 3.4: NDWI values and their ranges (Source: EOS, 2023) 23
Table 3.5: SPI values and their categories (Source: McKee et al., (1993)).....24
Table 4.1: Showing the Mann-Kendall trends of the processed variables on monthly and seasonally.....56

LIST OF FIGURES

Figure 3.1: Study area map of Intsika Yethu, Eastern Cape. 15
Figure 3.2 : Research methodological flow chart. 16
Figure 4.1: Landcover map of Intsika Yethu municipality adopted from SANLC 2018 29
Figure 4.2: The area percent of the Landcover classes at Intsika Yethu municipality 30
Figure 4.3: Mean NDVI time series for 2017 to 2021 (January to May) 31
Figure 4.4: The NDVI Map of Intsika Yethu for January to May for the period of 2017 to 2021..... 38
Figure 4.5: Mean annual NDVI values per growing season for 2017 to 2021 39
Figure 4.6: Difference in area coverage of NDWI during Months of January to May, 2017 to 2021..... 45
Figure 4.7: a) Interpolated Rainfall data from the Stutterheim weather station for months of January to May, 2017 to 2021. b) Interpolated Rainfall data from the Queenstown weather station for months of January to May, 2017 to 2021. c) Interpolated Rainfall data from the Mthatha weather station for months of January to May, 2017 to 2021. d) Interpolated Rainfall data from the Elliot weather station for months of January to May, 2017 to 2021. 48
Figure 4.8: a) Shows the Mann-Kendall trend of SPI from different weather stations. b) Shows the Mann-Kendall trend of maximum temperature from different weather stations. c) Shows the Mann-Kendall trend of minimum temperature from different weather stations. ... 50
Figure 4.9: Time series of the daily accumulated precipitation estimate for January to May of 2017 to 2021 51
Figure 4.10: Maps illustrating the average daily accumulated precipitation from January to May for the different years a) 2017, b) 2018, c) 2019, d) 2020, e) 2021. 52
Figure 4.11: Annual Average PCI for Intsika Yethu for 2017-2021 53
Figure 4.12: Time series, area averaged of volumetric soil moisture over 2017 to 2021, January to May..... 54
Figure 4.13: a) Time series, area averaged of volumetric soil moisture spatial distribution for January to May of 2017. b) Time series, area averaged of volumetric soil moisture spatial distribution for January to May of 2018. c) Time series, area averaged of volumetric soil moisture spatial distribution for January to May of 2019. d) Time series, area averaged of volumetric soil moisture spatial distribution for January to May of 2020. e) Time series, area averaged of volumetric soil moisture spatial distribution for January to May of 2021. 55
Figure 4.14: Average annual SMCI of Intsika Yethu 56

Figure 4.15: Spatial distribution of drought risk area of Intsika Yethu for January to May of 2017.....61
Figure 4.16: Spatial distribution of drought risk area of Intsika Yethu for January to May of 2018.....62
Figure 4.17: Spatial distribution of drought risk area of Intsika Yethu for January to May of 2019.....63
Figure 4.18: Spatial distribution of drought risk area of Intsika Yethu for January to May of 2020.....64
Figure 4.19: Spatial distribution of drought risk area of Intsika Yethu for January to May of 2021.....65
Figure 4.20: Drought severity of Intsika Yethu for 2017 to 2021 (January to May).....67
Figure 6.1: Average maximum temperature trend from Umthatha, Queenstown, Elliot and DOHNE – Agr weather stations 81
Figure 6.2: Average minimum temperature trend from Umthatha, Queenstown, Elliot and DOHNE – Agr weather stations 81
Figure 6.3: Time series, interpolated rainfall data from Umthatha, Queenstown, Elliot and Stutterheim weather stations (January to May of 2017). 82
Figure 6.4: Time series, interpolated rainfall data from Umthatha, Queenstown, Elliot and Stutterheim weather stations (January to May of 2018). 82
Figure 6.5: Time series, interpolated rainfall data from Umthatha, Queenstown, Elliot and Stutterheim weather stations (January to May of 2019). 83
Figure 6.6: Time series, interpolated rainfall data from Umthatha, Queenstown, Elliot and Stutterheim weather stations (January to May of 2020). 84
Figure 6.7: Time series, interpolated rainfall data from Umthatha, Queenstown, Elliot and Stutterheim weather stations (January to May of 2021). 85
Figure 6.8: Time series, interpolated Average Temperature data from Umthatha, Queenstown, Elliot and Dohne_Agr weather stations (January to May of 2017) 85
Figure 6.9: Time series, interpolated Average Temperature data from Umthatha, Queenstown, Elliot and Dohne_Agr weather stations (January to May of 2018) 86
Figure 6.10: Time series, interpolated Average Temperature data from Umthatha, Queenstown, Elliot and Dohne_Agr weather stations (January to May of 2019) 86
Figure 6.11: Time series, interpolated Average Temperature data from Umthatha, Queenstown, Elliot and Dohne_Agr weather stations (January to May of 2020). 87

Figure 6.12: Time series, interpolated Average Temperature data from Umthatha, Queenstown, Elliot and Dohne_Agr weather stations (January to May of 2021). 87

LIST OF ACRONYMS

AHP	Analytical Hierarchy Process
AI	Artificial intelligence
AMSR-E	Advanced Microwave Scanning Radiometer
ANN	Artificial Neural Network
AVHRR	Advanced Very High Resolution Radiometer
AWC	Available Water holding Capacity
BOA	Bottom-Of-Atmosphere
CDMM	Composite Drought Monitoring Model
CMI	Crop Moisture Index
CMIP5	Coupled Model Intercomparison Project
DFFE	Department of Forestry, Fisheries and the Environment
DISC	Data Information Services Center
ENSO	El Niño-Southern Oscillation
ESA	European Space Agency
ESI	Evaporative Stress Index
EVI	Enhanced Vegetation Index
GLDAS	Global Land Data Assimilation System
GIS	Geographic Information Systems
GPM	Global Precipitation Measuring Mission
IDMI	Integrated Drought Monitoring Index
ISDI	Integrated Surface Drought Index
LST	Land surface temperature
MCDA	Multi Criteria Decision Analysis
MERRA	Modern-Era Retrospective Analysis for Research and Applications
MDB	Municipal Demarcation Board
MODIS	Moderate Resolution Imaging Spectroradiometer
MSI	Multispectral Instrument
NASA	National Aeronautics and Space Administration
NDDI	Normalized Difference Drought Index
NDVI	Normalized Difference Vegetation Index
NDWI	Normalized Difference Water Index
NIR	Near Infra-Red

NMDI	Normalized Multi band Drought Index
NOAA	National Oceanic and Atmospheric Administration
OLI	Operational Land Imager
PCI	Precipitation Condition Index
PDSI	Palmer Drought Severity Index
RF	Random Forest
SANLC2018	South African National Land Cover 2018
SAS	Statistical Analysis System (SAS)
SATVI	Soil Adjusted Total Vegetation Index
SVM	Support Vector Machine
SAWS	South African Weather Services
SDI	Synthesized Drought Index
SMCI	Soil Moisture Condition Index
SPI	Standardized Precipitation Index
SPEI	Standardized Precipitation Evapotranspiration Index
SWIR	Short-wave infrared
SWSI	Surface Water Supply Index
TCI	Temperature Condition Index
TIRS	Thermal Infrared Sensor
TRMM	Tropical Rainfall Measuring Mission
USGS	United States Geological Survey
VCI	Vegetation Condition Index
VHI	Vegetation Health Index
VTCI	Vegetation Temperature Condition Index
WOA	Weighted Overlay Analysis
WDVI	Weighted Difference Vegetation Index

1. INTRODUCTION

1.1. BACKGROUND

Droughts are a recurring climatic event in South Africa that can adversely affect wide range of biophysical and socio-economic aspects (Rouault & Richard, 2003). The significant drought consequences are an extreme shortage of food and resultant social disintegration (Belal et al., 2014). Amongst all natural hazards, droughts is the worst because of its spread over a long period which results in serious ecological damages and socioeconomic losses across the globe (Meteorological and States, 2010, Hao et al., 2014). Food security is threatened by drought, as it has strong effect on production, access and distribution of food (Maponya and Mpandeli, 2012, Atif and Mahboob, 2016). Global production of food such as maize and wheat has been predicted to decline due to the increasing temperatures and decreasing precipitation (Daryanto et al., 2016). Droughts are caused by variations in climate that affects large geographic extents (Atif & Mahboob, 2016). Future climate projections show that Africa is enduring climate change-related harsh weather and rising temperatures (Masikati et al., 2019). Droughts causes water scarcity as it affects both ground water recourses and surface water leading to crop failure, deteriorated water quality, reduced water supply and disturbed riparian habitats (Belal et al., 2014).

Droughts affect agriculture more, because it is reliant on water resource conservation and soil moisture throughout the different crop growth stages (Orimoloye et al., 2019). Soil quality can be reduced due to less organic activity, extinction of some soil organisms and erosion (Orimoloye et al., 2019).This leads to vulnerability of mostly, farmers who survive on subsistence because they rely heavily on rain fed agricultural systems (Masikati et al., 2019). Climate change and its variability significantly affect developing countries that are heavily dependent on agriculture (Bryan et al., 2009). Major drought in the mid-eighties lead to extreme scarcity of food and in East Africa killed approximately a million people (Hao et al., 2014). Also, East Africa and South Eastern Asia experienced drought in in 2010-2011 that affected 9 million people and resulted in significant ecological impacts and extreme food scarcity (Hao et al., 2014).

South Africa including the Eastern Cape experienced severe drought in the years 1992-1995 and 2015-16 that lead to the economic decline, water resource scarcity and reduced agricultural

productivity that affected 3.7 million people (Baudoin et al., 2017; Bhaga et al., 2020) (Baudoin et al., 2017).

A lack of moisture in plant roots is a factor in agricultural drought, which results in crop growth stress, reduction in crop yields or crop failure because of long periods of low precipitation (Wu et al., 2020a). It causes both direct and indirect losses such as diminished pasture growth, reduced crop yields and livestock mortality that can be attributed to the former, while the latter will result to losses due land use changes and abandonment of land and lost opportunities in both livestock and agricultural sector (Meteorological & States, 2010).

1.2. RESEARCH PROBLEM STATEMENT

Droughts and floods are the most geographically extensive hazards that account for 7.5% and 11% respectively of earth's land surface area (Belal et al., 2014). Droughts are caused by climate change and can have catastrophic consequences as they develop slowly and increase in intensity and duration (Mukherjee et al., 2018). Future climate projections suggest that some South African regions, including the Eastern Cape will encounter warmer and arid conditions, with extreme events, which will lead to regular and intense droughts (Hewitson & Crane, 2006). Over the past five decades, South Africa's average annual temperature has risen by 0.97°C compared to the global mean of 0.65°C (Ziervogel et al., 2014). This temperature rise is projected to reach 3-6°C by 2081 to 2100 with less certain precipitation changes (Ziervogel et al., 2014).

The Eastern Cape has recently come under the influence of drought, leading to a decline in the local economy through reduced agricultural productivity and scarcity of water resources (Mahlalela et al., 2020). Recognizing areas that are vulnerable to drought and predicting the severity of a drought and the likelihood of a drought occurring is critical for the execution of programs aimed at improving food security (Rojas et al., 2011). Drought monitoring and mitigation have emerged as critical scientific concerns, particularly agricultural drought monitoring, which is essential for decreasing catastrophic loss and damage, however, those are underdeveloped (Liu et al., 2016). According to West, Quinn and Horswell, (2019) remote sensing based approaches have made drought monitoring easy through water levels and vegetation health mapping. However, little or no research has been found that utilized remote sensing approaches for monitoring conditions of agricultural drought in the Eastern Cape and Intsika Yethu, South Africa. Furthermore, little research has been done on the Eastern Cape's

climate in comparison to other areas of South Africa, despite it having a big rural population, being a significant agricultural region and the least developed (Mahlalela et al., 2020).

- The novelty of this research is to use Geographic Information Systems (GIS) and multi source satellite remote sensing data to monitor agricultural drought at the Intsika Yethu Municipality. Ultimately this research will create a Composite Drought Monitoring Model (CDMM) for the comprehensive assessment and mapping of drought vulnerability, providing valuable insights for drought management within the municipality.
- Possibility of saving much needed vegetation that will benefit subsistence farmers in particular and the community.

1.3. AIM AND OBJECTIVES

1.3.1. AIM

The research aims at developing a GIS based Composite Drought Monitoring Model for Spatio-temporal drought vulnerability assessment at Intsika Yethu municipality, South Africa.

1.3.2. OBJECTIVES

- To map spatio-temporal agriculture variability ranging from 2017-2021 at Intsika Yethu local municipality in the Eastern Cape, South Africa.
- To derive multi spectral indices using multi source satellite remote sensing data.
- To develop the Composite Drought Monitoring Model (CDMM) for Drought vulnerability mapping.

2. LITERATURE REVIEW

This chapter provides a brief review of the literature related to drought, ie types of droughts, the impact of drought, traditional and modern ways of monitoring drought.

2.1. AGRICULTURAL AND METERIOLOGICAL DROUGHT

Philip et al., (2020) undertook a study to understand whether changes in meteorological and agricultural droughts in the Netherlands were as severe as or worse than in 2018 due to increased global temperatures. And whether trends in these droughts differ in inland and coastal areas? Statistical modelling was used in the study. The study demonstrated that the summer drought (Apr.-Sep.) near the shore did not change in recent years. While for the inland region, where local precipitation is a major determinant of water supply, a pattern in agricultural drought was seen.

With the help of the Coupled Model Intercomparison Project's (CMIP5) five Global Climate Models (GCMs), over East Africa, Haile et al., (2020) carried out a study that attempted to predict future drought trends. Drought features in the near term (the 2020s; 2011-2040), mid-term (2050s; 2041-2070), and long-term (the 21st century) were examined under the Representative Concentration Paths (RCPs) 2.6, 4.5, and 8.5. (2080s; 2071–2,100). Comparisons were made between the variations in the Standardized Precipitation Evapotranspiration Index (SPEI and the Standardized Precipitation Index (SPI). The SPEI was then used to gauge the likelihood of future droughts as it demonstrated more pronounced changes, because it took temperature effects into account.

Agricultural drought can be seen as an external yet internal supply-side shock that is commonly acknowledged as directly causing dramatic decreases in agricultural productivity, decreased export earnings, extensive asset losses, decreases in employment, and losses related to reductions in rural income. (Benson & Clay, 1994). The National Weather Service (2020) defines agricultural drought as an instance where the soil's moisture content is insufficient to suit the needs of a specific crop. Likewise Rockström, (2000) believes that there is complete water scarcity when the cumulative plant accessible soil water is much less than the cumulative crop water requirements, causing an agricultural drought.

2.2. IMPACTS OF DROUGHT IN SOUTHERN AFRICA

Orimoloye (2022) examined how a drought affected the country's main commercial agricultural region's ability to provide food security. Data on crops and Earth observation was used covering 2011 to 2021. Maize and soghurm were assessed appropriately to calculate the effects of the drought on the two crops. The outcome illustrated that extremely serious drought events (<10%) occurred in the years 2015 and 2018 and impacted the whole study area. While Drought (>30%) had a significant influence on the agricultural industry in the years 2011, 2016, 2018, and 2019. Further research found that, with around 223,600 and 119,050 tons of maize produced each year, 2014 and 2015 saw the lowest levels ever recorded. The results also revealed that sorghum production had its lowest output in 2019, 2016, and 2015 with around 23,600, 24,640, and 24,150 tons produced, respectively.

2.3. MAPPING AND MONITORING OF DROUGHT

2.3.1. TRADITIONAL METHODS

Methods for monitoring the drought have historically centred on in-situ measurements made at stations, however, advances in technological developments in earth observation and remote sensing changed the paradigm (West et al., 2019). Nam et al., (2012) used the following four tactics: Management of drought records, drought countermeasures, drought outlook and forecast, and drought assessment and monitoring, to create a framework to assist in managing agricultural drought through risk-based decision making. The conclusion was that these tactics were effective in drought management and an improvement to conventional ways, which were based on weather measurements and water levels in reservoirs.

According to Brown et al., (2008) the primary sources of information on droughts have historically been climate and meteorological data, and the drought indices based on climate are widely utilised to guide planning decisions and spur mitigation measures. These indices are typically calculated using the following variables: snow pack, soil water holding capacity, temperature, rainfall, stream flow and other additional signs of the water supply. They typically compare the level of dryness to the long-term mean or usual situation.

2.3.2. GIS AND REMOTE SENSING METHODS

Since the advent of satellite observations, several researchers agree that indicators based on satellite remote sensing have been employed successfully to track drought at regional to global

scales (Jeyaseelan, 2003; Assal et al, 2016; West et al., 2019). Viña et al. (2019) designated spectral bands, primarily in the visible and near infrared ranges of the electromagnetic spectrum, as mixtures to create vegetation indices. Drought indices, according to a number of studies, are quantitative measurements that describe drought conditions by combining information from several sources, including temperature, streamflow, precipitation and evapotranspiration, and water supply (Nagarajan, 2009; Zargar et al., 2011; Mukherjee et al., 2018). During the last few decades, several multispectral indices have been generated to monitor the drought condition and its vulnerability, and are shown in Table 2.1.

Table 2.1: Various drought indices used to monitor and assess agricultural drought

Indices	Description	Mathematical expression	Reference
NDVI	Normalized Difference Vegetation Index	$\mathrm{NDVI} = \frac{\mathrm{NIR} - \mathrm{RED}}{\mathrm{NIR} + \mathrm{RED}}$	Tucker, (1979) & Kogan, (1991, 1995), Yengoh et al., (2015)
EVI	Enhanced Vegetation Index	$\mathrm{EVI} = \frac{\mathrm{NIR} - \mathrm{RED}}{\mathrm{NIR} + (6\ \mathrm{x\ RED} - 7.5\ \mathrm{x\ BLUE}) + 1}$	Huete et al., (2002) and Saleska et al., (2007)
VCI	Vegetation Condition Index	$\mathrm{VCI} = \frac{(\mathrm{NDVI} - \mathrm{NDVI_{min}})\ \mathrm{x}\ 100}{(\mathrm{NDVI_{max}} - \mathrm{NDVI_{min}})}$	Kogan, (1995)
NDWI	Normalized Difference Water Index	$\mathrm{NDWI} = \frac{\mathrm{GREEN} - \mathrm{NIR}}{\mathrm{GREEN} + \mathrm{NIR}}$	Zhang et al., (2017)
LSWI	Land Surface Water Index	$\mathrm{LSWI} = \frac{\mathrm{NIR} - \mathrm{SWIR}}{\mathrm{NIR} + \mathrm{SWIR}}$	Xiao et al., 2002)
SWISI	Shortwave Infrared Water Stress Index	$\mathrm{SWISI} = \frac{\mathrm{SWIR} - \mathrm{NIR}}{\mathrm{SWIR} + \mathrm{NIR}}$	Fensholt & Sandholt, (2003)

NDWI	Normalized Difference Water Index	$\mathrm{NDWI} = \frac{\mathrm{NIR} - \mathrm{SWIR}}{\mathrm{NIR} + \mathrm{SWIR}}$	Chen et al., (2005)
NMDI	Normalized Multiband Drought Index	$\mathrm{NMDI} = \frac{(\mathrm{NIR} - (\mathrm{SWIR}_1 - \mathrm{SWIR}_2))}{(\mathrm{NIR} + (\mathrm{SWIR}_1 + \mathrm{SWIR}_2))}$	Wang & Qu, (2007)
Combined Indices			
VTCI	Vegetation Temperature Condition Index	NDVI, Land surface temperature (LST)	Wan et al. 2004)
TVDI	Temperature Vegetation Dryness Index	NDVI, LST	Sandholt et al. 2002)
SDCI	Scaled Drought Condition Index	LST, NDVI, TRMM	Rhee et al. 2010)
NDDI	Normalized Difference Drought Index	$\mathrm{NDDI} = \frac{\mathrm{NDVI} - \mathrm{NDWI}}{\mathrm{NDVI} + \mathrm{NDWI}}$	Gu et al. 2007)
ESI	Evaporative Stress Index	LAI, LST, Modern-Era Retrospective Analysis for Research and Applications (MERRA), TRMM	M.C. Anderson et al. (2016) and W. Anderson et al. (2016)
ISDI	Integrated Surface Drought Index	NDVI, LST, ecological zoning, Available Water holding Capacity (AWC), irrigation water management distribution, DEM	Wu et al. (2015)
SDI	Synthesized Drought Index	NDVI, LST, TRMM	Du et al. 2013)

Drought monitoring has been carried out by several researchers using different sensors and spatial scales e.g. Neigh et al., (2008) used aerial photography, Ikonos, National Oceanic and Atmospheric Administration (NOAA), Landsat and auxiliary data to learn more about the regional vegetation patterns detected by the Normalized Difference Vegetation Index (NDVI) derived from Advanced Very High Resolution Radiometer (AVHRR) over the North American continent and discovered areas with significant yearly increases in photosynthetic capacity at different dates between 1982 and 2005. The utilization of multi resolution data, aerial photography, Ikonos, Landsat and auxiliary data to investigate these anomalous locations showed a variety of explanations for the NDVI rises, such as droughts and their aftermath.

Rojas et al., (2011) used Vegetation Health Index (VHI) and NDVI derived from AVHRR for the period of 1981 to 2009 and found that VHI was an efficient drought indicator for the African continent. Nicolai-Shaw et al., (2017) monitored a drought event by analysing several factors including soil moisture, surface temperature, evapotranspiration and precipitation derived from satellite data. It was found that remote sensing based soil moisture can investigate the Land - Vegetation - Atmosphere dynamics.

Remote sensing-based drought indices were utilized by Winkler et al., (2017) to track agriculturally important droughts across Africa from 2000 to 2016, particularly focusing on growing seasons. SPI based on the Tropical Rainfall Measuring Mission (TRMM) with 0.25° precision as well as Vegetation Condition Index (VCI) and NDVI derived from Moderate Resolution Imaging Spectro-radiometer (MODIS) were used in the study. Using these two distinct drought indices, spatial and temporal development of droughts affecting African agriculture and their relationship to El Niño-Southern Oscillation (ENSO) occurrences were looked at. Large-scale patterns of agriculturally important droughts were discovered using surface reflectance data and remotely detected anomalies in rainfall (SPI-3) linked to vegetation status.

Choi et al., (2013) studied the standard and regional remote sensing drought indices to analyze the differences amongst them and examine how they relate to the observed indicators of hydrological and agricultural droughts. VHI, Palmer Drought Severity Index (PDSI), Evaporation Stress Index (ESI) and Advanced Microwave Scanning Radiometer (AMSR-E) soil moisture were used. While the accuracy of the ESI was less effective in cases of severe droughts, it was still superior to other drought indicators in conditions of mild drought.

Belal et al., (2014) reviewed several studies looking at major findings on the impacts of drought, methods of evaluating drought utilizing Remote Sensing and GIS techniques including satellite based drought indicators such as PDSI, Crop Moisture Index (CMI), SPI, Surface Water Supply Index (SWSI), NDVI, VCI and Temperature Condition Index (TCI). The authors concluded that climate based indicators lacked spatial characteristics as they depend on data gathered from weather stations that, which sporadically have a sparse distribution, which affects the accuracy of indices of drought. Belal et al., (2014) suggested the need to develop different indices to study different droughts. Belal et al., (2014) proposed that drought regionalization using data from remote sensing needed to be researched as a significant atmospheric trends and regional drought could be a means to increase the space-time variability of drought from local to regional scales.

While Atif and Mahboob, (2016) used remote sensing data to chart the spatiotemporal variance in Tharparkar's vegetation, in Pakistan and performed statistical analysis for drought variation. MODIS derived NDVI data was utilized to analyze the vegetation stress for the period of 2009 to 2013. The NDVI was deemed valuable for monitoring of agricultural drought and can provide farmers with an early warning system. However, it was suggested that determining how drought will affect society, the economy, and the environment is a difficult task for scientists. The study concluded that even though the severity of drought is determined by period, intensity and geographic extent, it also depends on the water demands of the vegetation of the specific region.

Orimoloye et al., (2019) assessed drought in Cape Town, South Africa utilizing thermal infrared sensor (TIRS) and operational land imager (OLI) from Landsat 8 imagery taken between 2014 and 2018. The images were taken in the summer period (November to January, selecting a good image for that year within that period) Land Surface Temperature (LST) and five indices were utilized which included Soil Adjusted Total Vegetation Index (SATVI), Normalized Difference Drought Index (NDDI), Normalized Difference Water Index (NDWI), Weighted Difference Vegetation Index (WDVI) and NDVI. The study demonstrated the efficiency of the indices utilized to evaluate the status of the vegetation health concerning the severity of drought especially during the years 2017 and 2018.

Liu et al., (2020) suggested a Composite Drought Index utilizing multivariable linear regression (MCDIs) to incorporate TRMM generated precipitation, soil moisture generated

from Global Land Data Assimilation System Version 2.1 (GLDAS), LST derived from MODIS and NDVI from 2013 to 2017. The study was to see how effective single remote sensing indices are at observing drought. It was discovered that the MCDIs worked well for tracking meteorological drought however, the efficiency of these indices for drought monitoring varies due to regional characteristics, and many of them may not be enough to record the impact of single factors that can cause drought. Similarly Du et al., (2013) used a combination of TCI, MODIS derived VCI and precipitation condition index (PCI) derived from TRMM to develop a synthesised drought index (SDI) using principal component. This index was found to be an exhaustive drought monitoring tool that may include not only meteorological drought information but also the impact of agricultural drought.

Kumar et al., (2021) developed an integrated drought monitoring index (IDMI) utilizing time series datasets obtained from earth observation satellites in orbit. This study was done in the south eastern part of Indian peninsula called Tamil Nadu state, using MODIS datasets for the period of 2000 to 2016. The IDMI was found to be very robust in monitoring agricultural drought.

While Jiao et al., (2021) reviewed drought studies using multi sensor remote sensing motivated by improved sensing capabilities and advantages of coupled multi sensor approach to understanding the causes and effects of drought. The study concluded that utilizing multi sensor remote sensing provided a unique benefit for regional to global studies.

Assal et al., (2016) suggested that few studies have assessed heterogeneous and sparse vegetation at local scales using satellite images with a low resolution, such as MODIS, AVHRR though they proved successful at continental scales. Studies conducted using high spectral and spatial resolution satellite data have applied NDVI to monitor agricultural drought (Krofcheck et al., 2014). However, research conducted by West et al. (2019) highlighted the inefficiency of NDVI in order to monitor agricultural drought as it reflect long-term changes because it can show conditions relative to a specific date and at low vegetation density, and it is easily influenced by bright soil background.

Dutta., (2015) looked at the effectiveness of remote sensing and GIS methods for tracking the spatiotemporal extent of agricultural drought in Rajasthan which is located in India's North-Western region. Agricultural drought was monitored using NOAA-AVHRR NDVI, NDVI-

based Vegetation Condition Index where the results for 2002 and 2003 were compared with SPI. The effectiveness of this drought indicator generated from remote sensing was established. Mlenga & Jordaan, (2020) suggested that for spatiotemporal (drought) monitoring, the ability to track and foresee the characteristics of the drought (onset, frequency, duration, and severity) was essential. Therefore, they constructed a comprehensive tracking and early warning system for drought in Eswatini by creating a threshold for an early warning reaction through integrating the normalized differential vegetation index and the standardized precipitation index. They realised that the drought's size, duration, and severity in Eswatini were growing using and coordinating precipitation and remote sensing-based drought indices effectively.
Approaches for descriptive and predictive modeling of drought have been transformed by methods utilizing multi sensor remote sensing and AI methods such as SVM, random forest (RF), artificial neural network (ANN) (Houmma, 2022). Houmma et al., (2022) further stated that these modern methods detect the multifaceted, spatiotemporal complexity of drought by combining a variety of multisensor remote sensing products, climate model simulations and auxiliary data.

2.4. CLIMATE CHANGE AND DROUGHT

Droughts are a natural occurrence, but climate change has typically sped up the hydrological processes to cause them to begin more quickly and intensify, with numerous negative effects, not least of which is a rise in danger of wildfires (Mukherjee et al., 2018). Mukherjee et al., (2018) suggested that investigating drought characteristics in a warming climate requires correct construction of reliable drought indices and priority should be given to drought indices' resistance to changes in temperature and other factors. The study concluded that it may be preferable to estimate potential evapotranspiration (PET) using the energy budget framework as opposed to purely using temperature-based equations.

In East Africa, the Coupled Model Intercomparison Project (CMIP5), which is a collection of five Global Climate Models (GCMs) was used to assess projected drought trends by Haile et al., (2020). First, the changes in the SPI and the SPEI were compared. The SPEI was then utilized to gauge the likelihood of future droughts because it demonstrated more pronounced changes because it took temperature effects into account. Additionally, the findings demonstrate that drought variations in East Africa follow the pattern of "dry grows drier and wet gets wetter."

2.5. LIMITATIONS OF REMOTE SENSING

According to AghaKouchak et al., (2015) opportunities exist for the creation of composite and multi indicator drought models in both current and future satellite missions, however, data continuity, unquantified ambiguity, sensor modifications, and public acceptance are only a few of the significant difficulties. Also, the limited length of record among many of the presently accessible satellite observations is a significant drawback.

2.6. OPPORTUNITIES FOR IMPROVEMENT

AghaKouchak et al., (2015) contended that there were chances to improve early drought warning through data on near-surface air relative humidity from the Atmospheric Infrared Sounder mission, for example, are satellite observations that are not utilized at the moment for practical drought tracking. Also, indicators for defining what a drought's effects are on the carbon and nitrogen cycles, which are essential for determining how drought affects ecosystems, have a significant gap.

West et al., (2019) suggested that as technology develops in the future, where the utilization of remote sensing in drought tracking is expanded by launching new satellites or sensors or by creating fresh methods and methodologies to reassess previously collected data.

Jiao et al., (2021) suggested that by making use of opportunities offered by multi sensor remote sensing, that may improve the knowledge of crucial vegetation-water-carbon interactions, which may not only lead to these necessary advancements but also pave the way for mechanism-based drought prediction.

2.7. SUMMARY

At continental scales, the remote sensing indices were used by various authors to study the drought phenomenon with relative success. Neigh et al., (2008) showed that a combination of multiresolution data can identify drought patterns. Rojas et al., (2011) proved that Vegetation Health Index (VHI) was an efficient drought indicator for the African Continent than NDVI. Huge-scale trends in crucial agricultural droughts were discovered using remotely sensed rainfall anomalies (SPI-3) and surface reflectance data linked to vegetation status derived from VCI. At regional level, ESI was found to be a promising drought index for characterizing both the streamflow and soil moisture anomalies especially when precipitation is unavailable or sparsely distributed. The NDVI was found to be useful for agricultural drought tracking and

can provide early detection method to farmers. However, some suggested that for scientists, determining how drought will affect society, the economy, and the environment is a difficult task. Several indices including SATVI, NDWI, NDDI, WDVI and NDVI demonstrated their efficiency to reflect on the state of vegetation health regarding the severity of drought especially during the years 2017 and 2018 in Cape Town. The MCDIs was used successfully to keep track of meteorological drought, however, its efficiency is subject to regionalcharacteristics, and many may not be enough to capture the impact of single factors that can cause drought. However, the IDMI and SDI were found to be very robust in monitoring agricultural drought.

3. MATERIALS AND METHODS

3.1. STUDY AREA

Intsika Yethu municipality is a catergory B municipality within the district municipality of Chris Hani in the Eastern Cape province of South Africa. It is in the South Eastern side of South Africa between 31°40’0”S to 32°20’0”S latitudes and 27°15’0”E to 28°0’0”E longitudes, shown in Figure 3.1. It is one of the six local municipality falling under the district accounting for 8% (Area: 2711 km^2) of its geographical area. Intsika Yethu is a Xhosa name that literally means “our pillar”, it was named understanding that it will provide hope to the residents. It consists of two small towns, namely Tsomo and Cofimvaba. Tsomo is geographically located at 32° 2'16.06"S 27°49'12.19"E whereas Cofimvaba is at 32° 0'10.23"S 27°34'49.56"E. The Eastern Cape has the greatest percentage of households that depend on agriculture out of all the South African provinces (Walz et al., 2020). According to Census (2011), Intsika Yethu in particular, had 145,372 people and 40,448 households. Just over 58% (23,639) of the households are involved in some agricultural activities.

Small-scale livestock farming is eminent in the Eastern Cape (B. Mandleni, 2012). The province experiences cold front induced rainfall in winter which dominates at the coastal side and diminishes in the inland and summer rainfall (DEA, 2018). According to Palmer, (2004) the Eastern Cape is a dry to semi-arid province with a mean rainfall of 350-550 mm per annum. Mahlalela et al., (2020) suggested that rainfall projections indicate a shift in the Eastern Cape and will experience wetter winters and drier summers. The mean temperature for the region is 17.8°C and it can easily reach 40°C in summer season (Mills et al., 2005). According to South African Weather Services (SAWS), there are four weather stations around the study area located in Queenstown, Elliot, Stutterheim and Umtata. The distance ranges from 100 km to

170 kms (SAWS, 2021).

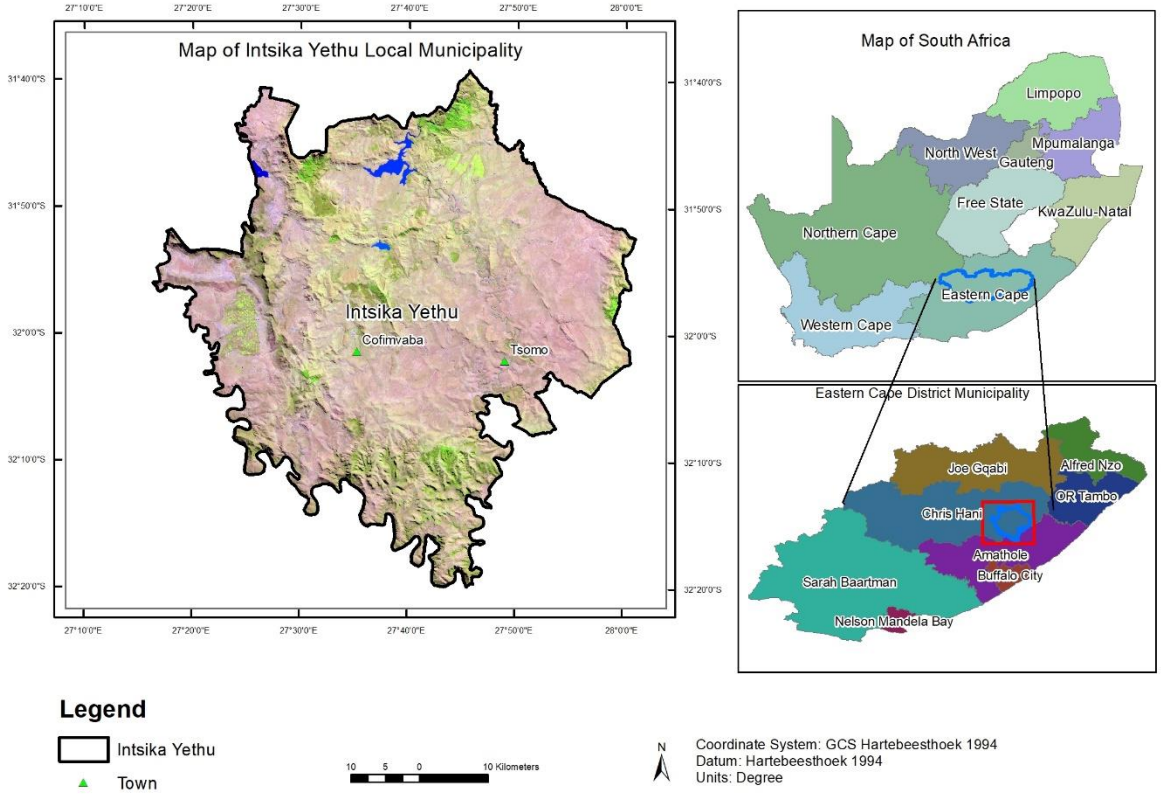

Figure 3.1: Study area map of Intsika Yethu, Eastern Cape.

3.2. RESEARCH DESIGN

The study followed the research design shown by the brief structure in Figure 3.2 below.

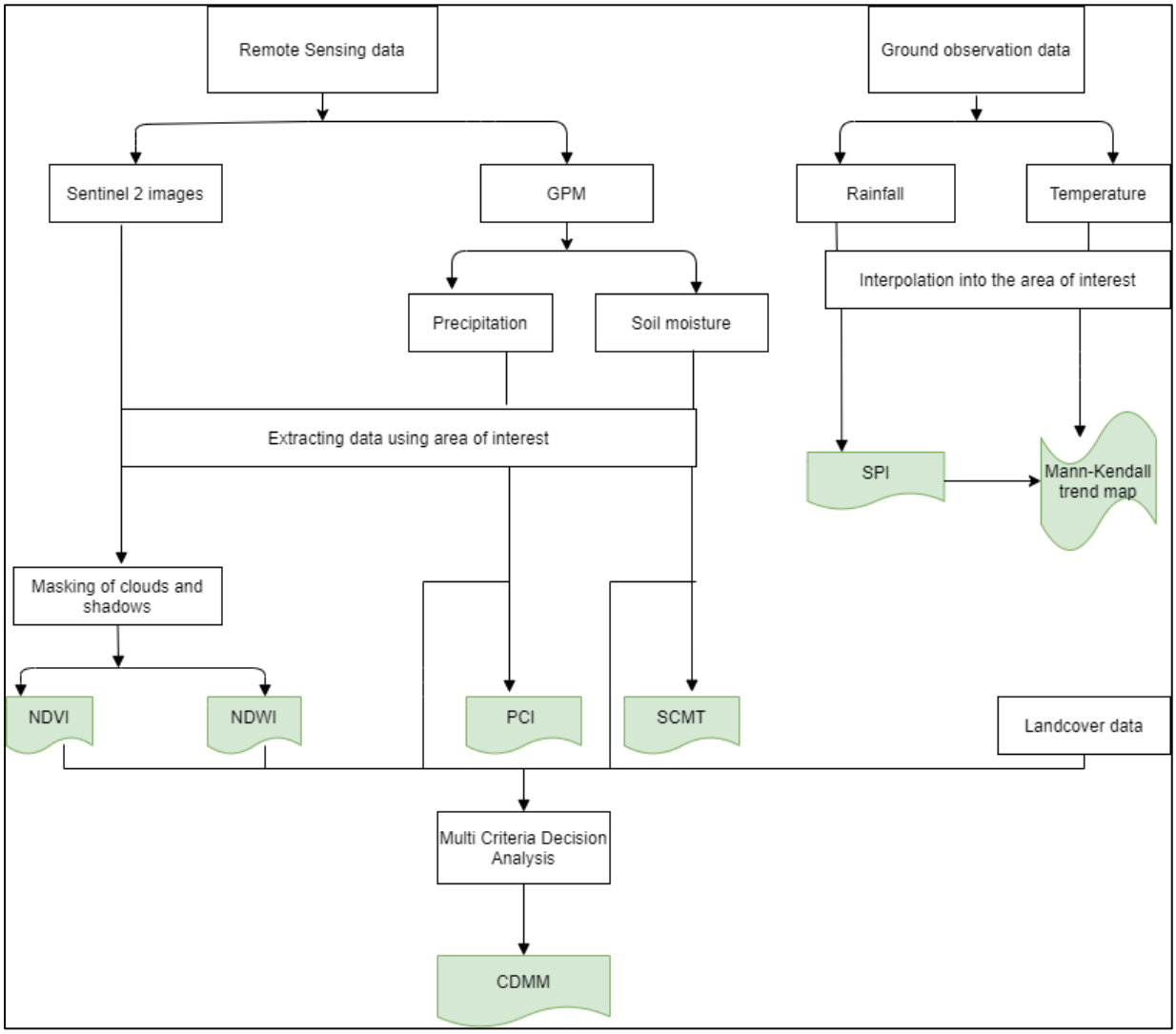

Figure 3.2 : Research methodological flow chart.

3.3. DATA REQUIREMENTS

The research used Sentinel-2 images covering the Intsika Yethu Local Municipality. The summary of the dataset information needed for this research is listed in table 3.1 below.

Table 3.1: Summary of data required for the research

Data Set	Details	Source
Sentinel-2 images	• 13 spectral bands (3 bands were used for the research i.e., band 4, band 8 and band 11. • Temporal resolution of five days (with Sentinel - 2A and Sentinel – 2B). • Swath width of 290 km. • The images were from January to May for years 2017 to 2021	United States Geological Survey (USGS) Earth Explorer
Meteorological Stations data	○ **Rainfall data** Data was provided from four stations data i.e. Queenstown, Elliot, Mthatha and Stutterheim ○ **Temperature data** Data was provided from Four stations i.e., Queenstown, Elliot, Mthatha and Dohne Agric. The data was from January to May for years 2017 to 2021.	South African Weather Service (SAWS)
Global Precipitation Mission (GPM) satellite precipitation data	• GPM_3IMERGDF v06 • Spatial resolution of 0.1° • Daily temporal resolution was used which will cover a five year period ranging from 2017 – 2021, for January to May	National Aeronautics and Space Administration's Giovanni available at https://giovanni.gsfc.nasa.gov/giovanni/
Advanced Microwave Scanning Radiometer 2 (AMSR-2) soil moisture	• Volumetric Soil Moisture (AMSR-2 LPRM_AMSR2_DS_A_SOILM3v001) • Spatial resolution of 10 km • Temporal resolution of daily	National Aeronautics and Space Administration's Giovanni available at https://giovanni.gsfc.nasa.gov/giovanni/
Municipal Boundaries	Municipality shape file	Municipal Demarcation Board (MDB)
South African National Landcover	South African National Landcover 30*30m resolution	Department of Forestry, Fisheries and the Environment

3.3.1. SENTINEL-2 DATA

Generation of consistent observation records of key biodiversity changes such as land use and land cover dynamics from local to global levels have been made possible by Satellite remote sensing (Townshend et al., 2012). According to Shen et al., (2011), it is possible to research land surface dynamics by keeping an eye on vegetation phenology, for example, dense time series supplied by regular satellite coverage. This dense time series also need high spatial resolution especially in heterogeneous areas, so fine scale land surface dynamics such as human related activities can be characterised (Zhu et al., 2016). Remote sensing technologies with high spatio-temporal resolution play a crucial role in tracking crop growth, land cover change detection and phenological parameter inversion (Zhang et al., 2013). The most suitable satellite data for observing drought, climate variability and surface water bodies is Sentinel-2 data because of its quality spatial, temporal and spectral characteristics and its availability (Bhaga et al., 2020). Amongst the series of Sentinels, Sentinel-2 consists of a high resolution sensor that combines Spot and Landsat type of data for services that include forestry, agricultural industry, humanitarian relief operations and disaster control (Aschbacher & Milagro-Pérez, 2012). Sentinel-2 consists of two satellite configurations that offer a global coverage of land surface, with five day temporal resolution (Baillarin et al., 2012).

Variables essential for climate and biodiversity such as leaf area index, fraction of photosynthetically active radiation, vegetation type, biomass, leaf water content, leaf chlorophyll, fire disturbance, fraction of vegetation cover and land cover (Malenovský et al., 2012). Sentinel-2's utility extends beyond climatic and biological monitoring to include local and global vegetation evaluation as a result of its improved spatial resolution and spectral band composition (Ramoelo et al., 2015). Also some of the commercial satellites such as Worldview-2 and Rapid Eye are comparable to Sentinel-2, because of the existence of the red edge band and including the short infrared bands (Ramoelo et al., 2015). According to Ramoelo et al., (2015), the red edge band is essential for tracking and evaluating vegetation. Sentinel-2 carries the Multi Spectral Instrument (MSI) having four bands at 10 m, six bands at 20 m and three bands at 60 m spatial resolution (Clevers & Gitelson, 2013). It has a swath width of 290 km at 20◦ field of view and has two spectral bands in the red edge region with spatial resolution of 20 m centred at 705 nm and 740 nm with a band width of 15 nm (Clevers & Gitelson, 2013) (Table 3.2).

Table 3.2: Different spectral bands of Sentinel-2 (Source: Wessel et al., (2018))

Spectral Band	Wavelength range (nm)	Width band	Spatial resolution (m)
B1(Coastal aerosol)	433 - 453	20	60
B2 (Blue)	458 - 523	65	10
B3 (Green)	543 - 578	35	10
B4 (Red)	650 - 680	30	10
B5 (Red edge)	698 - 713	15	20
B6 (Red edge)	733 - 748	15	20
B7 (Red edge)	773 - 798	20	20
B8 (Near infrared)	785 - 900	115	10
B8a (Red edge)	855 - 875	20	20
B9 (water vapor)	935 - 955	20	60
B10 (SWIR-cirrus)	1360 - 1390	30	60
B11 (SWIR)	1565 - 1655	90	20
B12 (SWIR)	2100 - 2280	180	20

The revisit time of Sentinel-2 is approximately 5 days at the equator (Wessel et al., 2018). High temporal resolution can be an important benefit in obtaining dynamic information on plant state (Somvanshi & Kumari, 2020). Therefore, Sentinel-2 images processed to level-2A were used for this research. Level-2A product, has an ortho-image, Bottom-Of-Atmosphere (BOA) adjusted reflectance product (ESA, 2021). The tiling grid 35HNE, which is 110km by 110km, was downloaded from https://earthexplorer.usgs.gov/. The images with cloud coverage of less than 10% were selected. To capture different plant phenological stages, the images must be from different seasons (Abdi, 2020).Therefore, the images covered the beginning, middle and end of the growing season just to ensure that seasonal variability is captured. The average number of images for each month were expected to be six or seven considering the revisit time of five days, however, due to cloud cover exceeding 10% some images could not be used.

3.3.2. FIELD BASED METEOROLOGICAL STATIONS DATA

The meteorological data utilized in this investigation was observed from the nearest stations surrounding the study area and there is none in the study area. The data was requested from SAWS via an email for four stations closer to the study area. The data covered months of January to May for the years, 2017 to 2021. It was duly received as an excel spreadsheet via an email.

3.3.3. SATELLITE BASED GLOBAL PRECIPITATION MEASURING MISSION DATA

Many hydrological and environmental research, such as climate change, drought, desertification and other strategic studies, rely heavily on precipitation data (Abdulrazzaqet al., 2019). Satellite based climate data, with a strong geographical and temporal coverage, is explored as an alternative for augmenting ground-based meteorological observations data and therefore, it is critical to employ drought indices and rainfall data from the TRMM (Abdulrazzaq et al., 2019) as well as its successor Global Precipitation Measuring Mission (GPM). TRMM was created primarily to study tropical rainfall however, it has been found to be a significant resource in areas such as drought and flood monitoring as well (Abdulrazzaqet al., 2018). However, falling snow and light-intensity precipitation (i.e., 0.5 mm h^{-1}), which make up a considerable occurrence of precipitation at the high and middle latitudes, is added to the range of measurements reached by TRMM owing to the GPM sensor (Kulie & Bennartz, 2009). International organizations NASA and JAXA are in charge of the GPM and the newest type of global precipitation and snow measurements are provided by this global network of satellites (Zhao et al., 2022). The GPM mission was created with the particular purpose of combining and improving precipitation observations from a network of research and operational microwave sensors (GPM, 2013). Therefore, this study used GPM_3IMERGDF v06 with a spatial resolution of 0.1° and daily temporal resolution. GPM data was downloaded from NASA's Giovanni available from https://giovanni.gsfc.nasa.gov/giovanni/.

3.3.4. ADVANCED MICROWAVE SCANNING RADIOMETER SOIL MOISTURE DATA

To accurately characterise agricultural droughts, it is essential to have reliable knowledge about soil moisture (Paredes-Trejo & Barbosa, 2017). The onset of an agricultural drought is generally regarded as occurring when soil moisture availability becomes so low as to adversely impact crop yield (Zhu et al., 2019). According to Spencer et al., (2010) soil moisture has a strong impact on plant growth and thus agricultural productivity, especially during times of water scarcity and drought. Thus, the accessibility of databases for soil moisture is crucial for the forecast of agricultural drought given the implications of soil moisture on agricultural output (Zhu et al., 2019). The data was acquired from the satellite and the product used in this study was Advanced Microwave Scanning Radiometer Soil Moisture Data (AMSR-2 LPRM_AMSR2_DS_A_SOILM3v001) with a spatial resolution of 10 km and daily temporal

resolution. Soil moisture data was downloaded from NASA's Giovanni) available from https://giovanni.gsfc.nasa.gov/giovanni/.

3.4. METHODOLOGY

3.4.1. LANDCOVER DATA OF STUDY AREA

The South African National Land Cover 2018 (SANLC2018) dataset was used to extract statistics of the different classes within the study area. One of the most crucial characteristics for monitoring, characterising, and analysing the environment is land cover (Herold et al., 2008). A range of activities, including economic growth, compliance monitoring, enforcement, and strategic decision making, are informed by land cover data, which is a vital reference dataset (Department of Forestry, Fisheries and the Environment (DFFE), 2023). In fact, information about the dynamics of land cover and change that is timely, comprehensive, and accurate is extremely helpful for decision making in numerous sectors, including policy assessment, sustainable development, food production, water and energy security, natural hazards, ecosystem services, and natural resource management (Bui et al., 2014). The SANLC 2018 was generated at pixel size of 20m by 20m using Sentinel 2 images (DFFE, 2023).

3.4.2. PRE-PROCESSING OF SENTINEL 2 IMAGERY USED

Sentinel-2 level 1 images are radiometrically calibrated and georectified data, and were usually the lowest accessible level with level 2A data already available with atmospheric adjustment (Frantz, 2019). ArcGIS 10.8.2 was used for extracting the images fitting the study area using the Intsika Yethu municipality shapefile. Eleven images with clouds were masked using ArcGIS 10.2 in order to remove effects of clouds and shadows.

3.4.3. PROCESSING OF THE VEGETATION INDICES

3.4.3.1. NORMALISED DIFFERENCE VEGETATION INDEX (NDVI)

The data was processed for NDVI, and the main objective was to map the spatio-temporal agriculture variability within the study area using seasonal images to record values. The data was also processed for other indices such as NDWI. Wu et al., (2020b) suggested that NDVI and some indices such as VCI, and NDWI are examples of vegetation indices that may characterize agricultural drought, its geographical extent, and vegetation stress (Wu et al., 2020b). NDVI is an indicator of the health of a plant based on how it reflects light at specific frequencies (Carlson & Ripley, 1997). It is also used to keep track of and forecast agricultural

output, drought evaluation, and forest fire danger zone mapping, and to quantify vegetation relative biomass (Somvanshi & Kumari, 2020). NDVI readings are typically low in areas of snow, barren rock or sand (for example, 0.1 or less), high NDVI values (about 0.6 to 0.9) are associated with vegetation that is dense, such as that found in tropical and temperate and tropical vegetation or crops that are at their peak development stage. Moderate NDVI levels can be generated by sparse vegetation, such as grasslands and shrubs, as well as senescing crops (between 0.2 and 0.5) (Brown, 2020). A higher NDVI rating implies that the vegetation is richer and healthier (Kumari & Somvanshi, 2019).

Because chlorophyll causes absorption in the red band and interior leaf structure causes relatively high reflection in the near infrared, a combination of the two is used to calculate NDVI (Somvanshi & Kumari, 2020). Equation 1 defines NDVI as follows:

$$\mathrm{NDVI} = \frac{\mathrm{NIR} - \mathrm{RED}}{\mathrm{NIR} + \mathrm{RED}} \qquad (1)$$

Where B8 and B4 are for NIR and red bands respectively were used for Sentinel 2 images. The pixel classification range is shown in table 3.3 below.

Table 3.3: Pixel classification range of NDVI (Source: Altunet al., (2020))

Pixel range	Class
< 0	Water
0 – 0.03	Bare soil
0.03 – 0.3	Sparse vegetation/Agriculture
0.3 to 0.5	Moderate vegetation
> 0.5	Dense vegetation

The range below 0.03 was excluded from the analysis as it does not constitute vegetation. The actual NDVI values were used to determine the monthly drought trends. According to Ali et al., (2019) the NDVI distribution pattern is a reliable indicator of regions that are vulnerable to drought, nonetheless on a bigger scale, it is challenging for NDVI readings to pinpoint a drought indication because vegetation is impacted by a number of other local factors in addition to climatic ones. Thus, NDWI was utilized to create spatial distribution maps, which were then compared to detect drought development trends in drought affected areas more precisely.

3.4.3.2. NORMALIZED DIFFERENCE WATER INDEX (NDWI)

Changes in the water content of leaves can be detected via an indicator based on remote sensing called the NDWI (Chen et al., 2005). Hence, it serves as a very accurate proxy for plant water stress (JRC European Commission, 2011). It is defined by equation 2 below:

$$\text{NDWI} = \frac{\text{NIR} - \text{SWIR}}{\text{NIR} + \text{SWIR}} \qquad (2)$$

Where Near Infra Red (NIR) and Short Wave Infra Red (SWIR) are Band 8 and B11 respectively. High vegetation water content and cover are correlated with high NDWI results and the opposite is true therefore NDWI will diminish during water stress periods (JRC European Commission, 2011).

Table 3.4: NDWI values and their ranges (Source: EOS, 2023)

Pixel range	Class
-1 - -0.3	Drought, non-aqueous surfaces Water
-0.3 – 0.0	Moderate drought, non-aqueous surfaces
0.0 – 0.2	Flooding, humidity
0.2 to 1	Water surface

To determine drought from NDWI, the study used ranges that are below 0, excluding water. According to McFeeters, (2013), NDWI values above zero are taken to indicate water surfaces, whereas those below or equal to zero are taken to represent non-water surfaces. According to Merriam-Webster (n.d.) non-aqueous solutions, therefore, are those in which a different solvent than water is utilized to create the solution.

3.4.4. PROCESSING OF METEOROLOGICAL STATIONS DATA

Even though the study area does not have any weather station, however, there are four weather stations around the area. These stations are situated in Mthatha (approximately 67 kms), Elliot (32 kms), Queenston and Stutterheim/Dohne Agric (approximately 35kms). The weather stations' monthly precipitation and temperature data was supplied by the SAWS and needed to be interpolated to the study area. The monthly data from all the stations that was missing was at 3% and 12% for rainfall and temperature data, respectively. GIS interpolation techniques were used to comprehend spatial and temporal trend and occurrence of drought in the research area. Drought conditions of unsampled places in areas where there aren't many weather stations

may be calculated using statistical approaches like a spatial interpolation of sampled data (Rhee,, et al. 2010). Inverse distance squared and kriging are two of the most popular GIS interpolating techniques (Conolly, 2020). Ordinary kriging was used to interpolate the data in order to produce surface maps of both rainfall and temperature using four stations and predicting the values in the study area using ArcGIS 10.8.2. Ordinary kriging is the interpolation technique that is used and compared the most, followed by IDW, IDS, and other methods (Li & Heap, 2008). Equation 3 as provided by Li & Heap (2008) is as follows:

$$(\hat{Z}(x_0) - \mu) = \sum_{i=1}^{n} \lambda_i [Z(x_i) - \mu(x_0)] \qquad (3)$$

Where μ recognized stationary mean that is determined as the data's average and is thought to be constant throughout the whole domain. The symbol n is the number of sampled points used to produce the estimation, the parameter λ_i is kriging weight and (x_0), which displays the sample mean within the search window. The kriging weight is determined by parameter I.

The interpolated rainfall data was processed for SPI with the main objective of deriving the spatial and temporal variation of meteorological drought that leads to agricultural drought.

3.4.5. STANDARDISED PRECIPITATION INDEX (SPI)

The SPI, which provides a rapid measure with little data needs, is among the highly prominent index based on precipitation used to track drought (Mlenga & Jordaan, 2020). The solely based on precipitation data, SPI is a highly useful tool and an index for tracking meteorological dryness (Dutta et al., 2015). Equation 4 below is used for calculating SPI:

$$SPI = \frac{(x_j - x_k)}{\sigma} \qquad 4$$

Where X_i is precipitation value at a station, X_m is the mean value for the month across the stations and **σ** is the standard deviation. The SPI classes are shown in table 3.5.

Table 3.5: SPI values and their categories (Source: McKee et al., (1993))

SPI value	Category
> 2.0	Extremely wet
1.5–1.99	Very wet

1.0–1.49	Moderately wet
0.99 to -0.99	Near normal
-1.0 to -1.49	Moderately dry
-1.5 to -1.99	Very dry
<-2	Extremely dry

To determine the regional pattern of meteorological dryness and the threshold value for several forms of drought, the SPI values were interpolated.

3.4.6. PROCESSING OF GLOBAL PRECIPITATION MISSION (GPM) SATELLITE DATA

Disputes in rainfall data are defined by a combination of challenges, these include a shortage of rain gauges, a limited coverage of rain gauges, a lack of rain gauge data, inadequate data sharing procedures, or poor data management (Mahmud et al, 2020). Without an adequate network of meteorological stations across the region, it is impossible to accurately determine the spatial extent of the drought (Dutta et al., 2015). Mahmud et al., (2020) suggested that satellite precipitation data can be utilized to support sub-catchments that are not gauged or that have data conflicts, albeit their utility is restricted by the geographic resolution and sub-catchment size restrictions. The data was sourced from NASA's GES DISC and was extracted using the study area boundary. Both statistical information and raster representing the precipitation information in the study area were extracted. The precipitation condition index (PCI) was processed using equation 5 as follows:

$$PCI = \frac{PGM_i - GPM_{min}}{PGM_{max} - PGM_{min}} \qquad (5)$$

Where $TRMM_i$ stands for the precipitation in the ith month, whereas $TRMM_{max}$ and $TRMM_{min}$ refer to the historical maximum and lowest values at each required time step during the study period.

3.4.7. PROCESSING OF ADVANCED MICROWAVE SCANNING RADIOMETER (AMSR-2) SOIL MOISTURE

Despite the fact that there are extremely few monitoring facilities that gauge soil moisture directly, it is a key predictor of drought (Ford & Quiring, 2019). Ford & Quiring, (2019) suggested that high-quality models as well as satellite remote sensing soil moisture estimates

can close the gaps in in-ground soil moisture observations. Advanced Microwave Scanning Radiometer 2 (AMSR-2) soil moisture was used in this study and was sourced from NASA's Giovanni. Both statistical information and raster representing the soil moisture information in the study area were extracted. The soil moisture-based soil moisture condition index (SMCI) was processed using equation 6 as follows:

$$SMCI = \frac{SM_i - SM_{min}}{SM_{max} - SM_{min}} \quad (6)$$

Where SM_i is the soil moisture in the ith month, and SM_{max} and SM_{min} are the maximum and minimum historical values at each specified time step within the study period.

3.4.8. MANN-KENDALL TREND ANALYSIS

The Mann-Kendall trend test was used to determine the trend from the processed information. Therefore, to evaluate whether the pattern of maximum, minimum, average temperatures and average rainfall and the processed indices in the study area was consistently rising or decreasing, the Mann-Kendall Trend Test was performed. According to Kamruzzaman et al., (2018) in order to establish whether a time series has a monotonic upward or decreasing trend, the Mann-Kendall test can be utilized.

A non-parametric rank-based test called the Mann-Kendall test is utilized to assess if a time series exhibits a monotonic trend. It was first devised by Mann (1945), and Kendall (1975) later determined the test-statistic distribution.

The alternative hypotheses for this test are that there is a pattern in the two-sided test or that there is an upward (or a downward) trend in the one-sided test, with the null hypothesis for this test being that there is no trend (Mann, 1945). For a time series x1 to xn, the Mann-Kendall test utilizes the following mathematical equations:

$$S = \sum_{k=1}^{n-1} \sum_{j=k+1}^{n} sgn\,(x_j - x_k) \quad (7)$$

$$sgn(x_j - x_k) = \begin{cases} +1 & \text{if } (x_j - x_k) > 0 \\ 0 & \text{if}(x_j - x_k) = 0 \\ -1 & \text{if}(x_j - x_k) < 0 \end{cases} \quad (8)$$

where n is the data set's length, x_k and x_j represent the data values at times k and j where l=1, 2, …, n-1 and k= l+1, …, n, The S value in this case reflects the trend's direction. An increasing trend is indicated by a positive value of S, and vice versa (Kamruzzaman et al., 2018).

3.4.9. DEVELOPING A COMPOSITE DROUGHT MONITORING MODEL (CDMM) FOR DROUGHT VULNERABILITY MAPPING

The calculated NDVI, NDWI, GPM Satellite precipitation, AMSR-2 soil moisture and the landcover map of the study area were combined using sensitivity analysis in ArcGIS 10.8.2 to delineate the vulnerable area to drought. The drought risk map can be created by combining the risk maps produced for agricultural drought and meteorological drought (Murad & Islam, 2011). The study adopted a Multi Criteria Decision Analysis (MCDA) method to select the areas affected by drought.

3.4.9.1. MULTI CRITERIA DECISION ANALYSIS (MCDA)

MCD is defined as a general term for a series of formal approaches that aim to explicitly account for various factors when assisting individuals or groups in exploring important issues (Mendoza & Martins, 2006). The evaluation of a range of potential actions or alternatives is a key component of the MCDA process (Durbach & Stewart, 2012). According to Durbach & Stewart, (2012) selecting a favorite alternative, ranking alternatives from best to worst, classifying alternatives into ordered categories like "good" or "bad," among other options, are some of the different ways this evaluation can be done.

To categorize the area for drought area determination, the Analytical Hierarchy Process (AHP) technique had been integrated with GIS and Weighted Overlay Analysis (WOA). The basic goal of multi criteria decision making is to figure out how to integrate data from multiple variables to provide one index of evaluation (Chen et al., 2010). According to Chen et al., (2010), a time and money-efficient analysis, GIS are ideally equipped to handle a variety of criteria data from many sources at several geographical, temporal, and scale levels.

Therefore this study used the time series data of multi source satellite remote sensing data such as NDVI, NDWI, precipitation, soil moisture and Landcover data to derive a drought risk profile of the study area.

Multiple layers were combined using cell statistics, in the spatial analyst tool of ArcGIS which calculates cell statistics from multiple raster layers. The process uses AHP to assign weighs to

different layers used. A five scale criterion was used where 5 is allocated to severe drought and 1 to a no drought. The layers were combined into four classes of drought risk profile.

4. RESULTS AND DISCUSSION

4.1. GENERAL STATISTICS OF THE STUDY AREA

This section gives an overview of the landcover classes at Intsika Yethu as provided by the (SANLC 2018) dataset. There are fifteen classes that can be found in the study area as shown in Figure 4.1. Spatially the grasslands are the dominant class followed by the cultivated subsistence class across the entire study area.

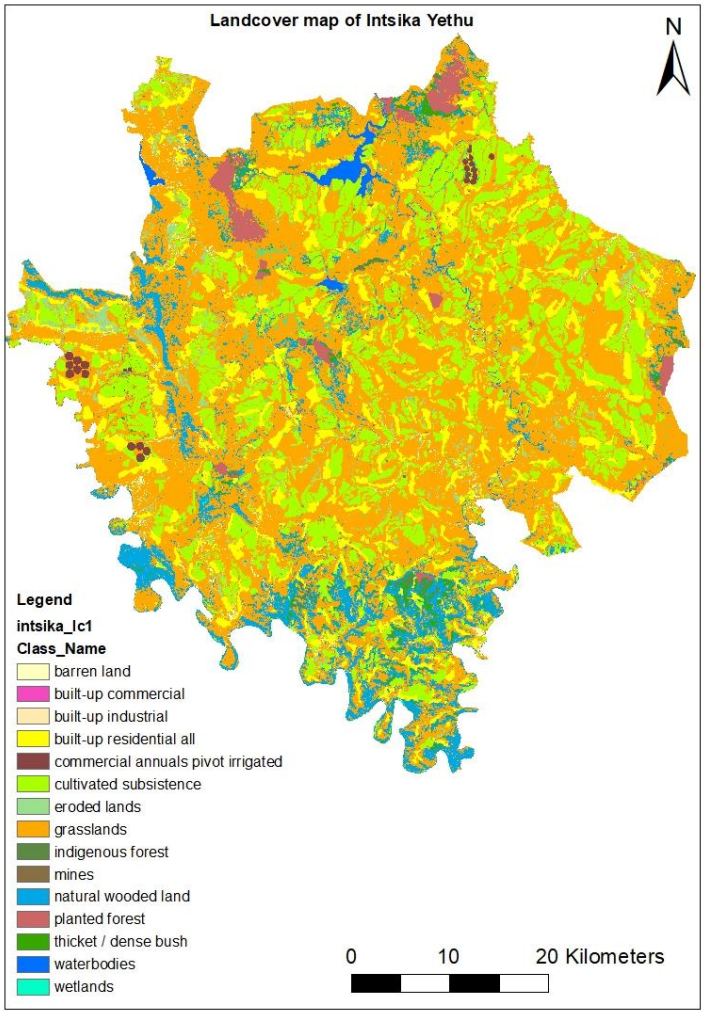

Figure 4.1: Landcover map of Intsika Yethu municipality adopted from SANLC 2018

More than 50% of the land is occupied by grasslands followed by cultivated subsistence and residential at 20% and 10% respectively as shown in Figure 4.2. The domination of grasslands is no surprise as according to (Abdel-Hamid et al., 2020) they make up over one-third of South Africa's total land area and are an important part of the natural vegetation of a country. Cultivated land is scattered across the adjacent to build up residential.

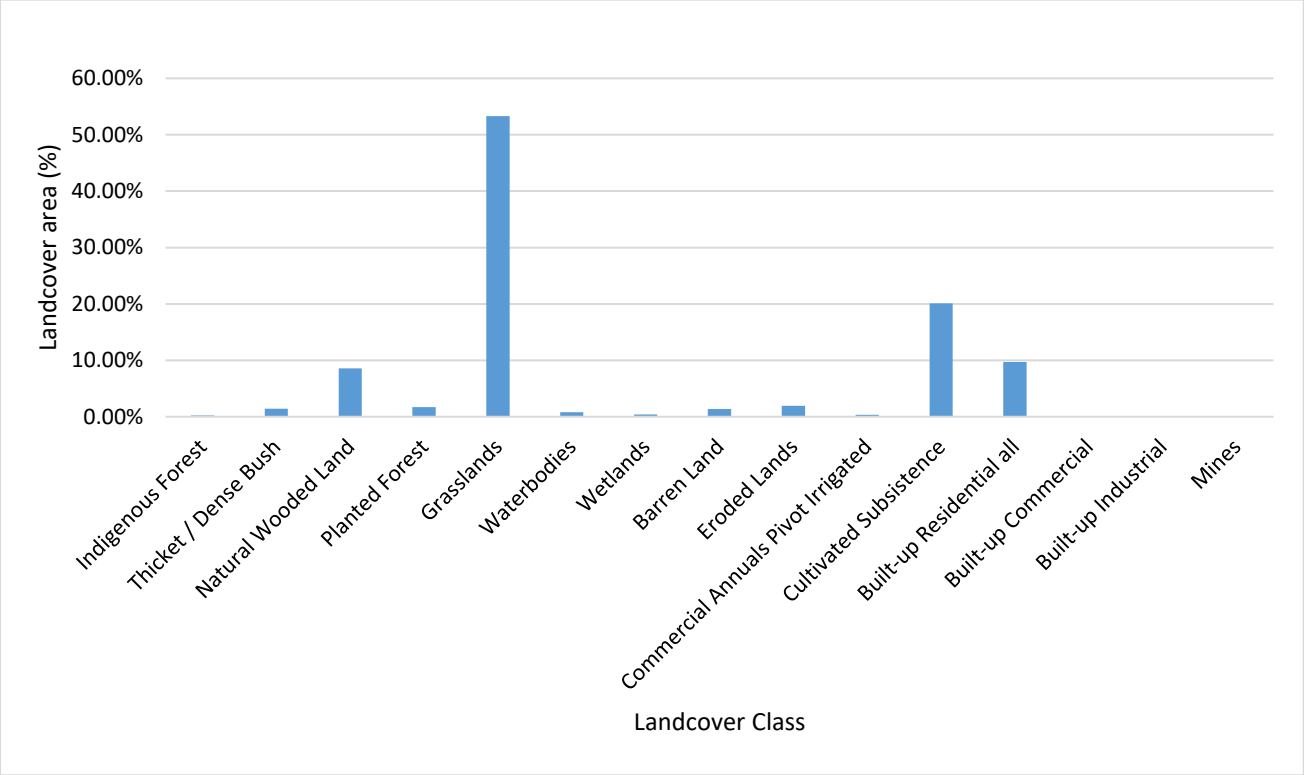

Figure 4.2: The area percent of the Landcover classes at Intsika Yethu municipality

All the other classes occupy less than 2% each of the land except Natural wooded land which is the fourth largest at close to 9%.

4.2. ANALYSIS OF AGRICULTURAL DROUGHT USING VEGETATION INDICES AT INTSIKA YETHU

4.2.1. ANALYSIS OF NDVI

This section provides the temporal overview of the vegetation variation at Intsika Yethu for 2017 to 2021, January to May. The crop season of growth was the time frame used in this study, and it is essential for capturing the spatiotemporal variance of NDVI in agriculture. The phenology of the crops and the climatic circumstances were the key factors considered in selecting the study period. Using the mean NDVI, the temporal variance of agricultural drought patterns and severity was examined. The association between spectral variability and variations in vegetation under different growth rates is demonstrated by the use of NDVI index in the remote sensing field (Shashikant et al., 2021).

Figure 4.3 demonstrates the temporal variability of mean NDVI for months of January to May for years 2017 to 2021, respectively. The few number of useful images have limited the variation as no image was selected for January and May as they were more than 10% cloud coverage, with only one image used in February and March while there were two usable images for April. The mean NDVI increases from just below 0.38 in February to a peak of 0.53 in March before dropping to 0.46 in April.

For 2018, the mean NDVI reading was at 0.42 in January and increases to 0.45 in February. It peaks to 0.55 in March and drops to 0.45 in April before dropping further to 0.40 in May.

In 2019, the mean NDVI for January was very low at 0.27. It increases slightly to 0.34 in February and remains constant in March. It peaks at 0.49 in April before dropping to 0.47 in May.

In 2020, low NDVI was observed in January and February at 0.32 and 0.38 respectively and started increasing in March to 0.52 before reaching a peak at 0.56 in April. It dropped slightly in May to 0.52.

While 2021 showed high values in January, February and March at 0.54, 0.55 and 051 respectively. It started dropping in April and May to 0.40 and 0.42 respectively.

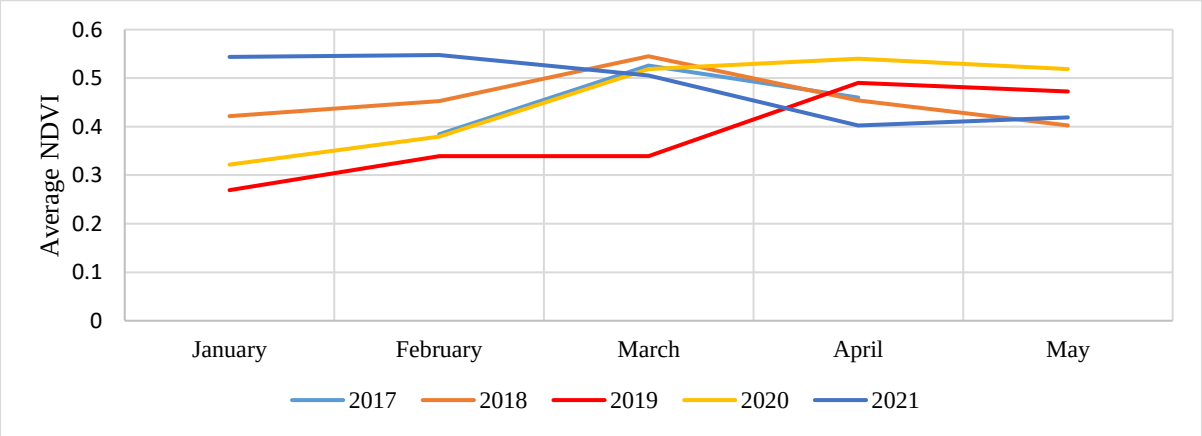

Figure 4.3: Mean NDVI time series for 2017 to 2021 (January to May)

In comparison to non-drought conditions (NDVI > 0.6), NDVI readings are lower when there is a drought (NDVI =~ 0.5) (Gu et al., 2007). Therefore the mean NDVI readings shown in Figure 4.3 demonstrated an NDVI lower than 0.6 throughout the study period.

4.2.2. ANALYSIS OF SPATIO-TEMPORAL VARIATION OF NDVI AT INTSIKA YETHU

The NDVI products in each year demonstrated a very similar pattern where January and February had a low NDVI value and peaked in March before declining in April and May (see Figure 4.4). The trend was consistent with the vegetation growing season of the area generally observed in years 2017 to 2020, however, for 2021 showed a decreasing trend where January had a higher NDVI mean and showed a decreasing trend in the subsequent months.
The temporal variation was observed in each year, where the NDVI was diverse month by month indicating difference in vegetation health within the study area. Generally, the northern and southern parts of the study area showed higher NDVI values than the western, central and eastern strip across the different months and years.

Year 2017 observed an NDVI that was low in February from east, central and west of the study area. The situation changed in March as the NDVI showed healthy vegetation in the study area which decreased in April.

For year 2018, January showed a similar pattern where the north and the south parts showed high NDVI while east, central and west sides showed a decreased NDVI values. The pattern continued in February before it improved significantly in March and April. The NDVI showed a decline in the May images.

Year 2019 showed very low NDVI values in January and the beginning of February indicating drought and slightly increased at the end of February before decreasing again as the month ends. April and May showed the same pattern as the east, central and west observe a slight lower NDVI values.

Year 2020 showed January with low NDVI values and the pattern was consistent until March when it improved significantly for the duration of the period. Year 2021 started with the high NDVI values that were consistent until April when they decreased slightly going to May. This was in line with what was reported by Archer et al., (2022) who stated that from 2015 until the beginning of 2020, when some improvement was observed, the Eastern Cape Province was affected by a severe multi year drought. In general, 2019 exhibits very low NDVI values compared to other years.

NDVI MAPS 2017

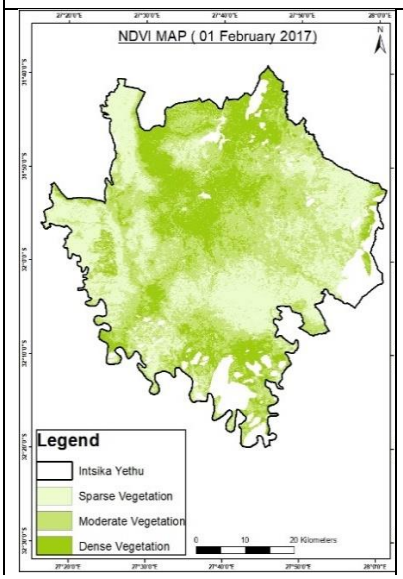

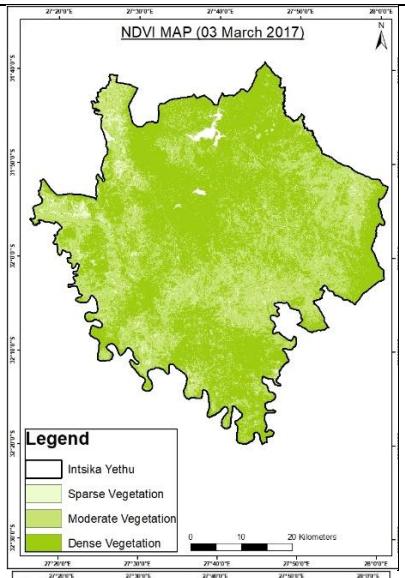

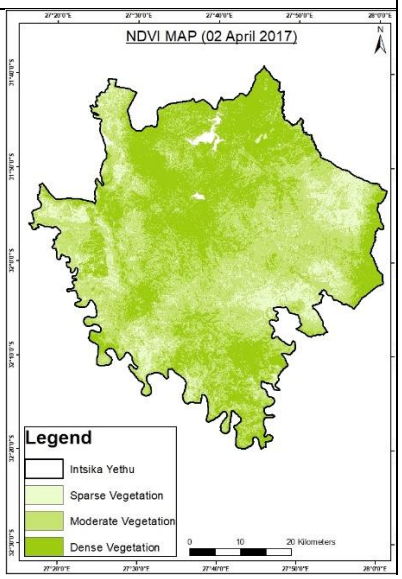

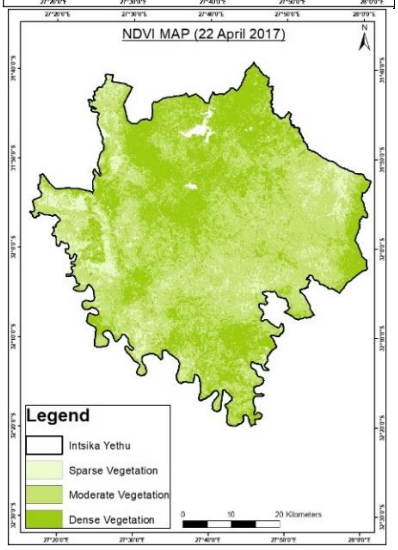

NDVI MAPS 2018

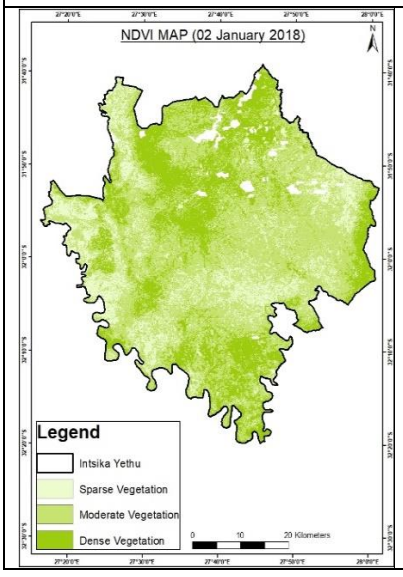

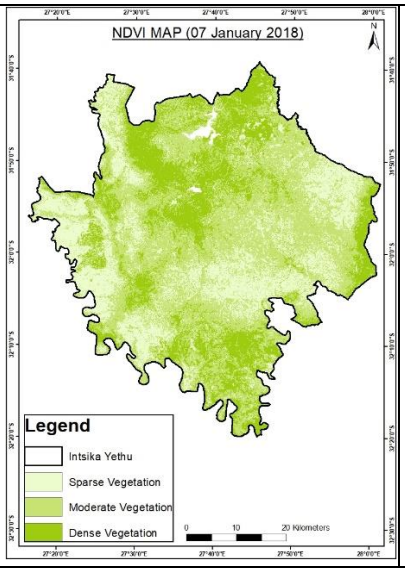

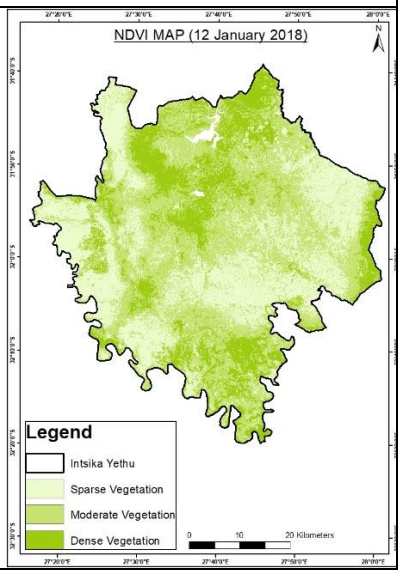

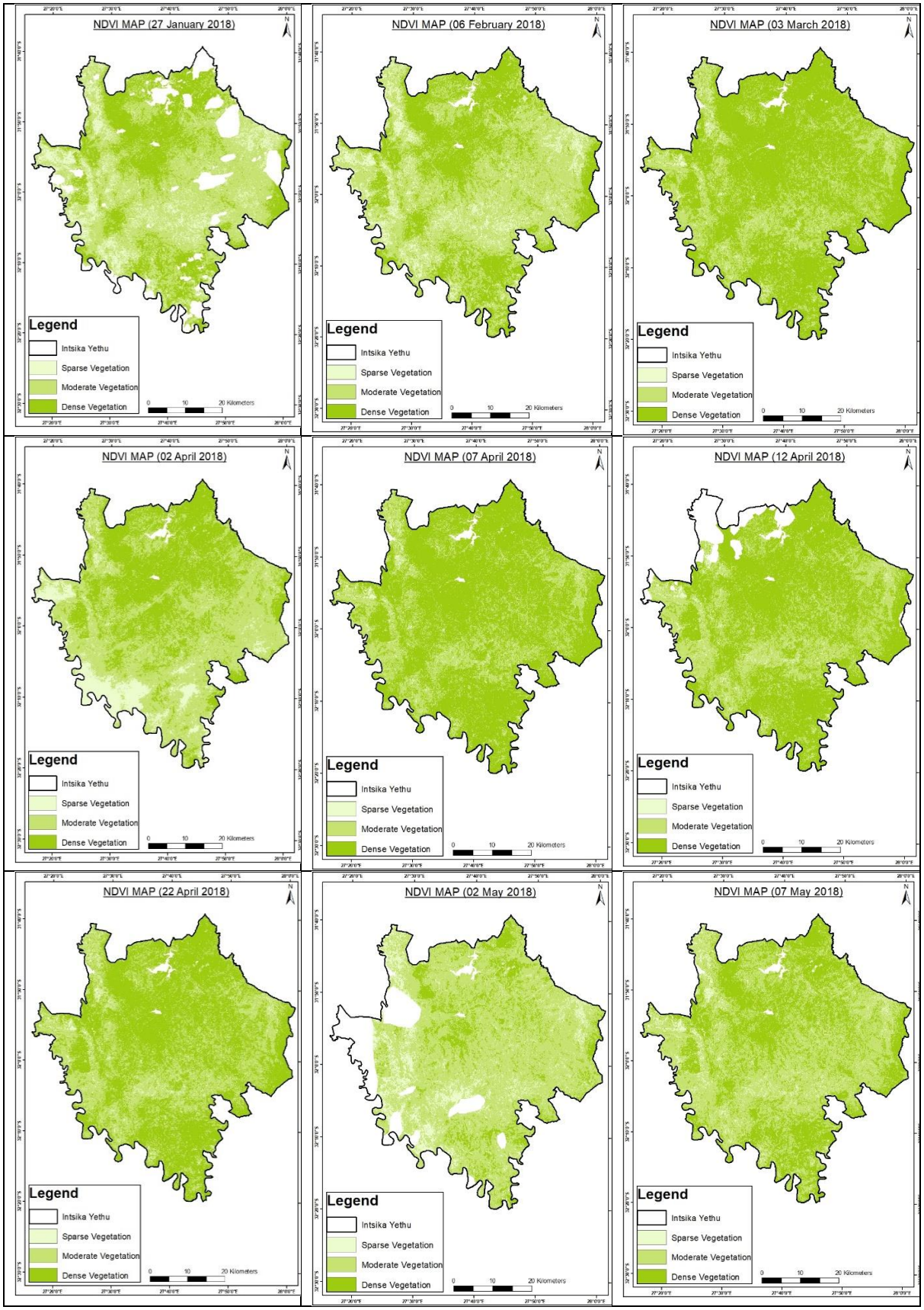
NDVI MAP (27 January 2018)
NDVI MAP (06 February 2018)
NDVI MAP (03 March 2018)
NDVI MAP (02 April 2018)
NDVI MAP (07 April 2018)
NDVI MAP (12 April 2018)
NDVI MAP (22 April 2018)
NDVI MAP (02 May 2018)
NDVI MAP (07 May 2018)
Legend
Intsika Yethu
Sparse Vegetation
Moderate Vegetation
Dense Vegetation
0 10 20 Kilometers

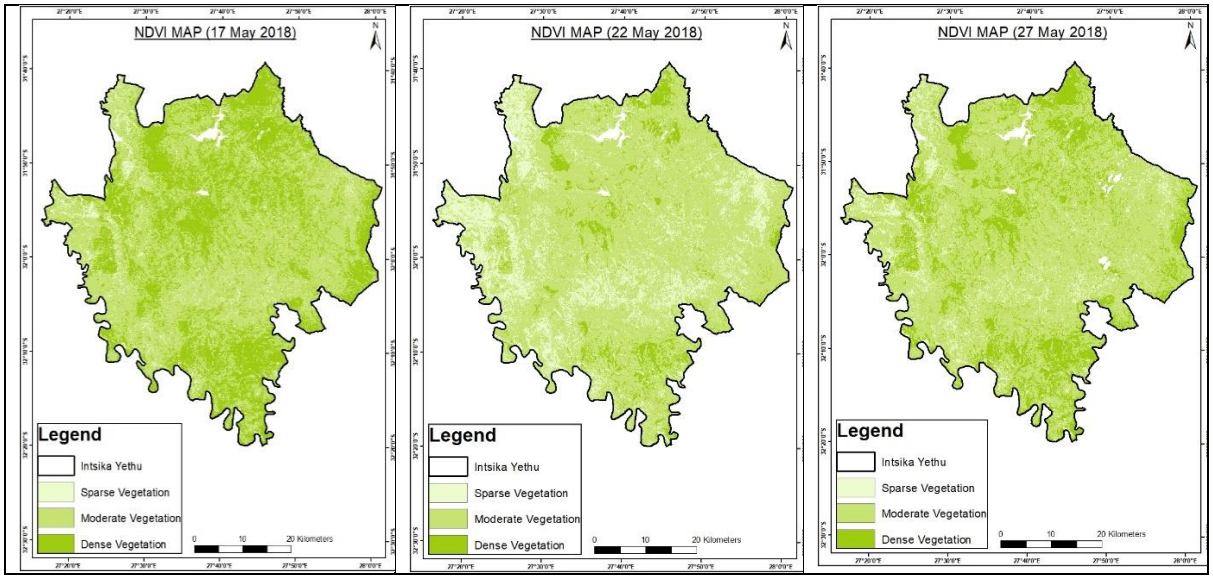

NDVI MAPS 2019

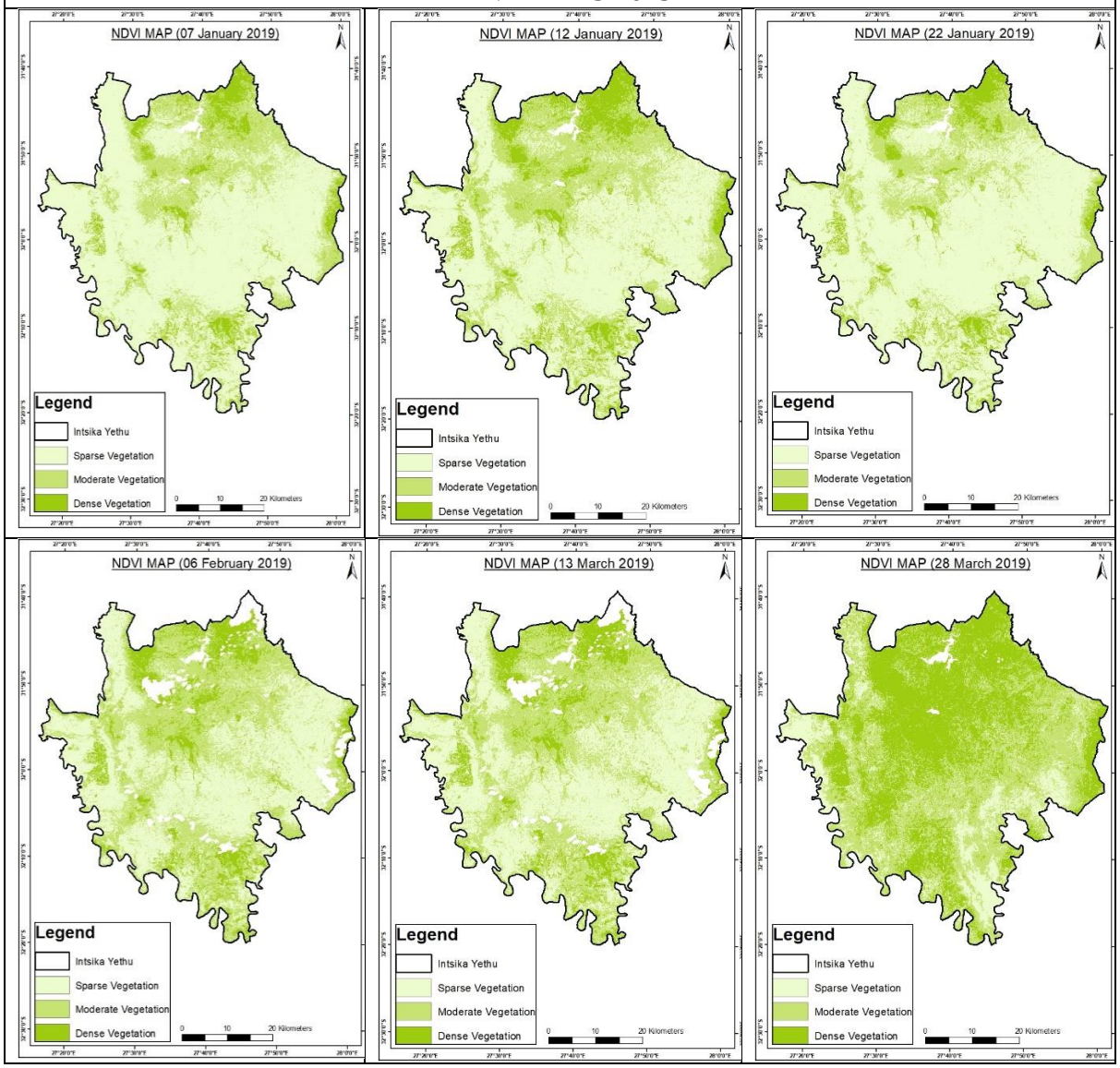

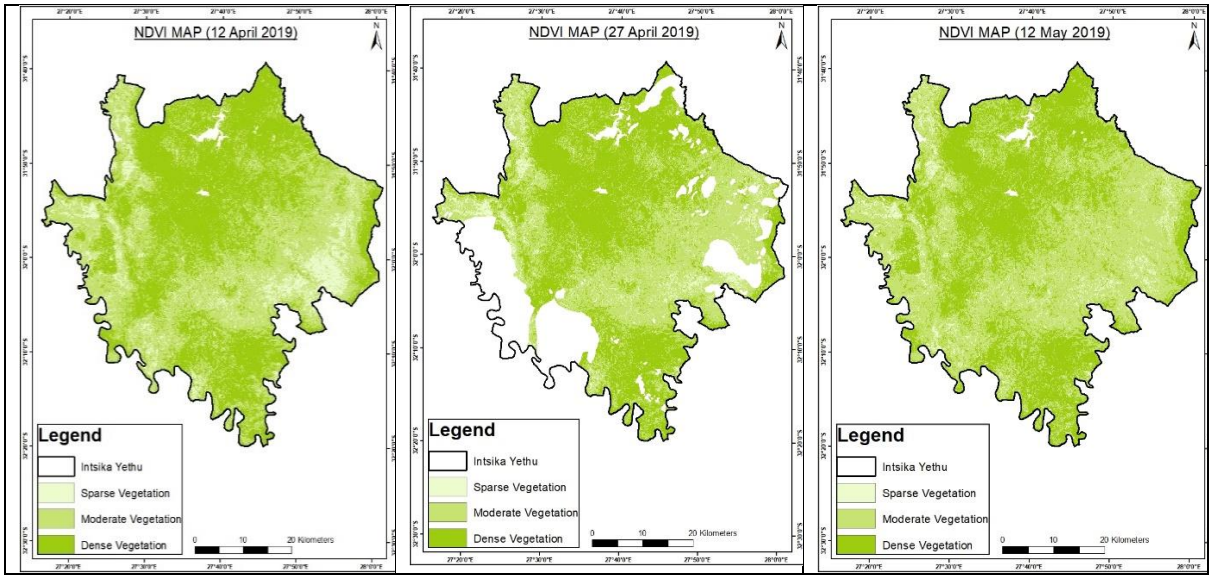

NDVI MAPS 2020

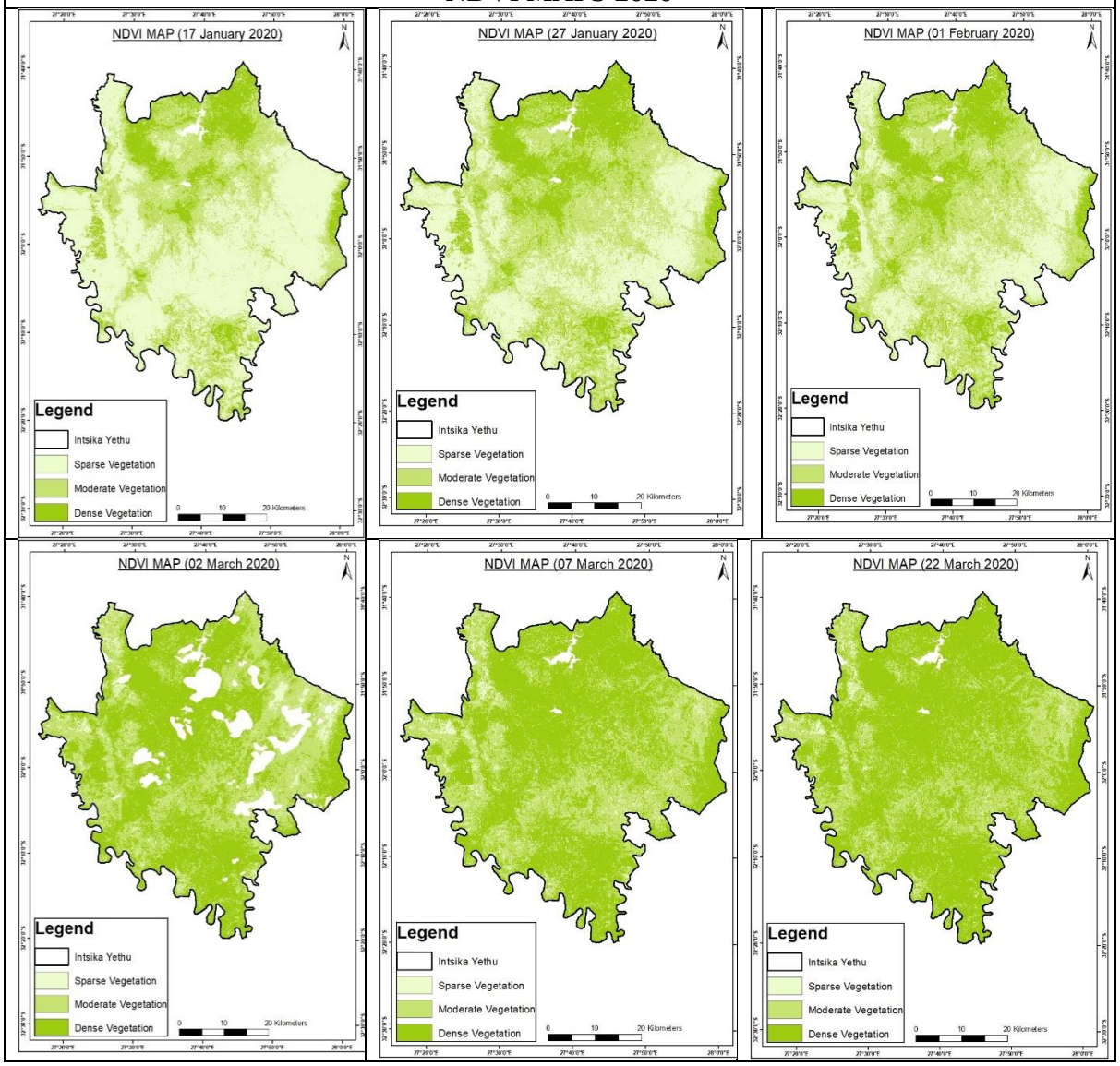

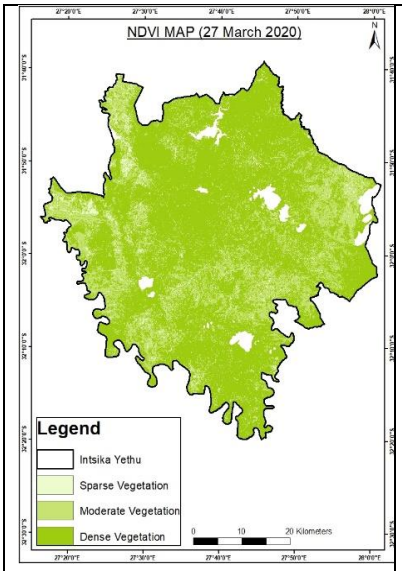

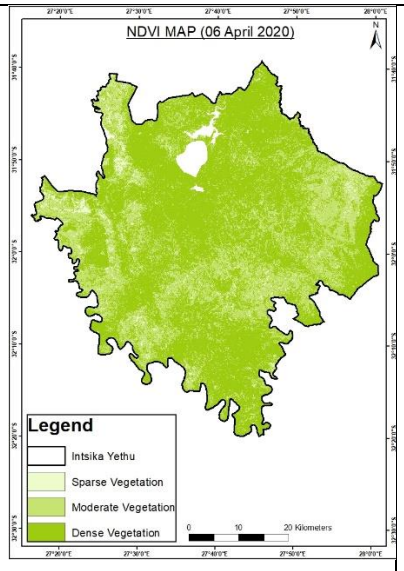

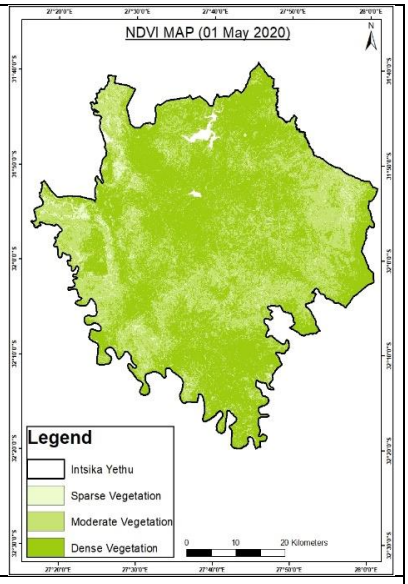

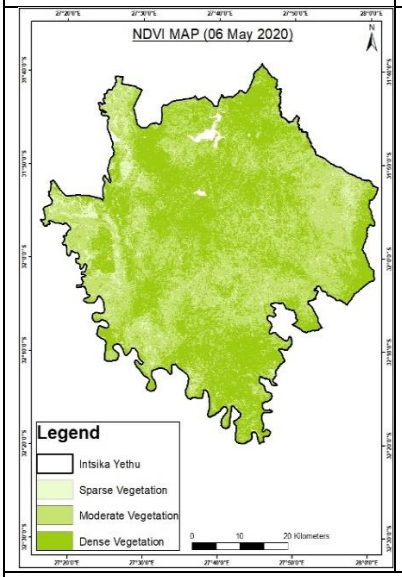

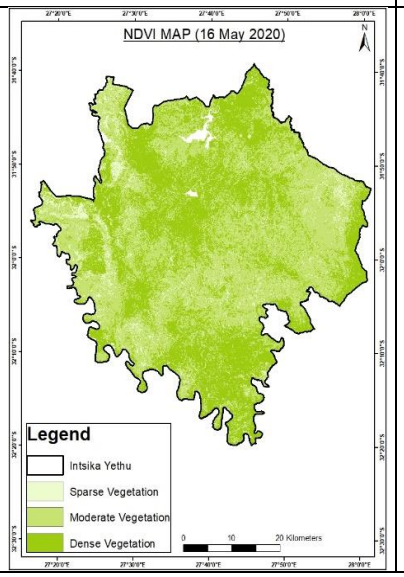

NDVI MAPS 2021

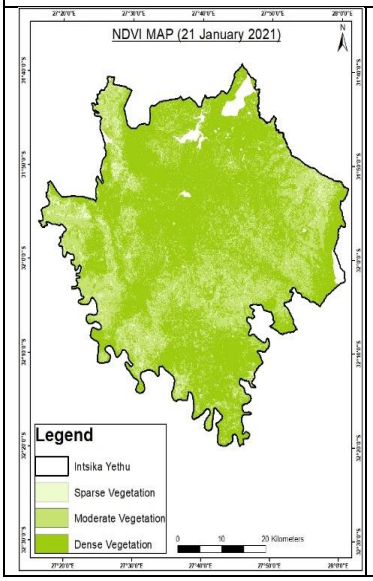

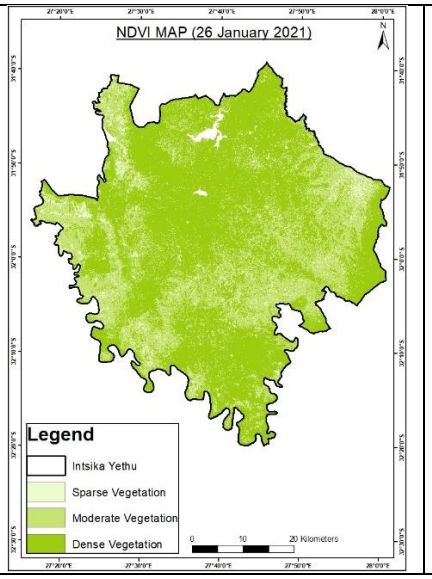

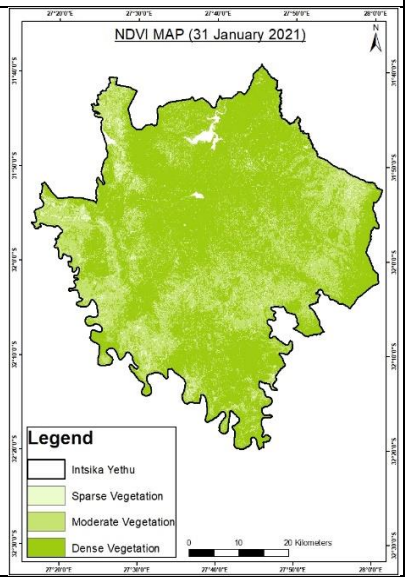

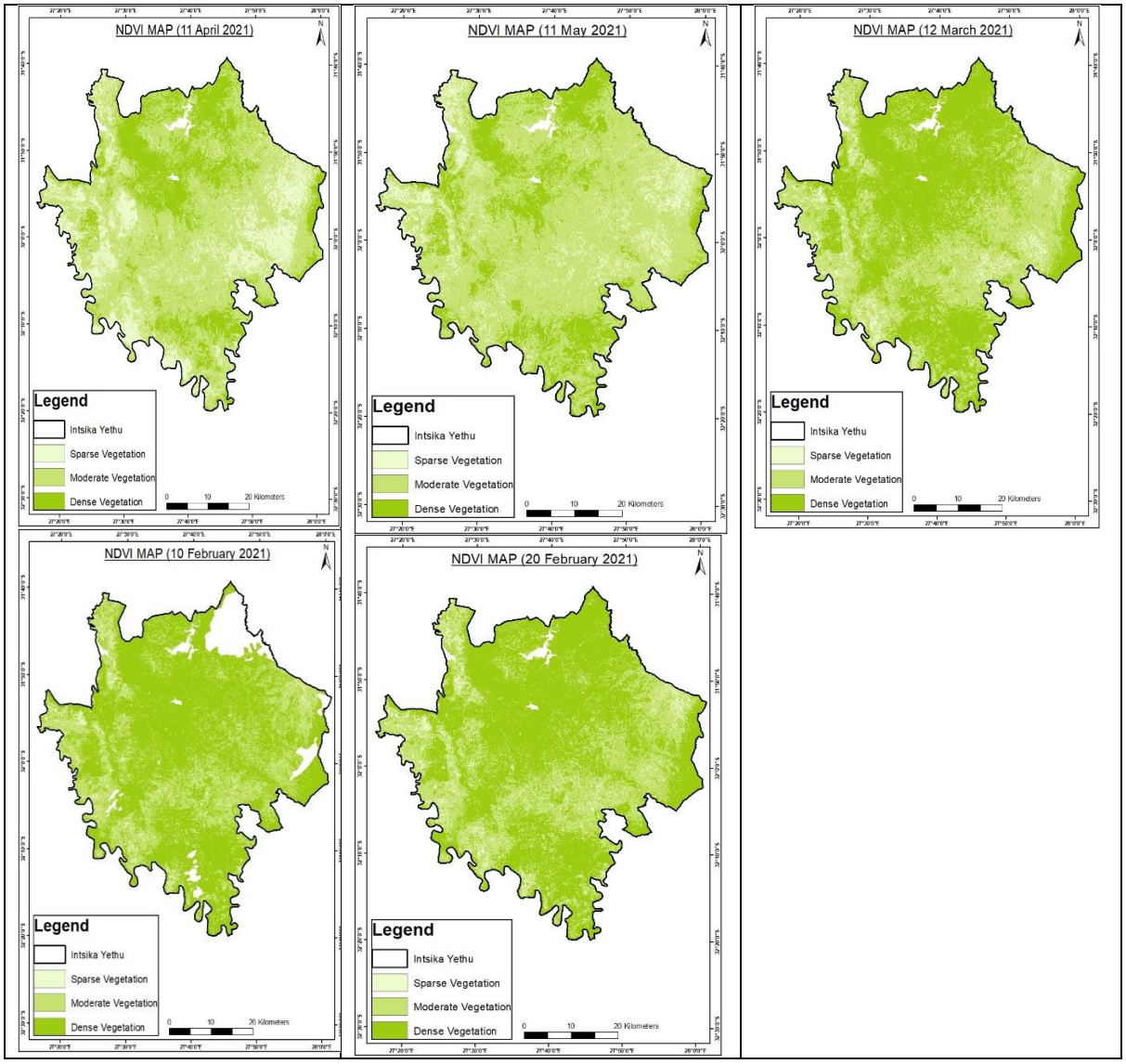

Figure 4.4: The NDVI Map of Intsika Yethu for January to May for the period of 2017 to 2021.

The average NDVI for each growing season is displayed in Figure 4.5. It reflects an average of 0.46 and 0.47 for 2017 and 2018, it dropped significantly in 2019 to 0.42 before it picked up again to 0.47 and 0.46 for 2020 and 2021, respectively. According to Gu et al., (2007) the NDVI and NDWI values lower or equal to 0.5 and 0.3 indicate drought while NDVI greater than 0.6 and NDWI greater than 0.4 indicate no drought. Therefore, the average seasonal NDVI values are less than 0.47 for the study period and this indicates drought. According to Shahzaman et al., (2021) a good way to spot agricultural drought is by looking at the NDVI distribution pattern. However, because the crops are impacted by various local elements in addition to climate factors, it is challenging to observe agricultural drought at a larger scale by focusing solely on NDVI readings.

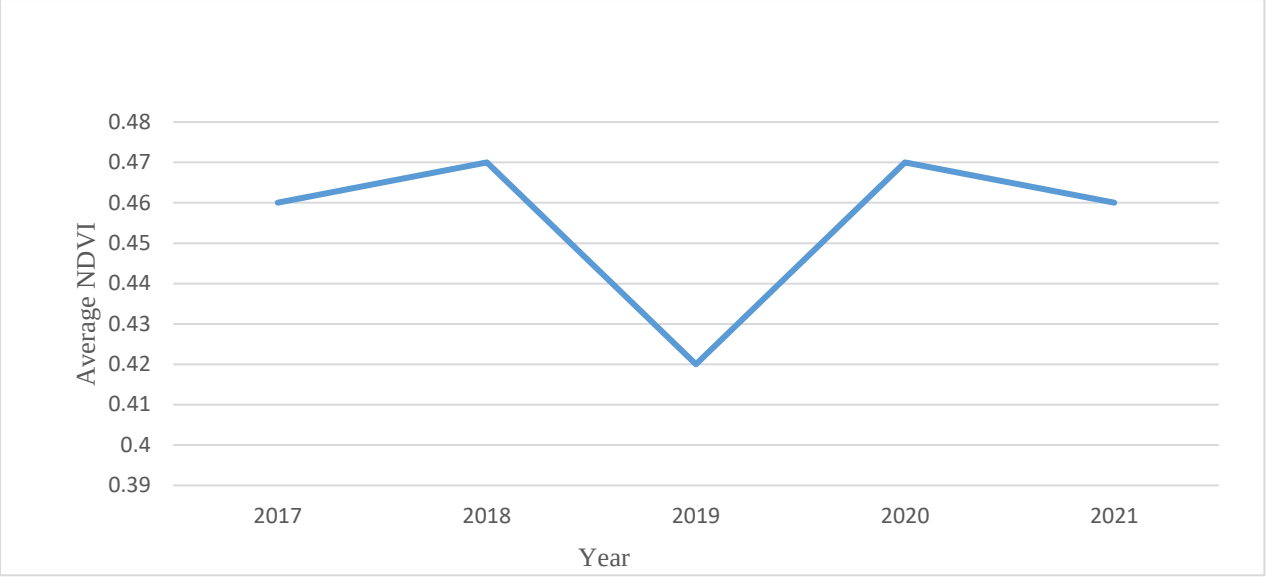

Figure 4.5: Mean annual NDVI values per growing season for 2017 to 2021

4.2.3. SPATIAL PATTERN OF NORMALIZE DIFFERENCE WATER INDEX

In this investigation, NDWI was utilized to examine how well the water content of the soil and plant surfaces reflected light (Shashikant et al., 2021). There are no set measurements for the NDWI unit as it varies from -1 to +1 based on the presence of surface water (JRC European Commission, 2011). A greater NDWI value signifies that the plant has a high water content. Low NDWI measurements imply low vegetation water content, hence during times of water stress, the NDWI rate declines (Zhang et al., 2017). The NDWI value rises as precipitation increases (Yaa'Cob et al., 2020). The spatio-temporal NDWI drought was mapped using the drought range of less than 0 in order to understand the drought pattern in the area.

February of year 2017 demonstrated drought in the bottom centre of the area, while generally the area was showing moderate drought except the southern, central and northern side of the region as shown in Figure 4.6. Sparsely moderate drought was observed in March in particular central to the northern eastern side. It intensified a bit in April especially in the east to north eastern portion of the region.

Moderate drought was observed in January 2018 and improved towards the end of January. However, February showed intense moderate drought except the north and some parts at the south part of the area. The situation improved in March going to early May before it got worse again in May.

For year 2019, the drought conditions can be observed at the centre to the south of the area in January and a small extent in February. Also moderate drought conditions can be observed in the study area except at the northern part of the area. February observed improved drought conditions compared to January while moderate drought improved slightly in the northern and southern part in March going to May.

The drought was observed in January 2020 going to February and improved in March to May. While in 2021 it showed slight moderate drought in the beginning of the year until April when moderate drought affected the study area.

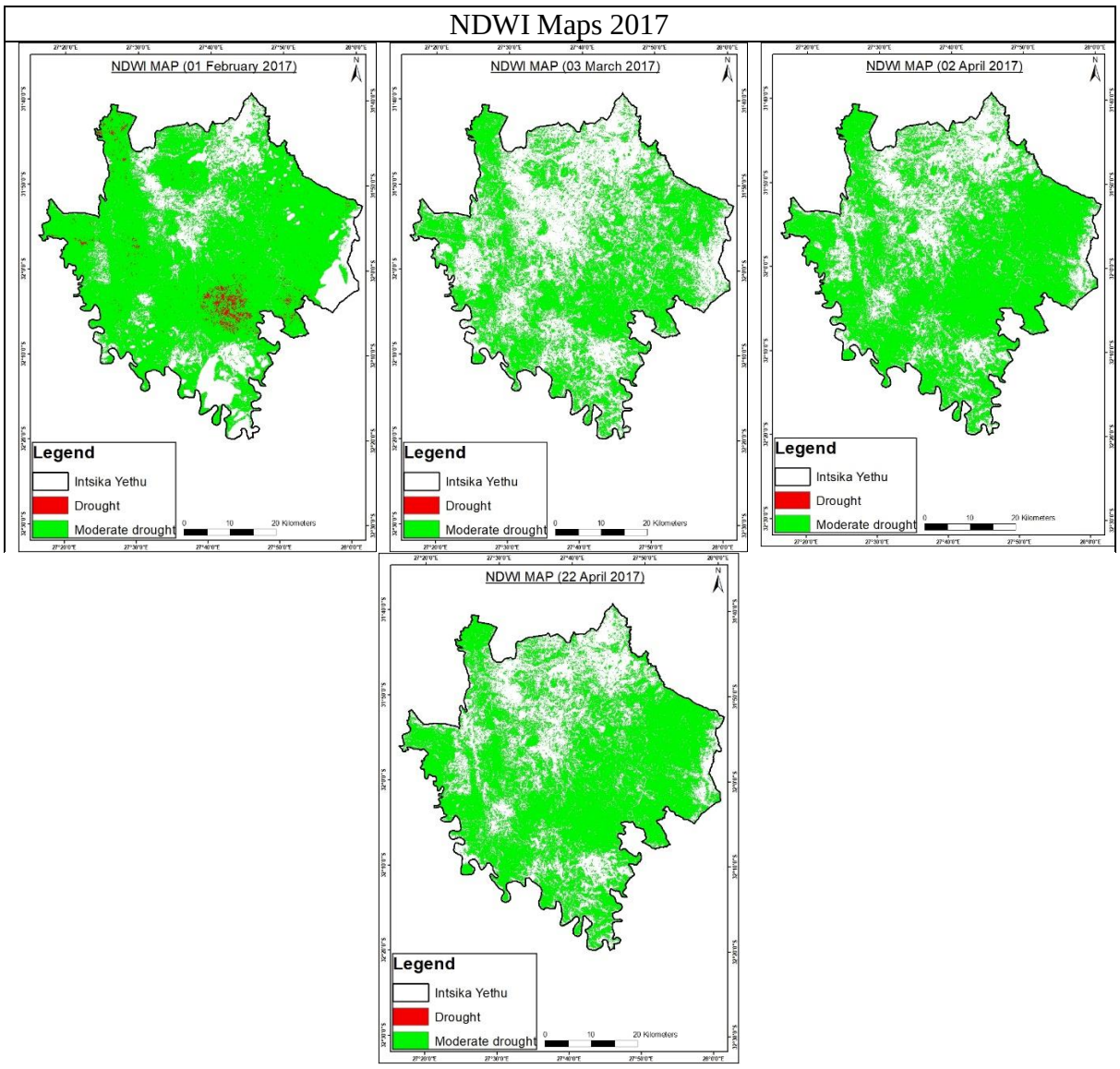

NDWI Maps 2018

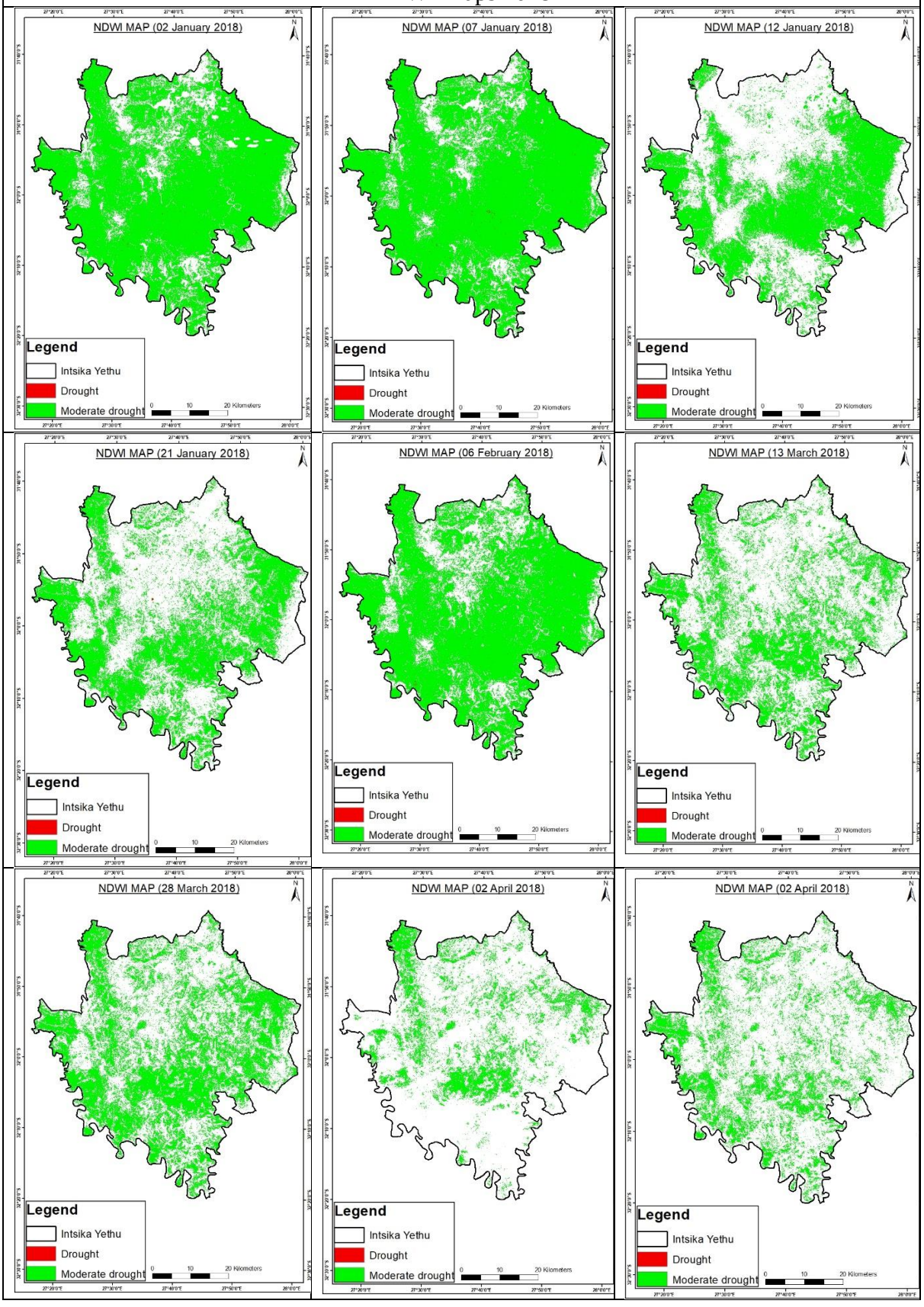

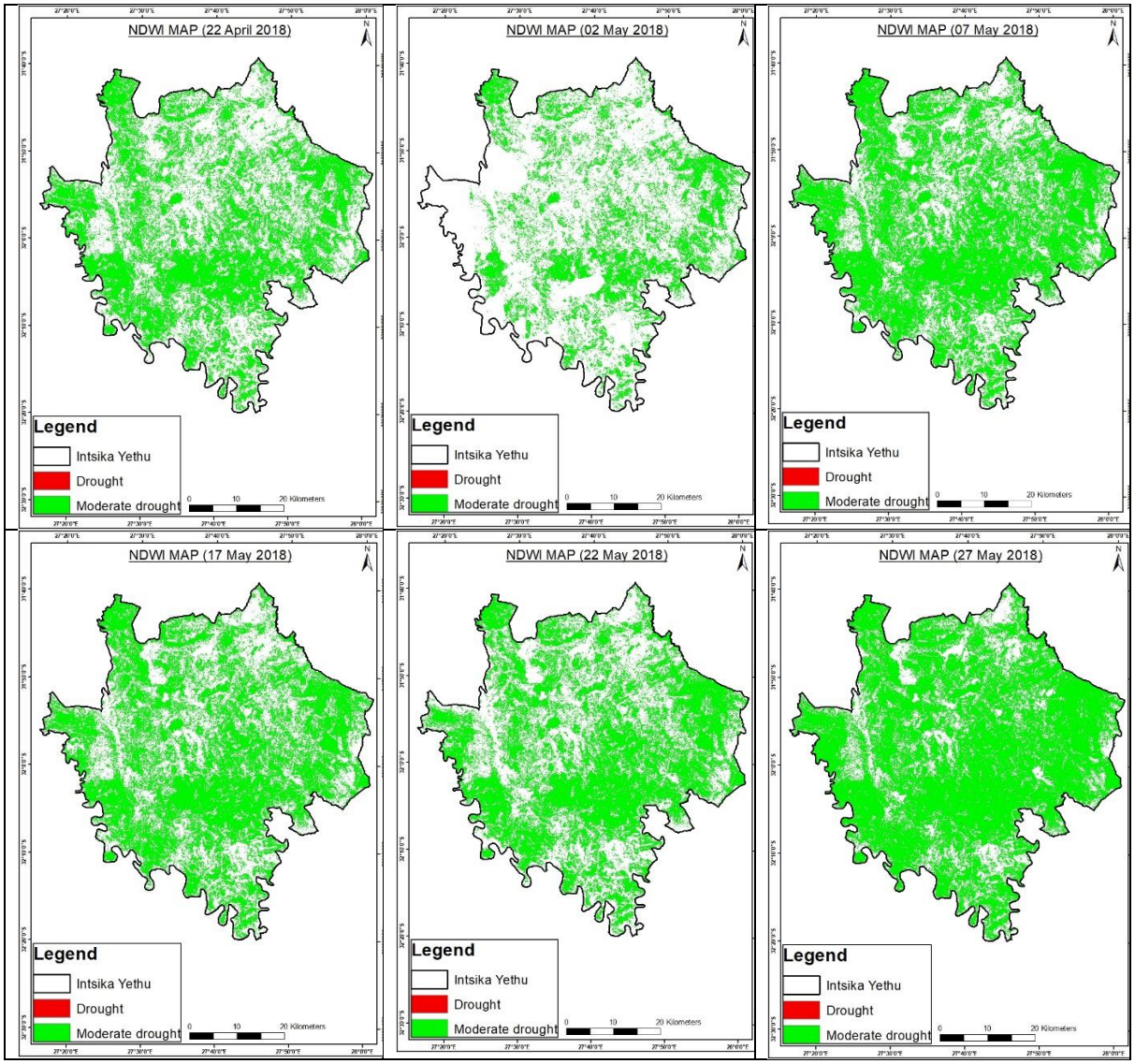

NDWI Maps 2019

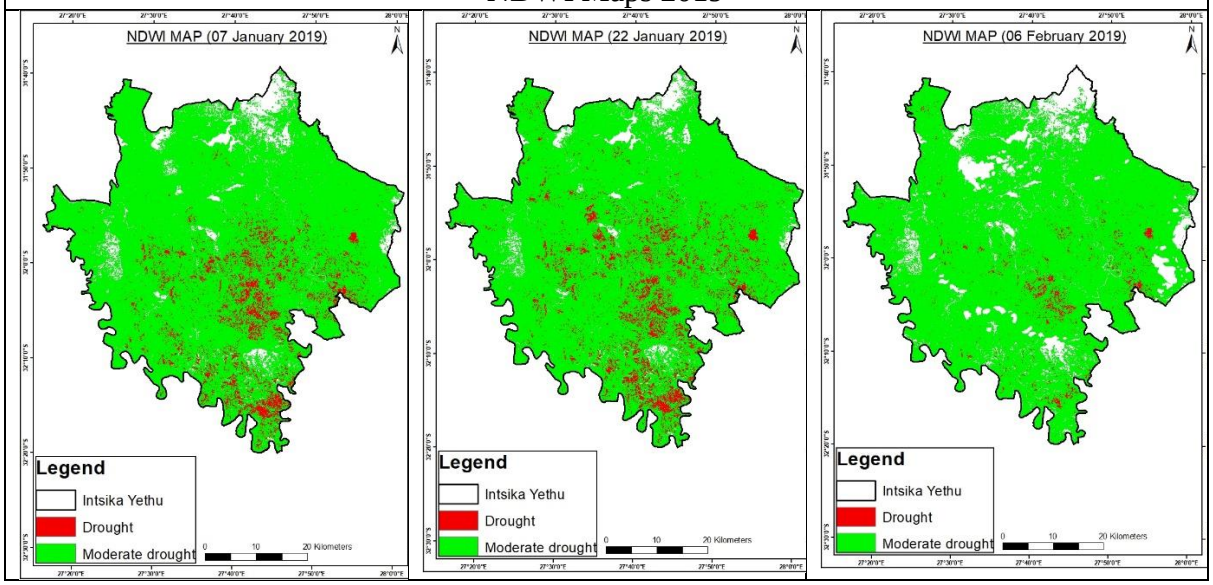

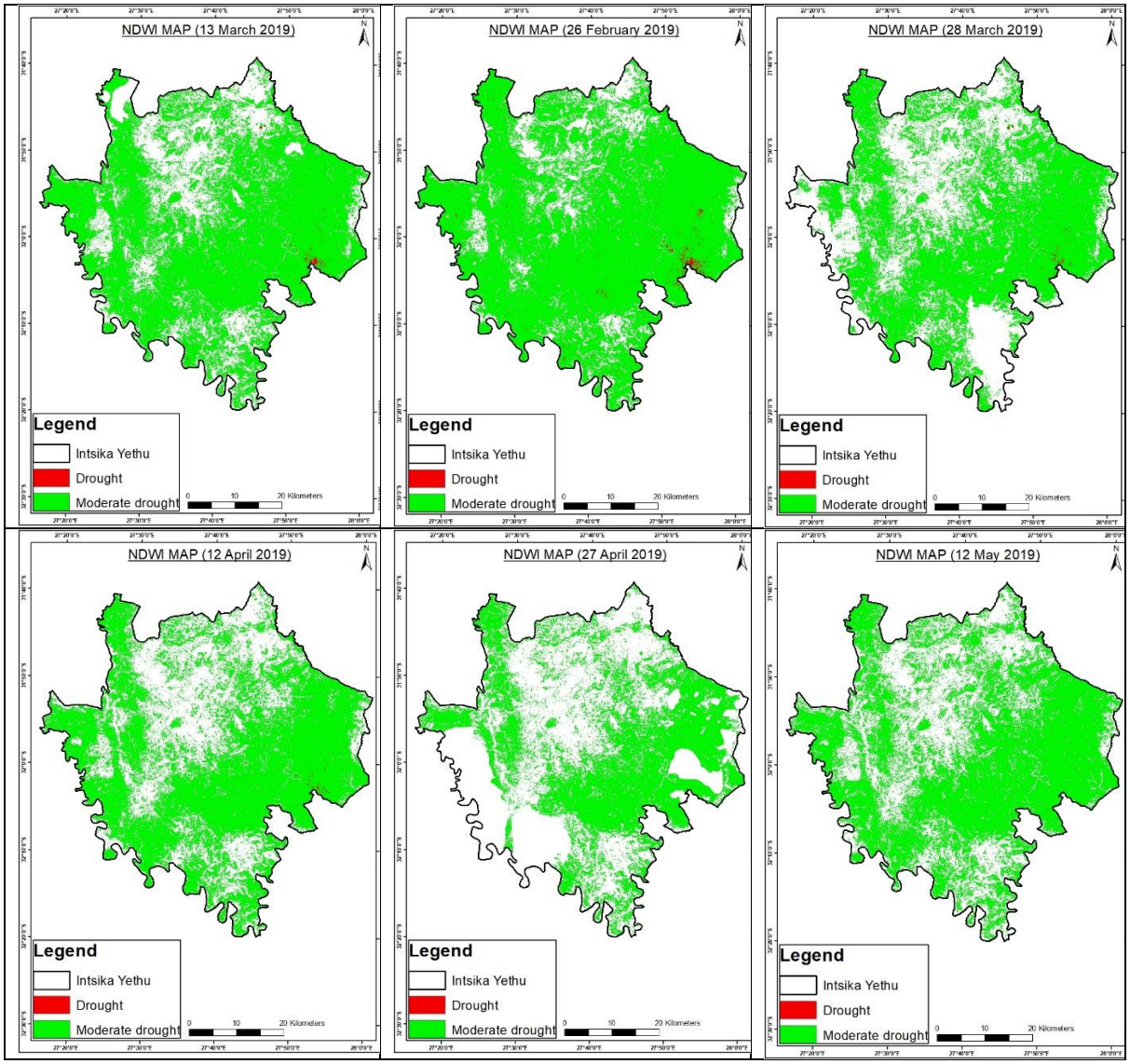

NDWI Maps 2020

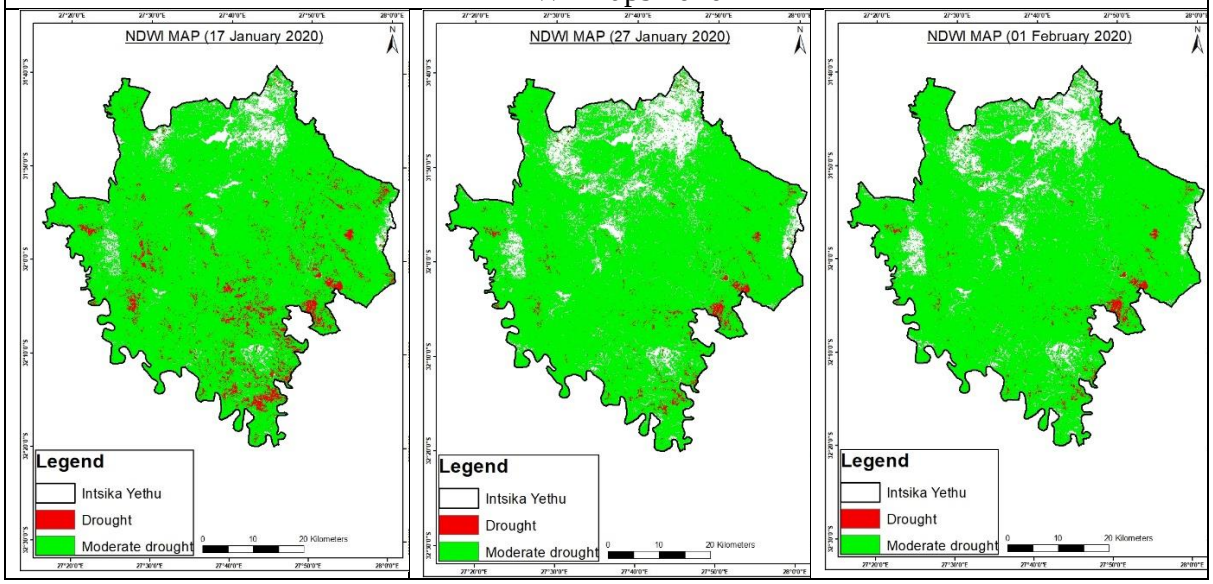

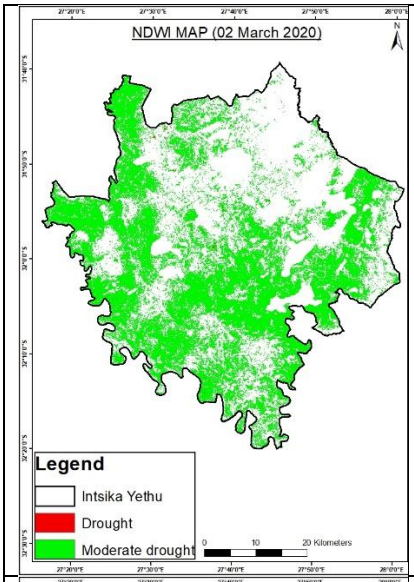
NDWI MAP (02 March 2020)
Legend
Intsika Yethu
Drought
Moderate drought
0 10 20 Kilometers

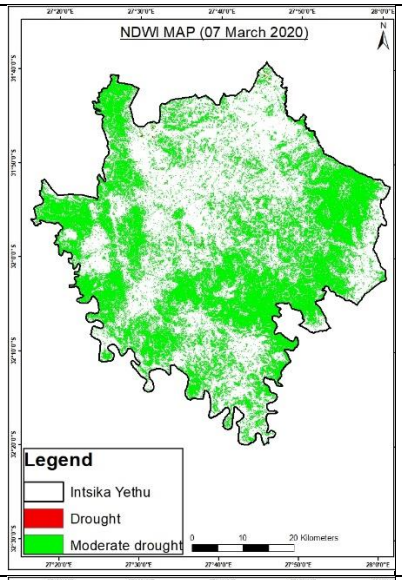
NDWI MAP (07 March 2020)
Legend
Intsika Yethu
Drought
Moderate drought
0 10 20 Kilometers

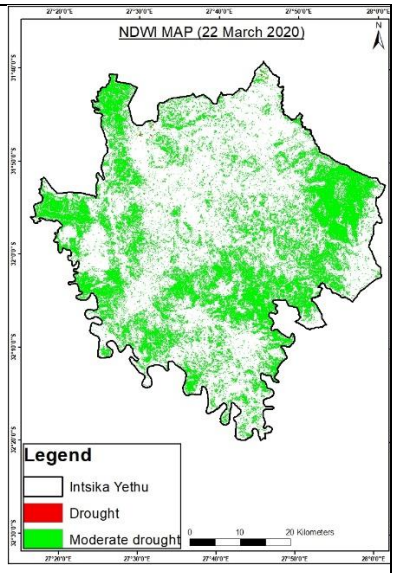
NDWI MAP (22 March 2020)
Legend
Intsika Yethu
Drought
Moderate drought
0 10 20 Kilometers

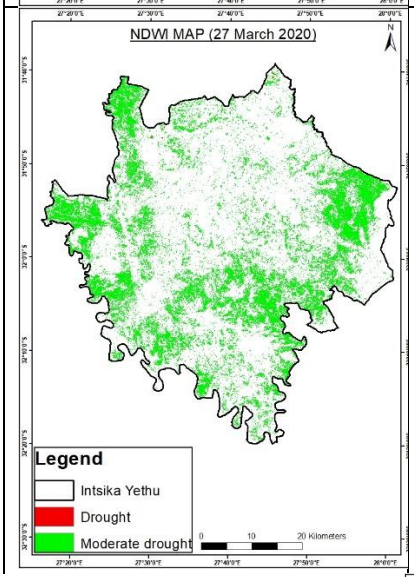
NDWI MAP (27 March 2020)
Legend
Intsika Yethu
Drought
Moderate drought
0 10 20 Kilometers

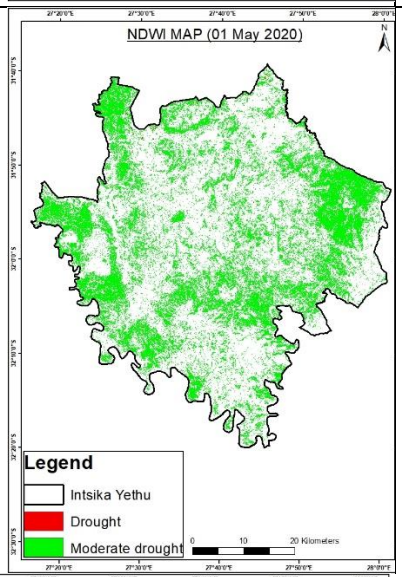
NDWI MAP (01 May 2020)
Legend
Intsika Yethu
Drought
Moderate drought
0 10 20 Kilometers

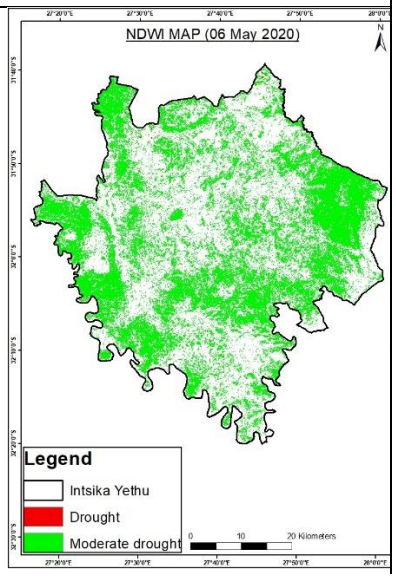
NDWI MAP (06 May 2020)
Legend
Intsika Yethu
Drought
Moderate drought
0 10 20 Kilometers

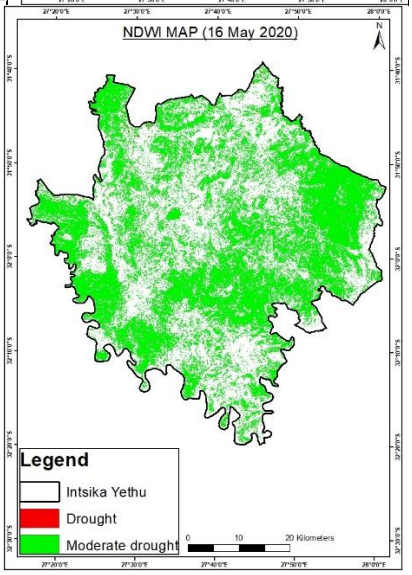
NDWI MAP (16 May 2020)
Legend
Intsika Yethu
Drought
Moderate drought
0 10 20 Kilometers

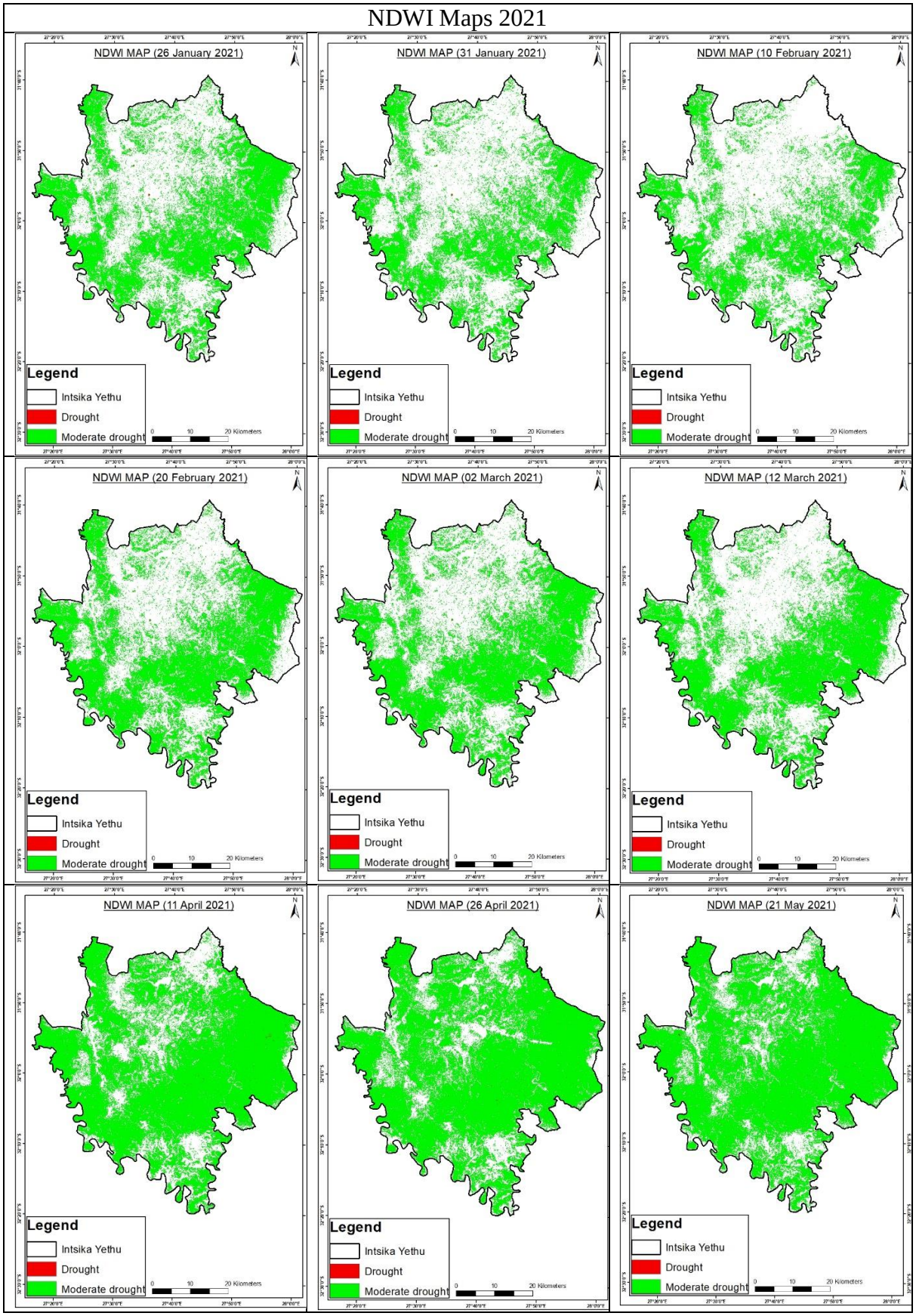

Figure 4.6: Difference in area coverage of NDWI during Months of January to May, 2017 to 2021

There is consistency in NDWI and NDVI results throughout the study period, for example, January 2019 results, demonstrated conditions that reflected moderate drought and drought observing from NDWI, while the NDVI showed low values in this period.

4.3. DATA FROM METEOROLOGICAL STATIONS

4.3.1. STANDARDIZED PRECIPITATION INDEX DERIVED FROM FOUR WEATHER STATIONS

SPI in Stutterheim showed that in 2017 there was mostly normal conditions for January and February as shown in Figure 4.7 a). The conditions improved slightly in March with SPI showing moderately wet conditions before it normalized in April. In May the SPI showed very dry conditions. In 2018 Conditions were moderately dry in January, normal in February. April was very wet. In 2020, there were moderately wet conditions with May 2020 becoming very wet. While 2021 started very dry in January and improved to moderately wet in March to May. Queenstown gauge station had an SPI that showed very dry conditions in January 2017 and improved slightly to dry conditions in February with May being moderately wet as shown in figure 4.7 b). While the other years were mostly normal.

Mthatha gauge was showing mostly normal conditions in 2017 except for March that was moderately dry as shown in Figure 4.7 c). February 2018, was very dry with March and May moderately wet. April 2019 and February 2021 were very wet.

The Elliot gauge showed very wet conditions in April 2017 and February 2019 and become normal in 2020 and 2021 although February and April of 2020 were very dry as shown in figure 4.7 d).

SPI as one of the drought indices, which are based on in-situ meteorological information from stations for weather, can be used to monitor drought effectively (Rhee et al., 2010).

a)

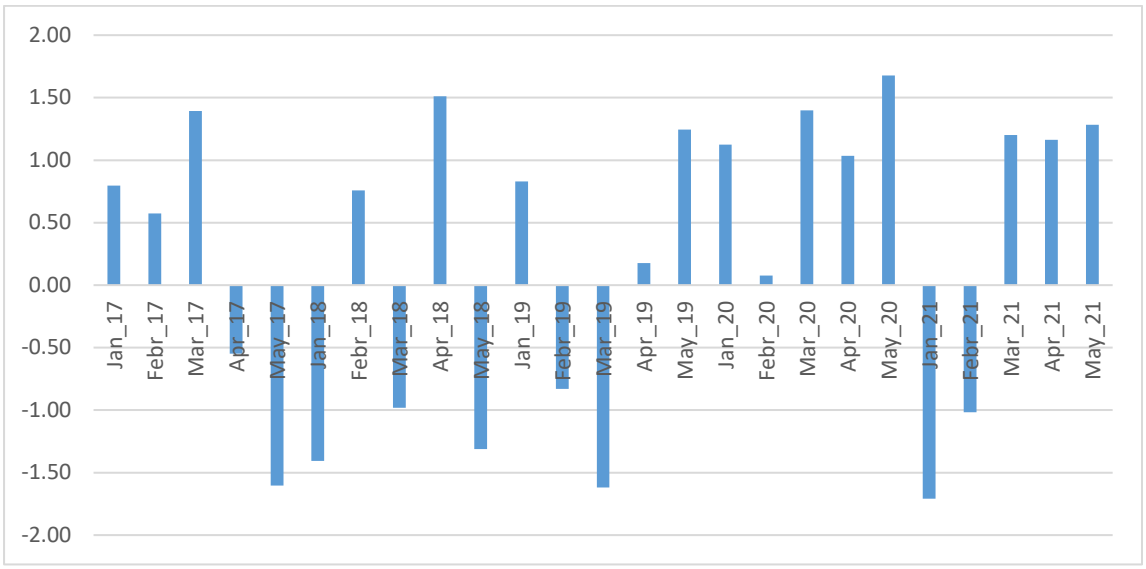
2.00
1.50
1.00
0.50
0.00
-0.50
-1.00
-1.50
-2.00
Jan_17
Febr_17
Mar_17
Apr_17
May_17
Jan_18
Febr_18
Mar_18
Apr_18
May_18
Jan_19
Febr_19
Mar_19
Apr_19
May_19
Jan_20
Febr_20
Mar_20
Apr_20
May_20
Jan_21
Febr_21
Mar_21
Apr_21
May_21

b)

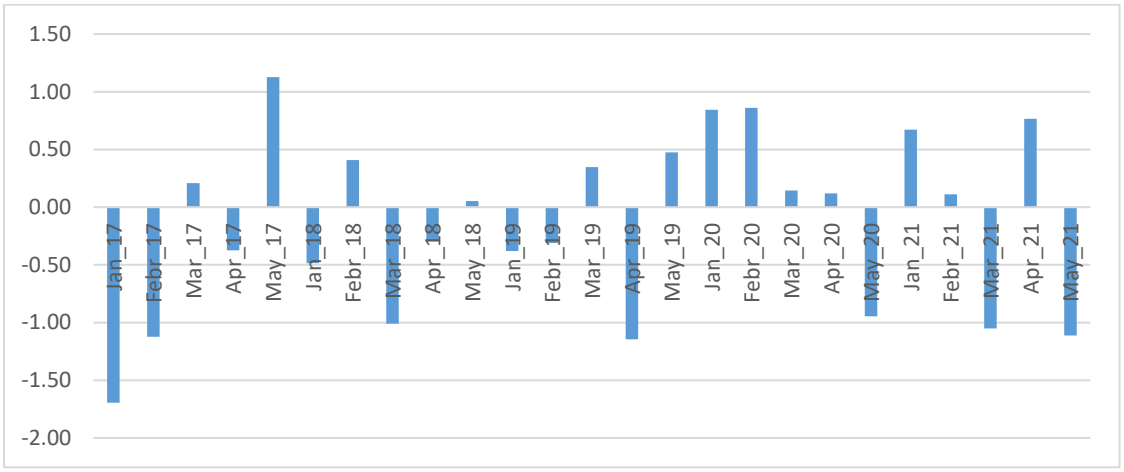
1.50
1.00
0.50
0.00
-0.50
-1.00
-1.50
-2.00
Jan_17
Febr_17
Mar_17
Apr_17
May_17
Jan_18
Febr_18
Mar_18
Apr_18
May_18
Jan_19
Febr_19
Mar_19
Apr_19
May_19
Jan_20
Febr_20
Mar_20
Apr_20
May_20
Jan_21
Febr_21
Mar_21
Apr_21
May_21

c)

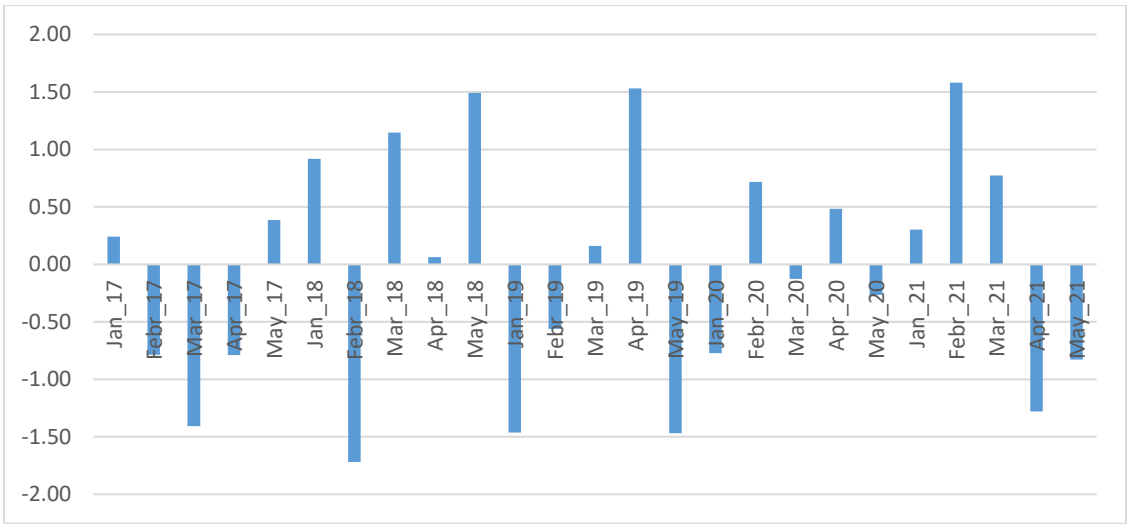
2.00
1.50
1.00
0.50
0.00
-0.50
-1.00
-1.50
-2.00
Jan_17
Febr_17
Mar_17
Apr_17
May_17
Jan_18
Febr_18
Mar_18
Apr_18
May_18
Jan_19
Febr_19
Mar_19
Apr_19
May_19
Jan_20
Febr_20
Mar_20
Apr_20
May_20
Jan_21
Febr_21
Mar_21
Apr_21
May_21

d)

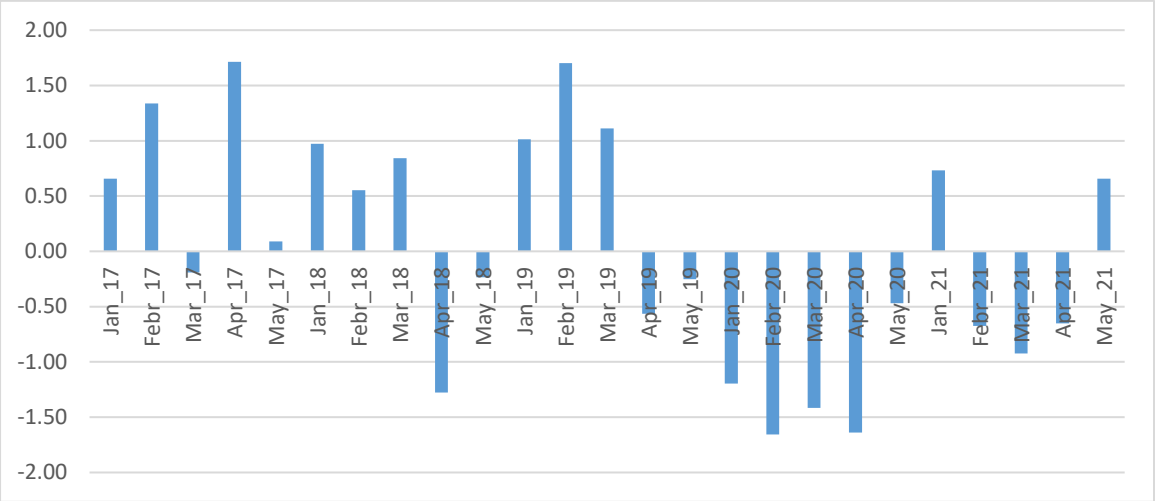

Figure 4.7: a) Interpolated Rainfall data from the Stutterheim weather station for months of January to May, 2017 to 2021. b) Interpolated Rainfall data from the Queenstown weather station for months of January to May, 2017 to 2021. c) Interpolated Rainfall data from the Mthatha weather station for months of January to May, 2017 to 2021. d) Interpolated Rainfall data from the Elliot weather station for months of January to May, 2017 to 2021.

Since unequal distribution of rainfall, wet times are unpredictable and variable, which has a significant impact especially on communal and small-scale farmers (Jordaan et al., 2019).

4.3.2. MANN-KENDALL TREND OF METERIOLOGICAL VARIABLES

The analysis of the spatial variation trends were conducted on the SPI, precipitation and average annual maximum and minimum temperature in the weather stations using ArcGIS 10.8.2. A decreasing trend in SPI was observed in Elliot while there is an increasing trend of 0.2 mm in Queenstown over the study period was experienced as shown in Figure 4.8 a. The decreasing SPI indicated drought risks at the station. Mthatha observed a decreasing trend in average annual maximum temperature by 0.4°C while Queenstown had experienced an increasing trend of 0.2°C in the study period as shown in Figure 4.8 b. The average minimum temperature was decreasing in Mthatha by 0.6°C as shown in Figure 4.8 c.

a)

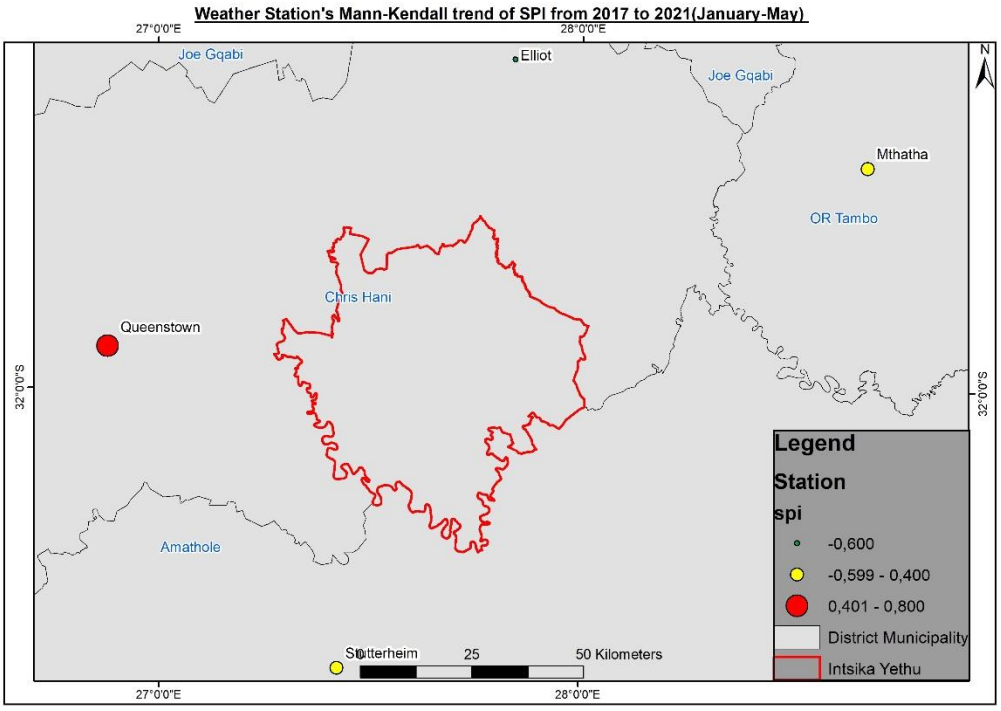
Weather Station's Mann-Kendall trend of SPI from 2017 to 2021(January-May)
27°0'0"E
28°0'0"E
Joe Gqabi
Elliot
Joe Gqabi
Mthatha
OR Tambo
Chris Hani
Queenstown
32°0'0"S
Amathole
Sutterheim
25
50 Kilometers
N
Legend
Station
spi
-0,600
-0,599 - 0,400
0,401 - 0,800
District Municipality
Intsika Yethu

b)

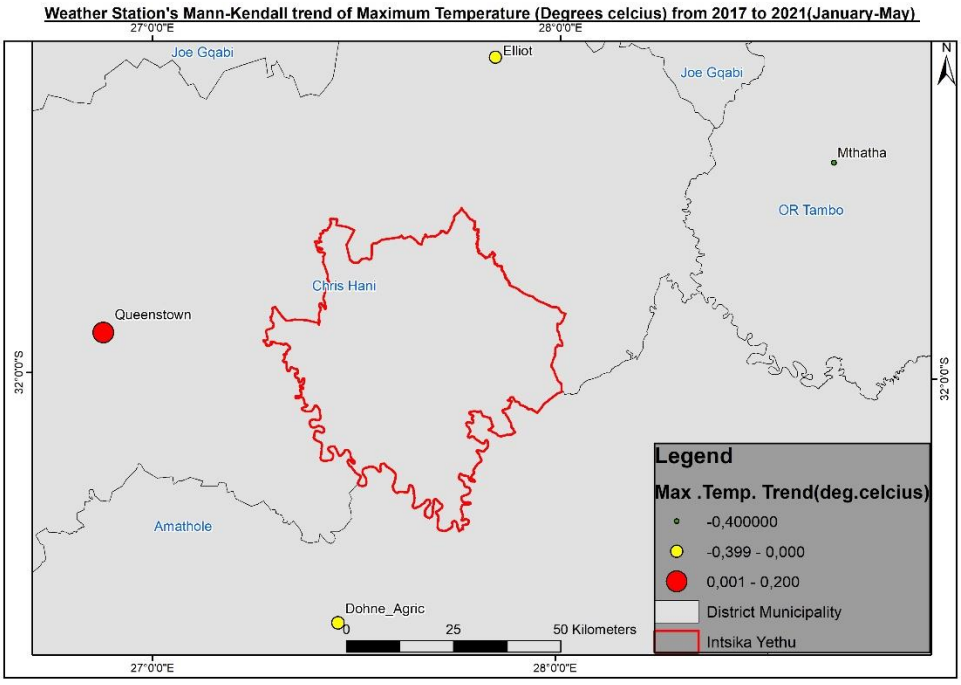
Weather Station's Mann-Kendall trend of Maximum Temperature (Degrees celcius) from 2017 to 2021(January-May)
27°0'0"E
28°0'0"E
Joe Gqabi
Elliot
Joe Gqabi
Mthatha
OR Tambo
Chris Hani
Queenstown
32°0'0"S
Amathole
Dohne_Agric
0
25
50 Kilometers
N
Legend
Max .Temp. Trend(deg.celcius)
-0,400000
-0,399 - 0,000
0,001 - 0,200
District Municipality
Intsika Yethu

c)

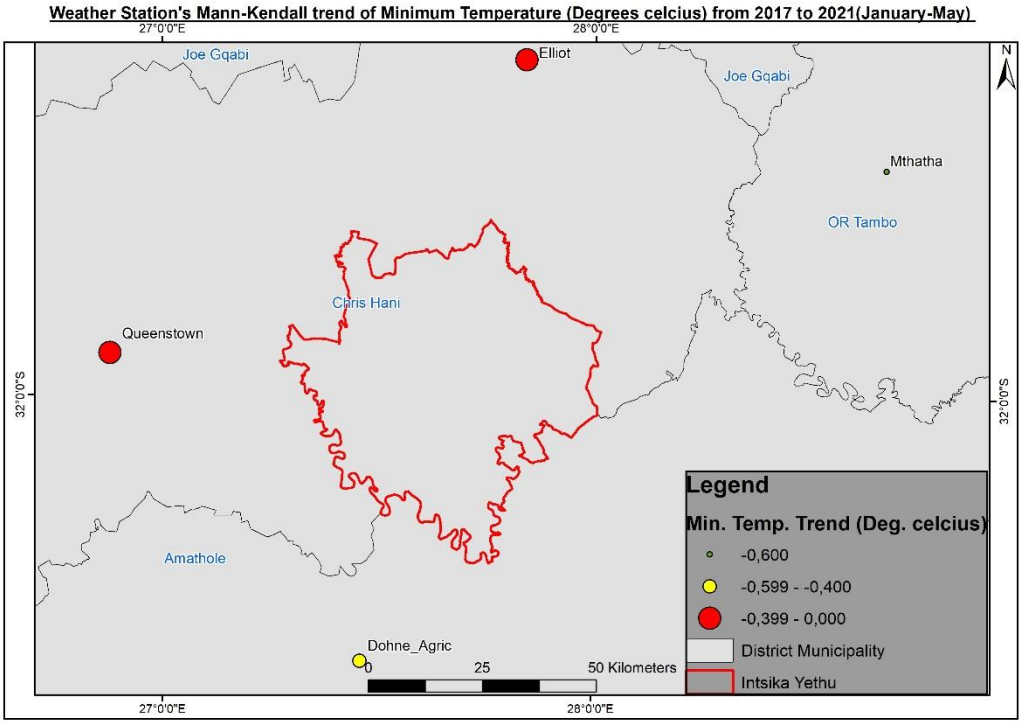

Figure 4.8: a) Shows the Mann-Kendall trend of SPI from different weather stations. b) Shows the Mann-Kendall trend of maximum temperature from different weather stations. c) Shows the Mann-Kendall trend of minimum temperature from different weather stations.

4.4. GPM SATELLITE PRECIPITATION DATA

4.4.1. SPATIO-TEMPORAL VARIABILITY OF GPM SATELLITE PRECIPITATION DATA

The time series of the daily accumulated precipitation estimate at 0.1 degrees for January to May of 2017 to 2021 is displayed in Figure 4.9. Year 2017 to 2020 showed a similar pattern in January where the precipitation started very low and peaked in February and started dropping for the rest of the months while 2021 peaked in January and started dropping. It can be observed that 2019 showed the least precipitation experienced in the study area with 2021 being the highest. The same trend was observed in February with 2018 experiencing slightly more precipitation than the other years followed by 2017 while 2021 being the lowest. In March, 2018 experienced the highest precipitation with 2021 being the lowest.

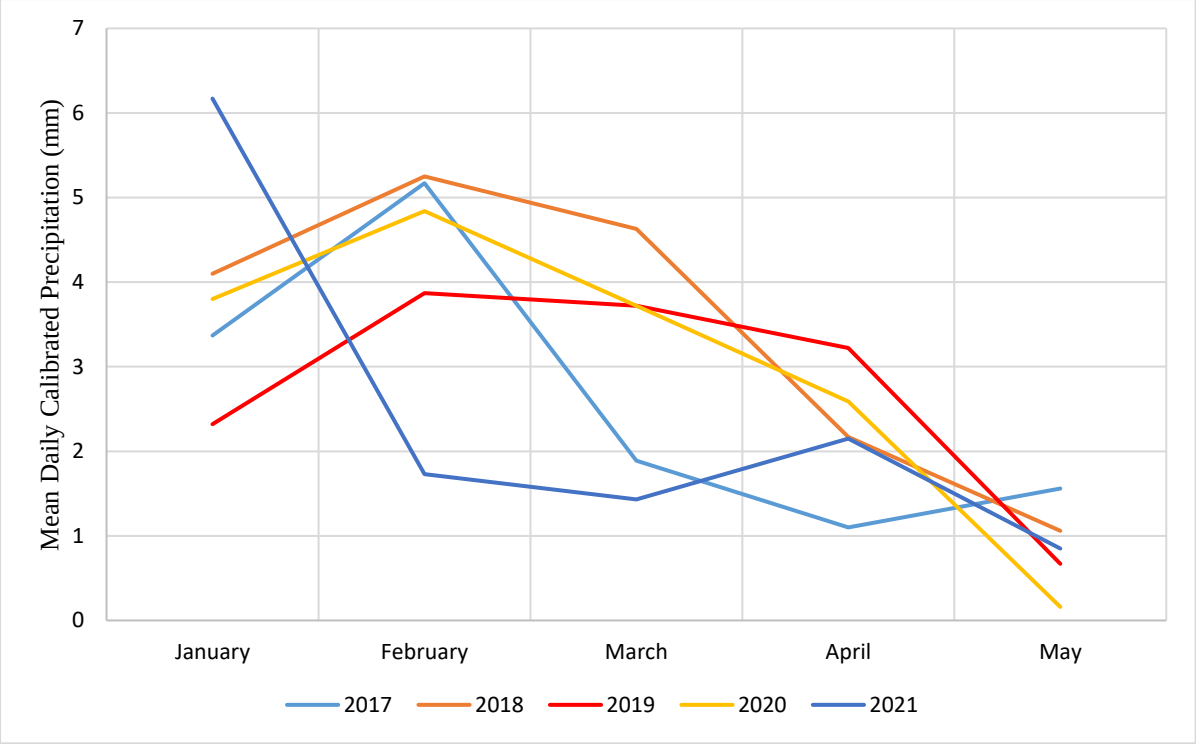

Figure 4.9: Time series of the daily accumulated precipitation estimate for January to May of 2017 to 2021

Figure 4.10 displays the averaged map of daily accumulated precipitation estimate for January to May of 2017 to 2021. The map of 2017 as shown in Figure 4.10 a) demonstrates that the North Eastern part of the area experienced more accumulated precipitation estimate of up to 4 days together central and western side of the study area. The same pattern was observed in 2018 as shown in Figure 4.10 b).

North eastern side displayed better daily accumulated precipitation in 2019 contrasted with the rest of the area as shown in Figure 4.10 c). The northern side showed the worst daily accumulated precipitation in 2020 of closer to 2 days contrasted with the rest of the area as shown in Figure 4.10 d). South eastern regions experienced a better precipitation than all the other regions in 2021 as shown in Figure 4.10 e). It can be observed that 2019 showed a very low daily accumulated precipitation overall compared to other years. The Eastern Cape's precipitation regime exhibits significant variability on a range of time scales, including inter-annual, decadal, multi decadal and intra-seasonal (Kane, 2009).

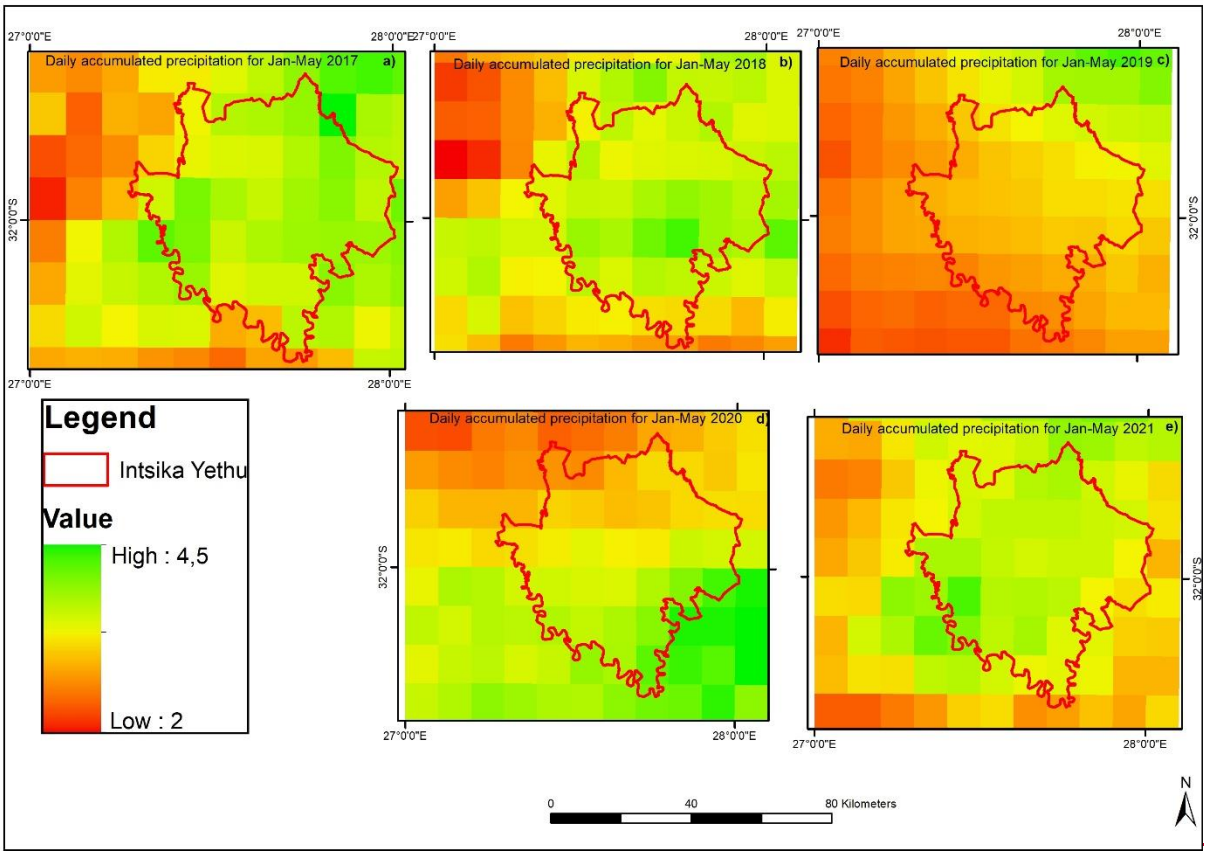

Figure 4.10: Maps illustrating the average daily accumulated precipitation from January to May for the different years a) 2017, b) 2018, c) 2019, d) 2020, e) 2021.

4.4.2. PRECIPITATION CONDITION INDEX (PCI)

The PCI for the study period shows a general declining precipitation as shown in Figure 4.11 below. The average PCI per growing season shows a low precipitation in 2017, 2019 and 2021 of 0.39, 0.42 and 0.38, respectively, while high values were observed in 2018 and 2020 at 0.53 and 0.46, respectively.

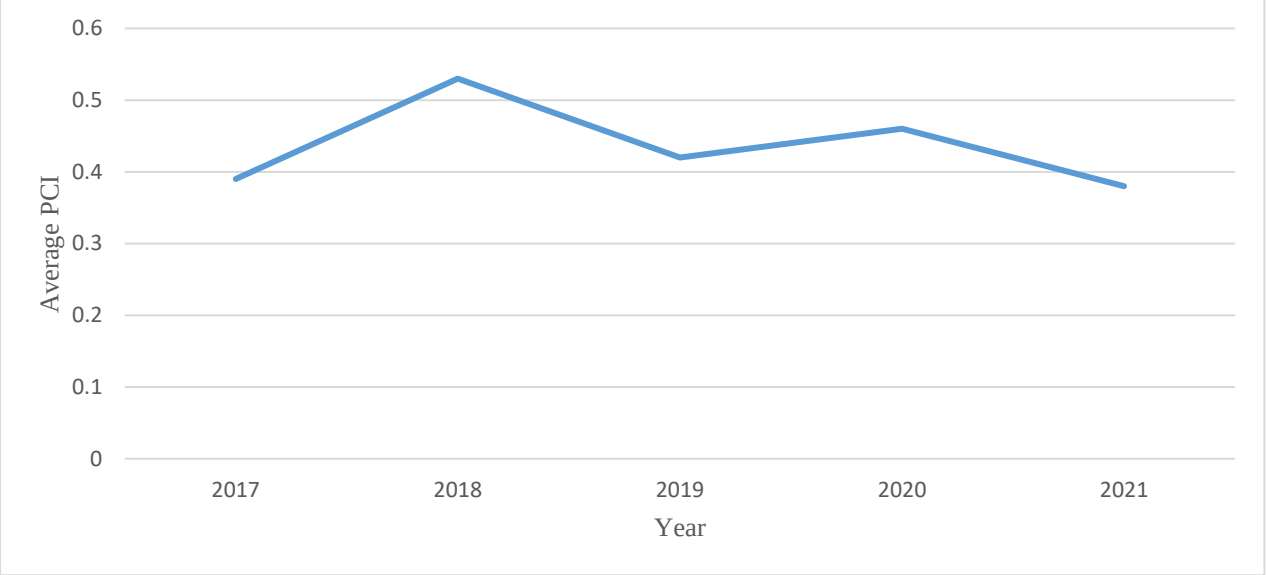

Figure 4.11: Annual Average PCI for Intsika Yethu for 2017-2021

4.5. AVERAGE SEASONAL AMSR-2 SOIL MOISTURE PATTERN

4.5.1. SPATIO_TEMPORAL VARIABILITY OF AMSR-2 SOIL MOISTURE

Figure 4.12 displays time series, area averaged of volumetric soil moisture at 10 km % over 2017 to 2021, January to May.

The maximum soil moisture percentage was experienced in February and in May at just below 25% in 2017. Year 2018 observed the highest soil moisture in March and April at just below 25%. While year 2019 observed a soil moisture of 10% and 15% which peaked in April. Year 2020 had a higher soil moisture in January and February of around 8% and dropped in March to May to just above zero. The soil moisture for 2021 was around zero.

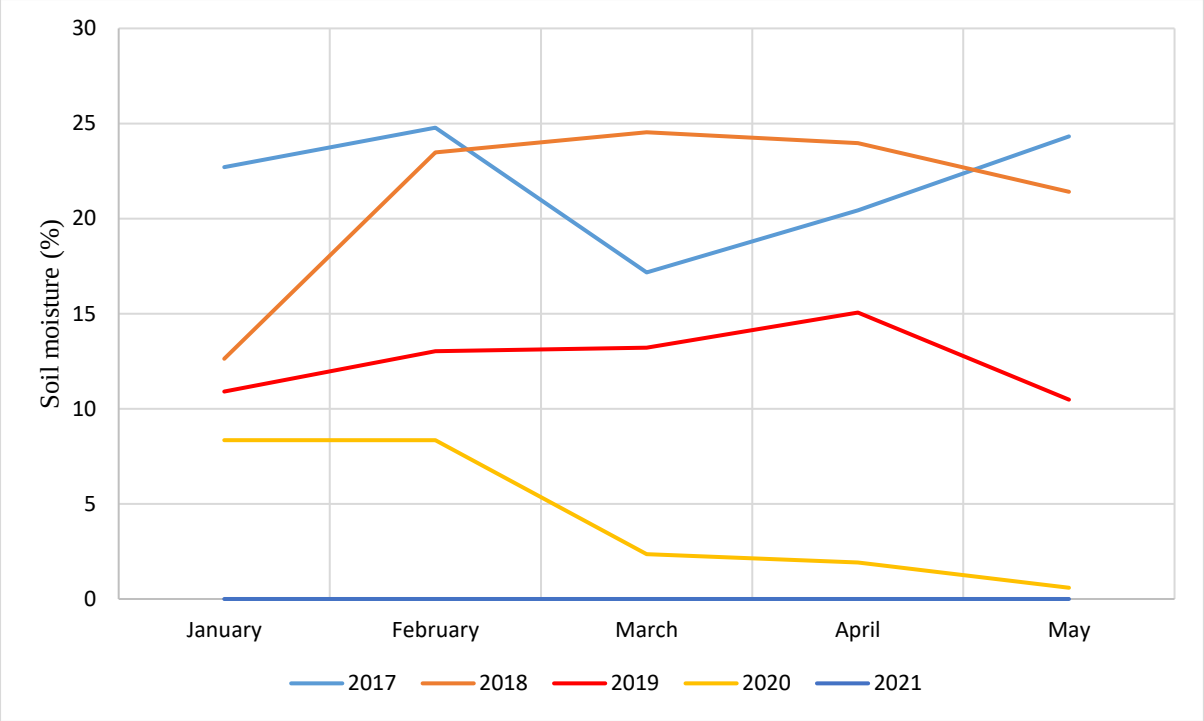

Figure 4.12: Time series, area averaged of volumetric soil moisture over 2017 to 2021, January to May

Figure 4.13 displays the time averaged map of volumetric soil moisture from daily 10km % over 2017 to 2021(January to May). The northern region showed a better average percentage in 2017 while the eastern region was very low on soil moisture percentage as shown in Figure 4.13 a). Slight improvement in 2018 as the eastern region showed improvement as shown in Figure 4.13 b). Year 2019 showed the North Eastern region with better percentage while eastern and southern regions showed very low percentage as shown in Figure 4.13 c). Years 2020 and 2021 are showing the same trend with only the northern region showing better soil

moisture percentage as shown in Figure 4.13 d) and Figure 4.13 e), respectively.

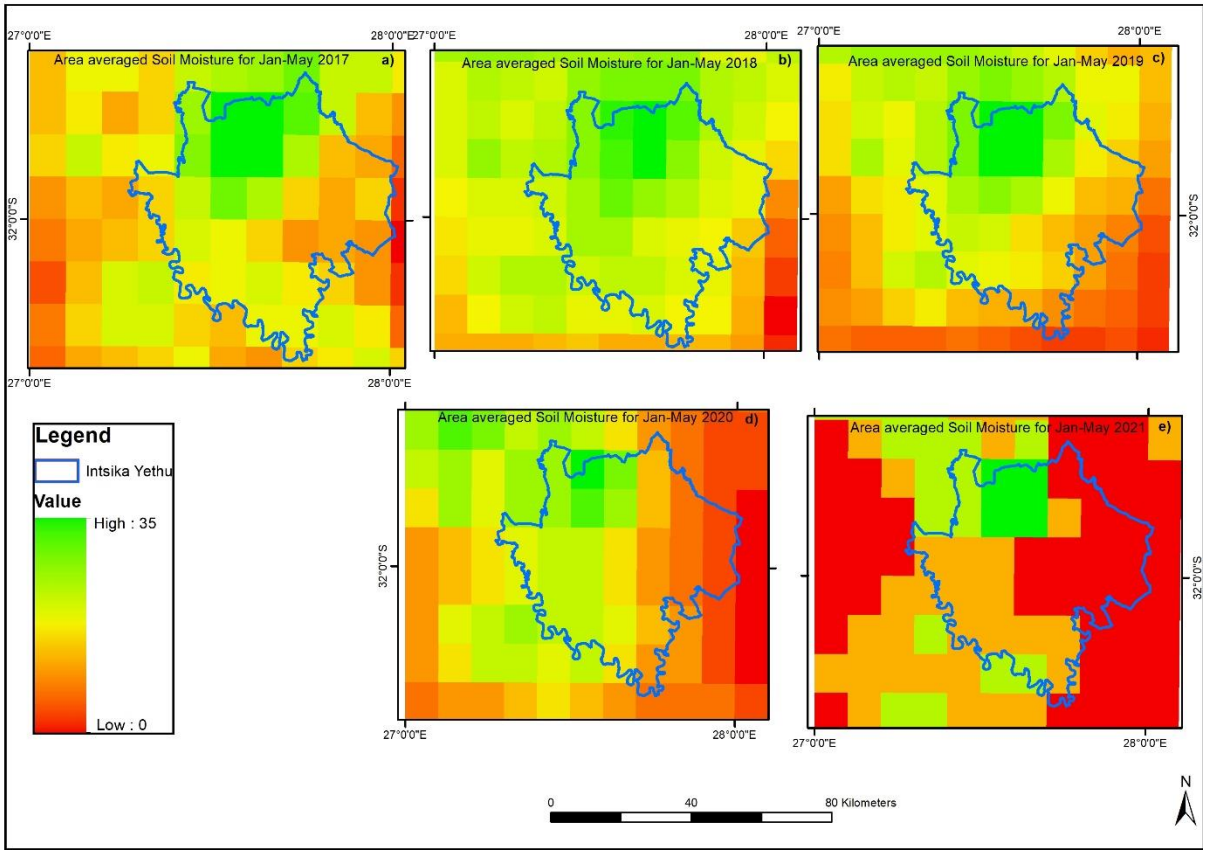

Figure 4.13: a) Time series, area averaged of volumetric soil moisture spatial distribution for January to May of 2017. b) Time series, area averaged of volumetric soil moisture spatial distribution for January to May of 2018. c) Time series, area averaged of volumetric soil moisture spatial distribution for January to May of 2019. d) Time series, area averaged of volumetric soil moisture spatial distribution for January to May of 2020. e) Time series, area averaged of volumetric soil moisture spatial distribution for January to May of 2021.

4.5.2. SOIL MOISTURE CONDITION INDEX (SMCI)

The average SMCI per growing season is displayed in Figure 4.14 and it shows a general declining soil moisture over the study period. The SMCI drops from 0.8 to 0 over the study period.

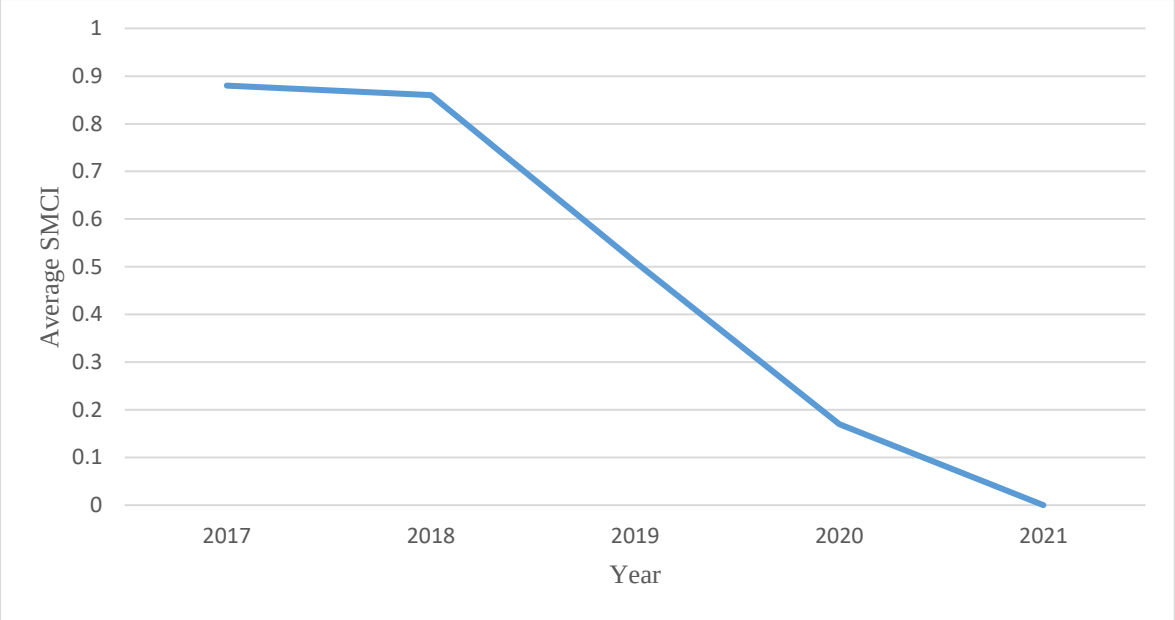

Figure 4.14: Average annual SMCI of Intsika Yethu

4.6. MANN-KENDALL TREND TEST FOR ALL THE DROUGHT VARIABLES

There was no trend observed from the Mann-Kendall trend test for both seasonal NDVI and seasonal NDWI across the study period as shown in Table 4.1. The meteorological rainfall showed a decreasing trend in February across the study period with similarly to the meteorological average temperature while both Meteorological Maximum temperature and Meteorological Minimum temperature showed no trend.

GPM Precipitation and PCI showed no trend AMSR-2 while AMSR-2 Soil Moisture and AMSR-2 SMCI both showed a decreasing trend across the years.

Table 4.1: Showing the Mann-Kendall trends of the processed variables on monthly and seasonally

Variable	Time	P value	Nature of trend
Seasonal NDVI	2017 to 2021	1	No trend
Seasonal NDWI	2017 to 2021	0.8065	No trend
Meteorological Rainfall	January (2017 - 2021)	0.8065	No trend
	February (2017 - 2021)	0.027486	decreasing
	March (2017 - 2021)	0.46243	No trend

	April (2017 - 2021)	0.8065	No trend
	May (2017 - 2021)	0.22067	No trend
SPI Queenstown station	2017 to 2021	0.86411	No trend
SPI Mthatha station	2017 to 2021	0.46243	No trend
SPI Elliot station	2017 to 2021	0.22067	No trend
SPI Stutterheim	2017 to 2021	0.46243	No trend
Meteorological Minimum temperature	January (2017 - 2021)	0.086411	Increasing
	February (2017 - 2021)	0.22067	No trend
	March (2017 - 2021)	1	No trend
	April (2017 - 2021)	0.22067	No trend
	May (2017 - 2021)	0.8065	No trend
Minimum Temperature Queenstown station	2017 to 2021	1	No trend
Minimum Temperature Mthatha station	2017 to 2021	0.22067	No trend
Minimum Temperature Elliot station	2017 to 2021	1	No trend
Minimum Temperature Dohne_Agric station	2017 to 2021	0.46243	No trend
Meteorological Maximum temperature	January (2017 - 2021)	0.8065	No trend
	February (2017 - 2021)	1	No trend
	March (2017 - 2021)	0.8065	No trend
	April (2017 - 2021)	0.8065	No trend
	May (2017 - 2021)	1	No trend
Maximum Temperature Queenstown station	2017 to 2021	0.8065	No trend

Maximum Temperature Mthatha station	2017 to 2021	0.46243	No trend
Maximum Temperature Elliot station	2017 to 2021	0.8065	No trend
Maximum Temperature Dohne_Agric station	2017 to 2021	1	No trend
Meteorological Average temperature	January (2017 - 2021)	0.8065	No trend
	February (2017 - 2021)	0.086411	decreasing
	March (2017 - 2021)	0.46243	No trend
	April (2017 - 2021)	0.8065	No trend
	May (2017 - 2021)	1	No trend
GPM Precipitation	2017 to 2021	0.30719	No trend
GPM PCI	2017 to 2021	0.8065	No trend
AMSR-2 Soil Moisture	2017 to 2021	2.22e-16	decreasing
AMSR-2 SMCI	2017 to 2021	0.027486	decreasing

4.7. DEVELOPING A COMPOSITE DROUGHT MONITORING MODEL (CDMM) FOR DROUGHT VULNERABILITY MAPPING

The spatio-temporal patterns of the agricultural drought risk for 2017 to 2021 vegetation growing season of January to May are depicted in Figure 4.15 to Figure 4.19. The agricultural drought vulnerability map was created by combining several data sources, and it acts as a guide to the regions that need a thorough assessment of their drought susceptibility and risk (Wilhelmi & Wilhelmi, 2002). Therefore, the spatial seasonal drought maps were derived by combining vegetation indices (NDVI and NDWI) with the GPM satellite precipitation data, AMSR-2 soil moisture data, with the landcover data in ArcGIS 10.8.2. Areas at risk for drought can be identified by fusing satellite imagery and weather information (Murad & Islam, 2011).

To display the spatial patterns of the several levels of drought severity risks, from no drought to slight drought, moderate drought to severe drought, drought risk maps have been created as

shown in Figure 4.15 to Figure 4.19. In the generated maps, the dark green color represents no drought while light green, orange and brown represent area that have slight drought risk, moderate drought risk and severe drought risk, respectively. The outcomes demonstrate that the study area as a whole had severe drought occurrences in all the years in isolated areas, however, small as compared to other types of drought risks.

The severe drought patch was observed in the eastern region of the study area as shown in Figure 4.15. Moderate drought was observed from the east through the central part to the west of the area. The Northern part was not experiencing any drought. This is the area with a huge dam and the possibility of irrigation is huge in this area as landcover data shows a significant portion of cultivated subsistence on the southern side of the dam (Thompson, 2018). Also this area is dominated by the planted forest. According to Bruijnzeel (2004), it is reasonable to ascribe the deterioration and decimation in some areas of the forests to the shift in meteorological conditions as manifested in the drop of rainfall and moisture deficiency in the soil. Because it is well recognized that forests have a significant impact on rainfall.

Similar pattern was observed in 2018 as shown in Figure 4.16. The pattern observed in 2019 was completely different and inconsistent with all the other years (see Figure 4.17). Only the northern part was not experiencing any kind of drought in the study period.

The January 2019 NDVI variation showed very low values suggesting a stressed vegetation similarly, the satellite GPM precipitation and soil moisture influenced the observed pattern. The NDWI processed from January 2019 also showed the similar drought pattern. The year had the highest average minimum temperature and had the third highest average maximum temperature after year 2017 and 2021 within the study period as shown in Figure 6.2 and Figure 6.1, respectively, and Figures 6.7 to 6.12 in Appendices. Also, 2019 experienced the second least high rainfall in a day at 150 mm after 2017 at 140 mm as shown in Figures 6.3 to 6.7 in Appendices. According to Mahlalela et al., (2020) the Eastern Cape Province was designated a drought disaster area in October 2019 as a result of severe water shortages in many urban and rural regions. The grasslands experienced drought in 2019 specifically as this research was motivated by personal experience of drought in that particular year. Droughts can happen at any time of year, but the growing season in the summer is when grasslands are most susceptible to them (Abdel-Hamid et al., 2020).

Figure 4.18 demonstrated a similar pattern in 2020 as with 2017 and 2018 though the severity of drought was conspicuous than the latter two years in the north eastern side. Similarly, Figure 4.20 showed the same pattern for year 2021 even though better than year 2020.

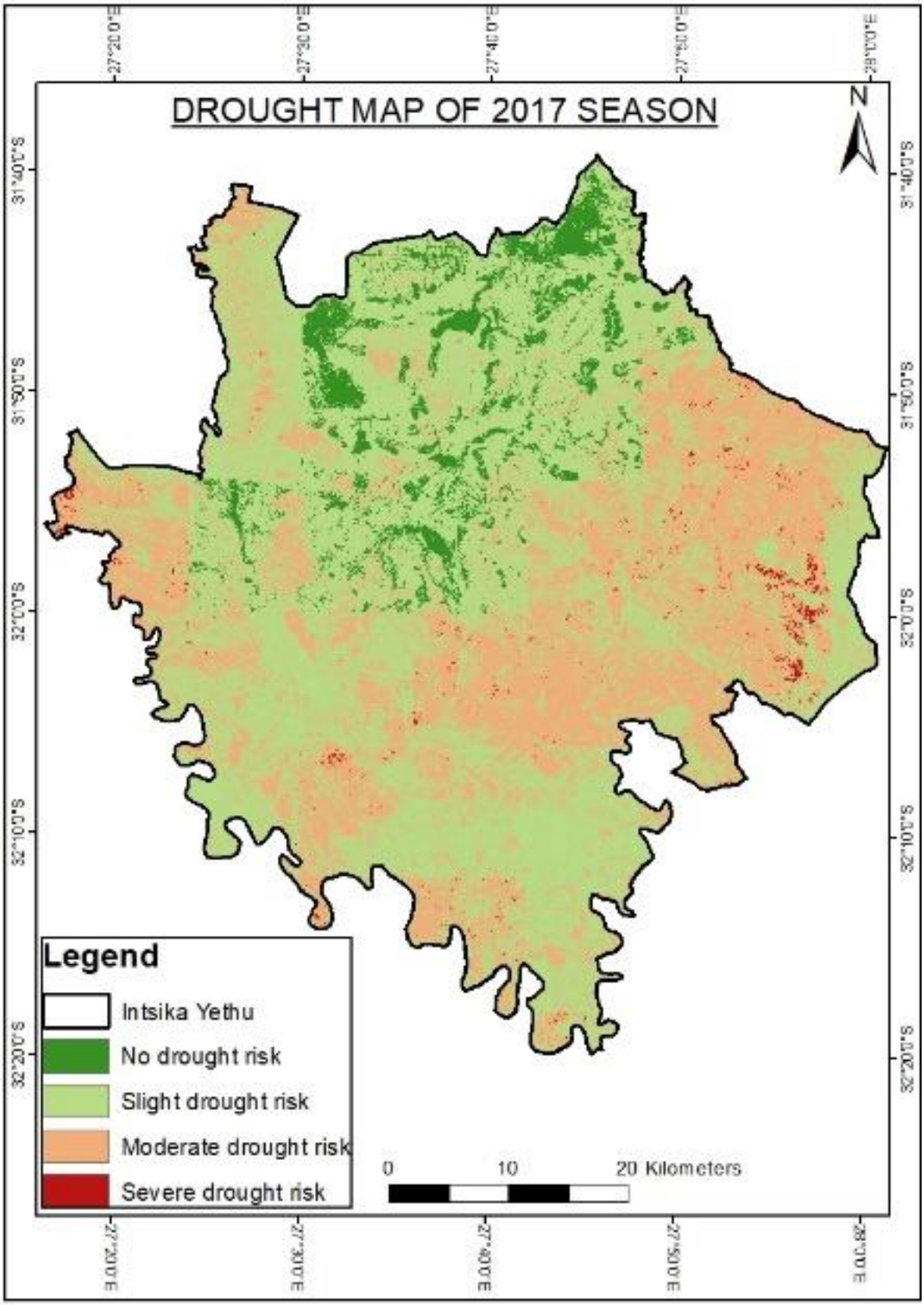

Figure 4.15: Spatial distribution of drought risk area of Intsika Yethu for January to May of 2017

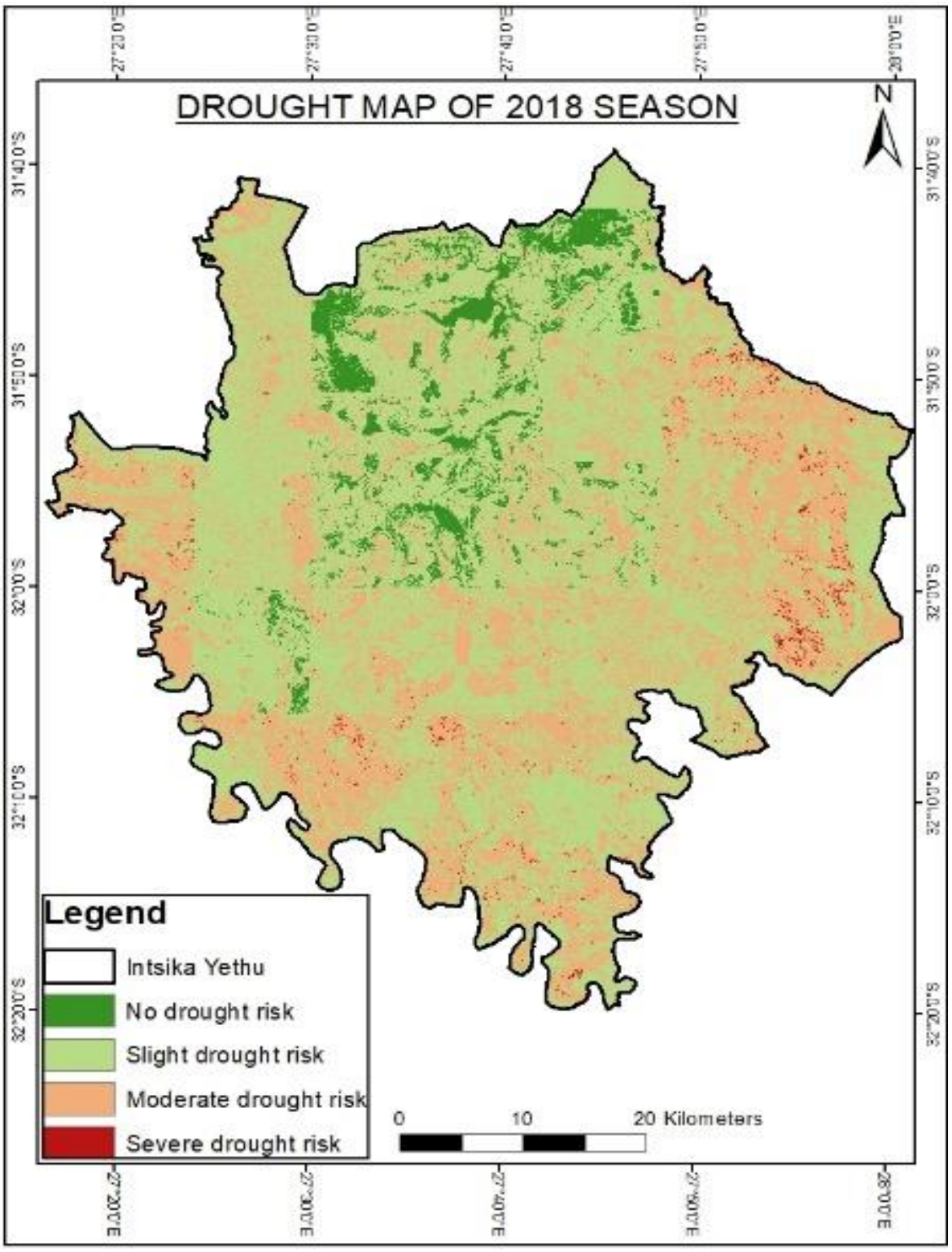

Figure 4.16: Spatial distribution of drought risk area of Intsika Yethu for January to May of 2018

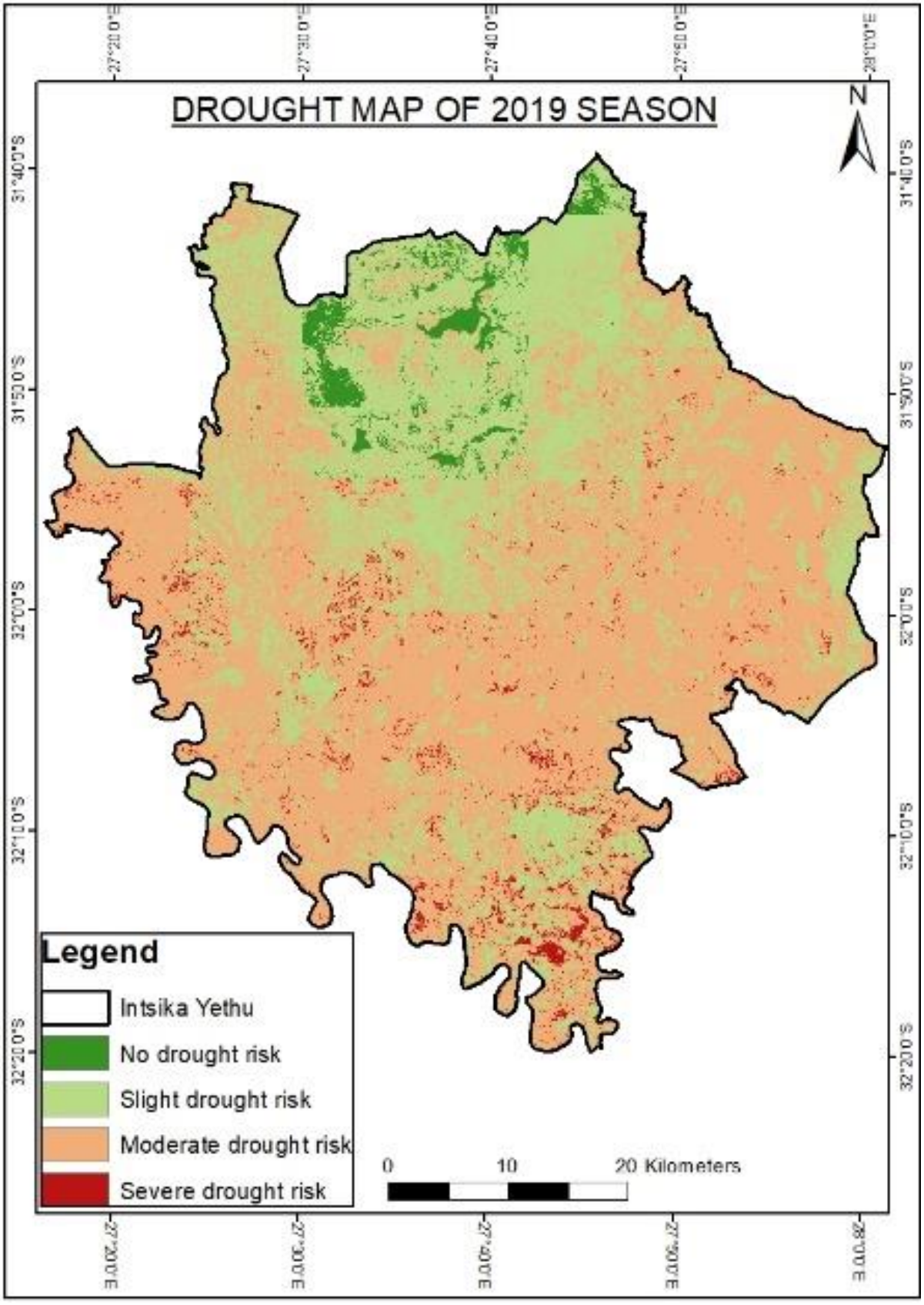

Figure 4.17: Spatial distribution of drought risk area of Intsika Yethu for January to May of 2019

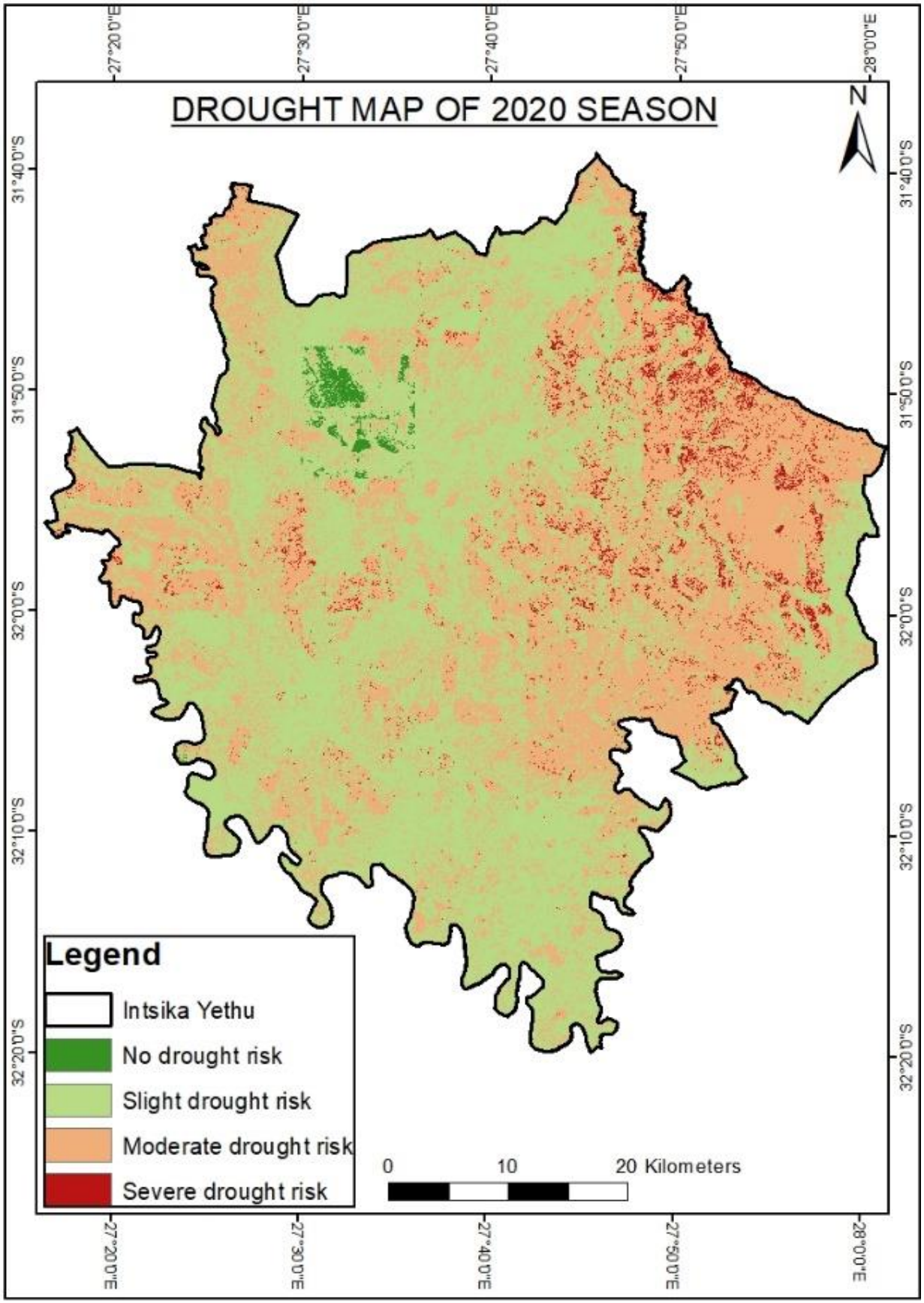

Figure 4.18: Spatial distribution of drought risk area of Intsika Yethu for January to May of 2020

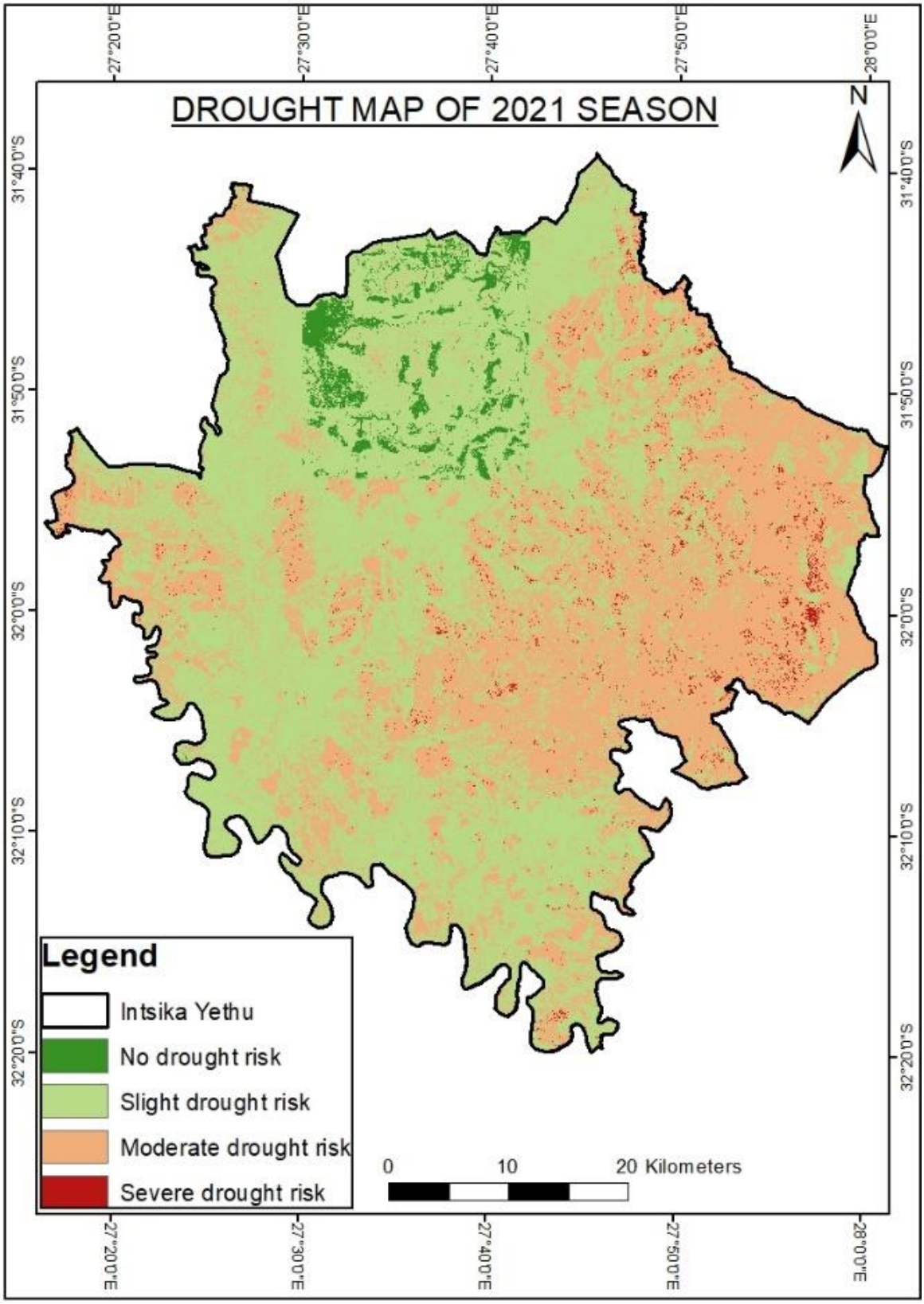

Figure 4.19: Spatial distribution of drought risk area of Intsika Yethu for January to May of 2021

The proportion of the drought risk area determined for each year from 2017 to 2021 is shown in Figure 4.20. Slight risk range dominated 2017 as 59.3% of the study area experienced this type of drought and this was followed by moderate drought risk which occupied 33.4% of the area. It was further noted that 2017 had the highest no drought area of 6.7% and the lowest severe drought 0.6%.

Year 2018 saw no drought risk slightly decreasing by 0.8% to 5.9% and slight risk also decreased by 1.1% while moderate risk increased by 1.8 % with severe drought remaining constant in comparison with the previous year.

A different pattern was observed in 2019 with moderate drought risk exceeding 60% and becoming the highest in the whole study period, also severe drought risk increased to 2.4% while both no drought risk and slight drought risk classes decreased by 3.2% and 24.2%, respectively, compared to the previous year. The increase by both moderate drought risk and severe drought risk indicated drought vulnerability in the area.

For year 2020, the no drought and moderate drought classes decreased by 2% and 18.1% while slight drought risk and severe drought risk classes increased by 19.6% and 0.5%, respectively. While year 2021 observed an increase of no drought risk and slight drought risk class by 1.9% and 2.6 %, respectively. While moderate and severe drought risk classes decreased by 2.7% and 1.9% respectively. This showed an improvement in 2021 compared to 2020 and 2019. This holds true with the observations by Archer et al., (2022) who suggested that drought reached its peak severity and extent in 2019 in the Eastern Cape and that its severity in 2019 was as a result of cumulative impact of the extended dry spells since 2014. This agreement demonstrates that the CDMM can be used at Intsika Yethu to keep track of the drought over a lengthy period of time.

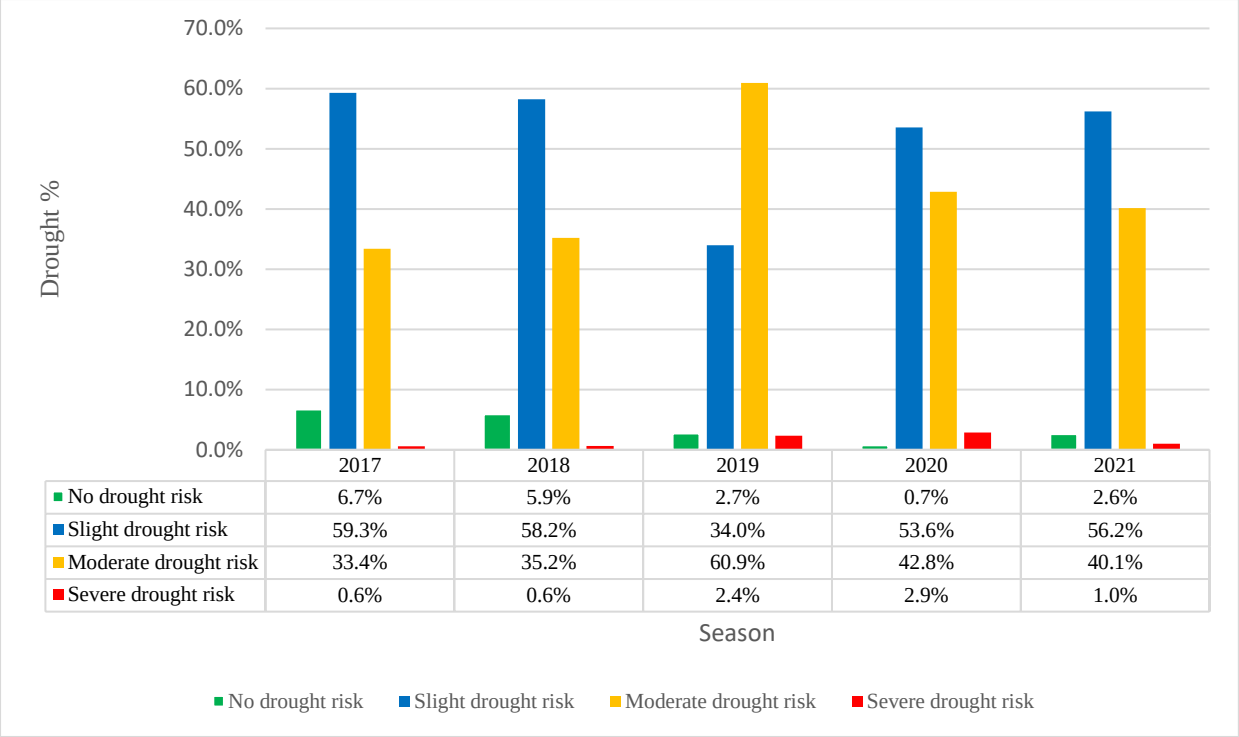

	2017	2018	2019	2020	2021
No drought risk	6.7%	5.9%	2.7%	0.7%	2.6%
Slight drought risk	59.3%	58.2%	34.0%	53.6%	56.2%
Moderate drought risk	33.4%	35.2%	60.9%	42.8%	40.1%
Severe drought risk	0.6%	0.6%	2.4%	2.9%	1.0%

Figure 4.20: Drought severity of Intsika Yethu for 2017 to 2021 (January to May)

5. CONCLUSION

The study demonstrated the ability of geospatial methods and statistics to monitor drought in remote areas such as Intsika Yethu. The study gave the first ground work and future studies can build on it to further the monitoring of the drought and setting of the early detection techniques within the municipality. GIS has the capacity to produce an enhanced monitoring system for agricultural drought that incorporates many aspects that have an impact on the drought and presents the findings to policy makers in a timely and relevant manner (Lourens & De Jager, 1997).

In addition to complementing in-situ measurements and meteorological observations, using satellite earth observation data, it is now possible to monitor changes in vegetation and consequently, agricultural droughts (Graw et al., 2017).

For phenological investigations, Sentinel-2 does have some drawbacks, particularly with regard to the inevitable data gaps caused by cloud cover which are a characteristic of optical sensors (Misra et al., 2020). The expected temporal variation was compromised by the poor quality of some images because of clouds resulting in gaps that could affect the accuracy of the findings, for example 2017, had the few usable images and some months did not have any usable images.

The data had to be interpolated into the study area from four meteorological stations, which range from 32 kms closest and 67 kms furthest. Despite the fact that the spatial interpolation of drought index values provide useful information on the state of the current drought, there may still be substantial uncertainty (Rhee et al., 2010). Furthermore, without an adequate network of meteorological stations across the area, it is impossible to accurately determine the spatial extent of the drought (Dutta et al., 2015).

Notwithstanding these difficulties, the study showed the ability of NDVI to map the spatio-temporal variability of agriculture at Intsika Yethu local municipality. To achieve better results, it is generally desirable to integrate the NDVI with other factors (Sruthi & Aslam, 2015). Therefore, spectral indices from multi sources such as NDWI, SPI, PCI and SMCI showed a collective potential in mapping agricultural drought in the area. There is a general agreement for example, with NDVI and NDWI especially in January, the results show a drought in the study area. These results were corroborated by SPI, PCI and satellite based precipitation which

demonstrated very low precipitation in 2019 especially. The weather stations provided a picture of precipitation and temperature trends in the area with the highest rainfall captured over these seasons being 210 mm and the lowest being zero. The combination of Agricultural and meteorological droughts and the local landcover dataset demonstrated the ability to track drought in real time in the study area. The influence of different variables is evident in 2019 map as both meteorological drought and agriculture drought experienced at different periods in 2019 influenced the final drought risk map. The results showed that Intsika Yethu has been experiencing slight drought risk followed by moderate drought risk for the study period, except for 2019 where moderate drought risk exceeded the slight drought risk. In order to protect the environment and ecosystems, it is essential to track the temporal and spatial dynamics of drought occurrences (Orimoloye eat al., 2021). Monitoring the drought is essential for carrying out drought plans (Vicente-Serrano et al., 2012).

This study can assist the municipality in identifying areas where support is needed. In South Africa, communal and small-scale farmers, for example, are especially vulnerable to drought shocks, and they perceive even routine dry spells as drought catastrophes (Jordan et al., 2013) and this is true at Intsika Yethu as well. With the identification and study of ecological sensitivity indicators to drought, it would be feasible to re-evaluate priorities for the government and municipality to adopt effective policy actions in response to drought and provide solutions to lessen drought susceptibility (Jordaan et al., 2019).

The study provided a good insight on the challenges that the drought can present to the municipality in the future. Also the study can be taken further to include the whole Chris Hani district municipality. The model accuracy can be improved by utilizing the high resolution satellite data. Future research should focus on increasing data accessibility and undertaking comprehensive validation to improve the usefulness and accuracy of the Composite Drought Monitoring Model (CDMM) for a wider range of applications.

REFERENCES

Abdel-Hamid, A., Dubovyk, O., Graw, V., & Greve, K. (2020). Assessing the impact of drought stress on grasslands using multi-temporal SAR data of Sentinel-1: a case study in Eastern Cape, South Africa. *European Journal of Remote Sensing*, *53*(sup2), 3–16. https://doi.org/10.1080/22797254.2020.1762514

Abdi, A. M. (2020). Land cover and land use classification performance of machine learning algorithms in a boreal landscape using Sentinel-2 data. *GIScience and Remote Sensing*, *57*(1), 1–20. https://doi.org/10.1080/15481603.2019.1650447

Abdulrazzaq, Z., Aziz, N., & Mohammed, A. (2018). Flood modelling using satellite-based precipitation estimates and digital elevation model in eastern Iraq. *International Journal of Advanced Geosciences*, *6*(1), 72. https://doi.org/10.14419/ijag.v6i1.8946

Abdulrazzaq, Z. T., Hasan, R. H., & Aziz, N. A. (2019). Integrated TRMM Data and Standardized Precipitation Index to Monitor the Meteorological Drought. *Civil Engineering Journal*, *5*(7), 1590–1598. https://doi.org/10.28991/cej-2019-03091355

AghaKouchak, A., Farahmand, A., Melton, F. S., Teixeira, J., Anderson, M. C., Wardlow, B. D., & Hain, C. R. (2015). Remote sensing of drought: Progress, challenges and opportunities. *Reviews of Geophysics*, *53*(2), 452–480. https://doi.org/10.1002/2014RG000456

Ali, S., Tong, D., Xu, Z. T., Henchiri, M., Wilson, K., Siqi, S., & Zhang, J. (2019). Characterization of drought monitoring events through MODIS- and TRMM-based DSI and TVDI over South Asia during 2001–2017. *Environmental Science and Pollution Research*, *26*(32), 33568–33581. https://doi.org/10.1007/s11356-019-06500-4

Altun, R., Kalkan, K., & Gürsoy, Ö. (2020). Determining The Forest Fire Risk with Sentinel 2 Images. *Turkish Journal of Geosciences*, *1*(1), 22–26. Retrieved from https://dergipark.org.tr/en/pub/turkgeo

Archer, E., du Toit, J., Engelbrecht, C., Hoffman, M. T., Landman, W., Malherbe, J., & Stern, M. (2022). The 2015-19 multi year drought in the Eastern Cape, South Africa: it's evolution and impacts on agriculture. *Journal of Arid Environments*, *196*(July 2021), 104630. https://doi.org/10.1016/j.jaridenv.2021.104630

Arun Kumar, K. C., Reddy, G. P. O., Masilamani, P., Turkar, S. Y., & Sandeep, P. (2021). Integrated drought monitoring index: A tool to monitor agricultural drought by using time-series datasets of space-based earth observation satellites. *Advances in Space*

Research, *67*(1), 298–315. https://doi.org/10.1016/j.asr.2020.10.003

Aschbacher, J., & Milagro-Pérez, M. P. (2012). The European Earth monitoring (GMES) programme: Status and perspectives. *Remote Sensing of Environment*, *120*(2012), 3–8. https://doi.org/10.1016/j.rse.2011.08.028

Assal, T. J., Anderson, P. J., & Sibold, J. (2016). Spatial and temporal trends of drought effects in a heterogeneous semi-arid forest ecosystem. *Forest Ecology and Management*, *365*, 137–151. https://doi.org/10.1016/j.foreco.2016.01.017

Atif, I., & Mahboob, M. A. (2016). Spatio-Temporal Mapping of Tharparkar Drought Using High, *28*(1), 257–264.

B. Mandleni. (2012). Climate change and adaptation of small-scale cattle and sheep farmers. *African Journal of Agricultural Reseearch*, *7*(17), 106–112. https://doi.org/10.5897/ajar10.747

Baillarin, S. J., Meygret, A., Dechoz, C., Petrucci, B., Lacherade, S., Tremas, T., … Spoto, F. (2012). Sentinel-2 Level 1 Products and Image Processing Performances. *ISPRS - International Archives of the Photogrammetry, Remote Sensing and Spatial Information Sciences*, *XXXIX-B1*(July), 197–202. https://doi.org/10.5194/isprsarchives-xxxix-b1-197-2012

Baudoin, M. A., Vogel, C., Nortje, K., & Naik, M. (2017). Living with drought in South Africa: lessons learnt from the recent El Niño drought period. *International Journal of Disaster Risk Reduction*, *23*(May), 128–137. https://doi.org/10.1016/j.ijdrr.2017.05.005

Belal, A. A., El-Ramady, H. R., Mohamed, E. S., & Saleh, A. M. (2014). Drought risk assessment using remote sensing and GIS techniques. *Arabian Journal of Geosciences*, *7*(1), 35–53. https://doi.org/10.1007/s12517-012-0707-2

Benson, C., & Clay, E. (1994). THE IMPACT OF DROUGHT ON SUB-SAHARAN AFRICAN ECONOMIES linkages and multiplier effects, implies that the final expenditure, the intensity of water usage, levels of GDi ’ per capita and natural resource Simple Economies - predominantly rain-fed duction, *25*(4).

Bhaga, T. D., Dube, T., Shekede, M. D., & Shoko, C. (2020). Impacts of climate variability and drought on surface water resources in sub-saharan africa using remote sensing: A review. *Remote Sensing*, *12*(24), 1–34. https://doi.org/10.3390/rs12244184

Brown, J. F., Wardlow, B. D., Tadesse, T., Hayes, M. J., & Reed, B. C. (2008). The Vegetation Drought Response Index (VegDRI): A new integrated approach for monitoring drought stress in vegetation. *GIScience and Remote Sensing*, *45*(1), 16–46. https://doi.org/10.2747/1548-1603.45.1.16

Bruijnzeel, L. A. (2004). *Hydrological functions of tropical forests: Not seeing the soil for the trees? Agriculture, Ecosystems and Environment* (Vol. 104). https://doi.org/10.1016/j.agee.2004.01.015

Bryan, E., Deressa, T. T., Gbetibouo, G. A., & Ringler, C. (2009). Adaptation to climate change in Ethiopia and South Africa: options and constraints. *Environmental Science and Policy*, *12*(4), 413–426. https://doi.org/10.1016/j.envsci.2008.11.002

Bui, Y. T., Orange, D., Visser, S. M., Hoanh, C. T., Laissus, M., Poortinga, A., … Stroosnijder, L. (2014). Lumped surface and sub-surface runoff for erosion modeling within a small hilly watershed in northern Vietnam. *Hydrological Processes*, *28*(6), 2961–2974. https://doi.org/10.1002/hyp.9860

Carlson, T. N., & Ripley, D. A. (1997). On the relation between NDVI, fractional vegetation cover, and leaf area index. *Remote Sensing of Environment*, *62*(3), 241–252. https://doi.org/10.1016/S0034-4257(97)00104-1

Chen, D., Huang, J., & Jackson, T. J. (2005). Vegetation water content estimation for corn and soybeans using spectral indices derived from MODIS near- and short-wave infrared bands. *Remote Sensing of Environment*, *98*(2–3), 225–236. https://doi.org/10.1016/j.rse.2005.07.008

Chen, Y., Yu, J., & Khan, S. (2010). Spatial sensitivity analysis of multi-criteria weights in GIS-based land suitability evaluation. *Environmental Modelling and Software*, *25*(12), 1582–1591. https://doi.org/10.1016/j.envsoft.2010.06.001

Choi, M., Jacobs, J. M., Anderson, M. C., & Bosch, D. D. (2013). Evaluation of drought indices via remotely sensed data with hydrological variables. *Journal of Hydrology*, *476*, 265–273. https://doi.org/10.1016/j.jhydrol.2012.10.042

Clevers, J. G. P. W., & Gitelson, A. A. (2013). Remote estimation of crop and grass chlorophyll and nitrogen content using red-edge bands on sentinel-2 and-3. *International Journal of Applied Earth Observation and Geoinformation*, *23*(1), 344–351. https://doi.org/10.1016/j.jag.2012.10.008

Conolly, J. (2020). Spatial Interpolation. *Archaeological Spatial Analysis*, 118–134. https://doi.org/10.4324/9781351243858-7

Daryanto, S., Wang, L., & Jacinthe, P. A. (2016). Global synthesis of drought effects on maize and wheat production. *PLoS ONE*, *11*(5). https://doi.org/10.1371/journal.pone.0156362

DEA. (2018). South Africa's Third National Communication, 368. Retrieved from https://unfccc.int/sites/default/files/resource/South African TNC Report to the

UNFCCC_31 Aug.pdf [accessed on 25 September 2018]

Du, L., Tian, Q., Yu, T., Meng, Q., Jancso, T., Udvardy, P., & Huang, Y. (2013). A comprehensive drought monitoring method integrating MODIS and TRMM data. *International Journal of Applied Earth Observation and Geoinformation*, *23*(1), 245–253. https://doi.org/10.1016/j.jag.2012.09.010

Durbach, I. N., & Stewart, T. J. (2012). Modeling uncertainty in multi-criteria decision analysis. *European Journal of Operational Research*, *223*(1), 1–14. https://doi.org/10.1016/j.ejor.2012.04.038

Dutta, D., Kundu, A., Patel, N. R., Saha, S. K., & Siddiqui, A. R. (2015). Assessment of agricultural drought in Rajasthan (India) using remote sensing derived Vegetation Condition Index (VCI) and Standardized Precipitation Index (SPI). *Egyptian Journal of Remote Sensing and Space Science*, *18*(1), 53–63. https://doi.org/10.1016/j.ejrs.2015.03.006

Ford, T. W., & Quiring, S. M. (2019). Comparison of Contemporary In Situ, Model, and Satellite Remote Sensing Soil Moisture With a Focus on Drought Monitoring. *Water Resources Research*, 1565–1582. https://doi.org/10.1029/2018WR024039

Frantz, D. (2019). FORCE-Landsat + Sentinel-2 analysis ready data and beyond. *Remote Sensing*, *11*(9). https://doi.org/10.3390/rs11091124

Graw, V., Ghazaryan, G., Dall, K., Gómez, A. D., Abdel-Hamid, A., Jordaan, A., … Dubovyk, O. (2017). Drought dynamics and vegetation productivity in different land management systems of Eastern Cape, South Africa-A remote sensing perspective. *Sustainability (Switzerland)*, *9*(10). https://doi.org/10.3390/su9101728

Gu, Y., Brown, J. F., Verdin, J. P., & Wardlow, B. (2007). A five-year analysis of MODIS NDVI and NDWI for grassland drought assessment over the central Great Plains of the United States. *Geophysical Research Letters*, *34*(6), 1–6. https://doi.org/10.1029/2006GL029127

Haile, G. G., Tang, Q., Hosseini-Moghari, S. M., Liu, X., Gebremicael, T. G., Leng, G., … Yun, X. (2020). Projected Impacts of Climate Change on Drought Patterns Over East Africa. *Earth's Future*, *8*(7), 1–23. https://doi.org/10.1029/2020EF001502

Hanadé Houmma, I., El Mansouri, L., Gadal, S., Garba, M., & Hadria, R. (2022). Modelling agricultural drought: a review of latest advances in big data technologies. *Geomatics, Natural Hazards and Risk*, *13*(1), 2737–2776. https://doi.org/10.1080/19475705.2022.2131471

Hao, Z., AghaKouchak, A., Nakhjiri, N., & Farahmand, A. (2014). Global integrated drought

monitoring and prediction system. *Scientific Data*, *1*, 140001. https://doi.org/10.1038/sdata.2014.1

Henry, M. (1945). Nonparametric Tests Against Trend Author (s): Henry B. Mann Published by : The Econometric Society Stable URL : https://www.jstor.org/stable/1907187 REFERENCES Linked references are available on JSTOR for this article : You may need to log in to JSTOR. *Econometrica*, *13*(3), 245–259.

Herold, M., Woodcock, C. E., Loveland, T. R., Townshend, J., Brady, M., Steenmans, C., & Schmullius, C. C. (2008). Land-cover observations as part of a global earth observation system of systems (GEOSS): Progress, activities, and prospects. *IEEE Systems Journal*, *2*(3), 414–423. https://doi.org/10.1109/JSYST.2008.925983

Hewitson, B. C., & Crane, R. G. (2006). Consensus between GCM climate change projections with empirical downscaling: Precipitation downscaling over South Africa. *International Journal of Climatology*, *26*(10), 1315–1337. https://doi.org/10.1002/joc.1314

INTERDISCIPLINARY DROUGHT RISK ASSESSMENT FOR AGRICULTURE : (2013), *41*, 44–58.

Jeyaseelan, A. T. (2003). Droughts & floods assessment and monitoring using remote sensing and GIS. *Satellite Remote Sensing and GIS Applications in Agricultural Meteorology*, 291–313. Retrieved from http://www.wamis.org/agm/pubs/agm8/Paper-14.pdf

Jiao, W., Wang, L., & McCabe, M. F. (2021). Multi-sensor remote sensing for drought characterization: current status, opportunities and a roadmap for the future. *Remote Sensing of Environment*, *256*(January), 112313. https://doi.org/10.1016/j.rse.2021.112313

Jordaan, A., Bahta, Y. T., Phatudi-, B., Management, D., Africa, S., State, F., … Bahta, Y. (2005). Ecological vulnerability indicators to drought : Case of communal farmers in Eastern Cape, South Africa Research methodology, 1–11.

JRC European Commission. (2011). NDWI (Normalized Difference Water Index). *Product Fact Sheet*, *5*(July), 6–7. Retrieved from http://edo.jrc.ec.europa.eu/documents/factsheets/factsheet_ndwi.pdf

Kamruzzaman, M., Rahman, A. T. M. S., Ahmed, M. S., Kabir, M. E., Mazumder, Q. H., Rahman, M. S., & Jahan, C. S. (2018). Spatio-temporal analysis of climatic variables in the western part of Bangladesh. *Environment, Development and Sustainability*, *20*(1), 89–108. https://doi.org/10.1007/s10668-016-9872-x

Kane, R. P. (2009). Periodicities, ENSO effects and trends of some South African rainfall series: An update. *South African Journal of Science*, *105*(5–6), 199–207. https://doi.org/10.4102/sajs.v105i5/6.90

Krofcheck, D. J., Eitel, J. U. H., Vierling, L. A., Schulthess, U., Hilton, T. M., Dettweiler-Robinson, E., … Litvak, M. E. (2014). Detecting mortality induced structural and functional changes in a piñon-juniper woodland using Landsat and RapidEye time series. *Remote Sensing of Environment*, *151*, 102–113. https://doi.org/10.1016/j.rse.2013.11.009

Kulie, M. S., & Bennartz, R. (2009). Utilizing spaceborne radars to retrieve dry Snowfall. *Journal of Applied Meteorology and Climatology*, *48*(12), 2564–2580. https://doi.org/10.1175/2009JAMC2193.1

Kumari, M., & Somvanshi, S. S. (2019). " Changing trends of land surface temperature in relation to vegetation cover of Gurugram district.," (August).

Li, J., & Heap, A. D. (2008). A Review of Spatial Interpolation Methods for Environmental Scientists. *Australian Geological Survey Organisation*, *GeoCat# 68*(2008/23), 154. https://doi.org/http://www.ga.gov.au/image_cache/GA12526.pdf

Liu, Q., Zhang, S., Zhang, H., Bai, Y., & Zhang, J. (2020). Monitoring drought using composite drought indices based on remote sensing. *Science of the Total Environment*, *711*(December), 134585. https://doi.org/10.1016/j.scitotenv.2019.134585

Liu, X., Zhu, X., Pan, Y., Li, S., Liu, Y., & Ma, Y. (2016). Agricultural drought monitoring: Progress, challenges, and prospects. *Journal of Geographical Sciences*, *26*(6), 750–767. https://doi.org/10.1007/s11442-016-1297-9

Lourens, U. W., & De Jager, J. M. (1997). A computerized crop-specific drought monitoring system: Design concepts and initial testing. *Agricultural Systems*, *53*(2–3), 303–315. https://doi.org/10.1016/s0308-521x(96)00004-2

Mahlalela, P. T., Blamey, R. C., Hart, N. C. G., & Reason, C. J. C. (2020). Drought in the Eastern Cape region of South Africa and trends in rainfall characteristics. *Climate Dynamics*, *55*(9–10), 2743–2759. https://doi.org/10.1007/s00382-020-05413-0

Mahmud, M. R., Yusof, A. A. M., Reba, M., & Hashim, M. (2020). Mapping the daily rainfall over an ungauged tropical micro-watershed: A downscaling algorithm using GPM data. *Water (Switzerland)*, *12*(6). https://doi.org/10.3390/W12061661

Malenovský, Z., Rott, H., Cihlar, J., Schaepman, M. E., García-Santos, G., Fernandes, R., & Berger, M. (2012). Sentinels for science: Potential of Sentinel-1, -2, and -3 missions for scientific observations of ocean, cryosphere, and land. *Remote Sensing of Environment*,

120, 91–101. https://doi.org/10.1016/j.rse.2011.09.026

Maponya, P., & Mpandeli, S. (2012). Impact of drought on food scarcity in Limpopo province , South Africa, *7*(37), 5270–5277. https://doi.org/10.5897/AJAR12.1453

Masikati, P., Descheemaeker, K., & Crespo, O. (2019). *Understanding the Role of Soils and Management on Crops in the Face of Climate Uncertainty in Zimbabwe: A Sensitivity Analysis*. *The Climate-Smart Agriculture Papers*. https://doi.org/10.1007/978-3-319-92798-5_5

McFeeters, S. K. (2013). Using the normalized difference water index (ndwi) within a geographic information system to detect swimming pools for mosquito abatement: A practical approach. *Remote Sensing*, *5*(7), 3544–3561. https://doi.org/10.3390/rs5073544

Mendoza, G. A., & Martins, H. (2006). Multi-criteria decision analysis in natural resource management: A critical review of methods and new modelling paradigms. *Forest Ecology and Management*, *230*(1–3), 1–22. https://doi.org/10.1016/j.foreco.2006.03.023

Meteorological, W., & States, U. (2010). Agricultural Drought Indices Proceedings of an, (June).

Mills, A. J., Cowling, R. M., Fey, M. V., Kerley, G. I. H., Donaldson, J. S., Lechmere-Oertel, R. G., … Rundel, P. (2005). Effects of goat pastoralism on ecosystem carbon storage in semiarid thicket, Eastern Cape, South Africa. *Austral Ecology*, *30*(7), 797–804. https://doi.org/10.1111/j.1442-9993.2005.01523.x

Misra, G., Cawkwell, F., & Wingler, A. (2020). Status of phenological research using sentinel-2 data: A review. *Remote Sensing*, *12*(17), 10–14. https://doi.org/10.3390/RS12172760

Mlenga, D. H., & Jordaan, A. J. (2020). Integrated drought monitoring framework for Eswatini applying standardised precipitation index and normalised difference vegetation index. *Jamba: Journal of Disaster Risk Studies*, *12*(1), 1–11. https://doi.org/10.4102/JAMBA.V12I1.749

Mukherjee, S., Mishra, A., & Trenberth, K. E. (2018). Climate Change and Drought: a Perspective on Drought Indices. *Current Climate Change Reports*, *4*(2), 145–163. https://doi.org/10.1007/s40641-018-0098-x

Murad, H., & Islam, A. K. M. S. (2011). Drought assessment using Remote Sensing and GIS in North-West region of Bangladesh. *3rd International Conference on Water and Flood Management*, 861–877.

Nagarajan, R. (2009). Drought Indices. *Drought Assessment*, 160–204. https://doi.org/10.1007/978-90-481-2500-5_5

Nam, W. H., Choi, J. Y., Yoo, S. H., & Jang, M. W. (2012). A decision support system for agricultural drought management using risk assessment. *Paddy and Water Environment*, *10*(3), 197–207. https://doi.org/10.1007/s10333-012-0329-z

Nicolai-Shaw, N., Zscheischler, J., Hirschi, M., Gudmundsson, L., & Seneviratne, S. I. (2017). A drought event composite analysis using satellite remote-sensing based soil moisture. *Remote Sensing of Environment*, *203*, 216–225. https://doi.org/10.1016/j.rse.2017.06.014

Orimoloye, I. R., Ololade, O. O., Mazinyo, S. P., Kalumba, A. M., Ekundayo, O. Y., Busayo, E. T., … Nel, W. (2019). Spatial assessment of drought severity in Cape Town area, South Africa. *Heliyon*, *5*(7), e02148. https://doi.org/10.1016/j.heliyon.2019.e02148

Orimoloye, Israel R. (2022). Agricultural Drought and Its Potential Impacts: Enabling Decision-Support for Food Security in Vulnerable Regions. *Frontiers in Sustainable Food Systems*, *6*(February). https://doi.org/10.3389/fsufs.2022.838824

Orimoloye, Israel R., Belle, J. A., & Ololade, O. O. (2021). Drought disaster monitoring using MODIS derived index for drought years: A space-based information for ecosystems and environmental conservation. *Journal of Environmental Management*, *284*(January), 112028. https://doi.org/10.1016/j.jenvman.2021.112028

Palmer, T. (2004). Makana LEAP: Vegetation of Makana, 1–39.

Paredes-Trejo, F., & Barbosa, H. (2017). Evaluation of the SMOS-derived soil water deficit index as agricultural drought index in Northeast of Brazil. *Water (Switzerland)*, *9*(6). https://doi.org/10.3390/w9060377

Philip, S. Y., Kew, S. F., Van Der Wiel, K., Wanders, N., Jan Van Oldenborgh, G., & Philip, S. Y. (2020). Regional differentiation in climate change induced drought trends in the Netherlands. *Environmental Research Letters*, *15*(9). https://doi.org/10.1088/1748-9326/ab97ca

Ramoelo, A., Cho, M., Mathieu, R., & Skidmore, A. K. (2015). Potential of Sentinel-2 spectral configuration to assess rangeland quality. *Journal of Applied Remote Sensing*, *9*(1), 094096. https://doi.org/10.1117/1.jrs.9.094096

Rhee, J., Im, J., & Carbone, G. J. (2010). Monitoring agricultural drought for arid and humid regions using multi-sensor remote sensing data. *Remote Sensing of Environment*, *114*(12), 2875–2887. https://doi.org/10.1016/j.rse.2010.07.005

Rockström, J. (2000). WATER RESOURCES MANAGEMENT IN SMALLHOLDER FARMS IN EASTERN AND SOUTHERN AFRICA : AN OVERVIEW, 1–20.

Rojas, O., Vrieling, A., & Rembold, F. (2011). Assessing drought probability for agricultural

areas in Africa with coarse resolution remote sensing imagery. *Remote Sensing of Environment*, *115*(2), 343–352. https://doi.org/10.1016/j.rse.2010.09.006

Rouault, M., & Richard, Y. (2003). Intensity and spatial extension of drought in South Africa at different time scales, *29*(4), 489–500.

Shahzaman, M., Zhu, W., Bilal, M., Habtemicheal, B. A., Mustafa, F., Arshad, M., … Iqbal, R. (2021). Remote sensing indices for spatial monitoring of agricultural drought in south asian countries. *Remote Sensing*, *13*(11). https://doi.org/10.3390/rs13112059

Shashikant, V., Shariff, A. R. M., Wayayok, A., Kamal, R., Lee, Y. P., & Takeuchi, W. (2021). Utilizing TVDI and NDWI to classify severity of agricultural drought in Chuping, Malaysia. *Agronomy*, *11*(6). https://doi.org/10.3390/agronomy11061243

Shen, M., Tang, Y., Chen, J., Zhu, X., & Zheng, Y. (2011). Influences of temperature and precipitation before the growing season on spring phenology in grasslands of the central and eastern Qinghai-Tibetan Plateau. *Agricultural and Forest Meteorology*, *151*(12), 1711–1722. https://doi.org/10.1016/j.agrformet.2011.07.003

Somvanshi, S. S., & Kumari, M. (2020). Comparative analysis of different vegetation indices with respect to atmospheric particulate pollution using sentinel data. *Applied Computing and Geosciences*, *7*(March 2019), 100032. https://doi.org/10.1016/j.acags.2020.100032

Spencer, M., Wheeler, K., White, C., West, R., Piepmeier, J., Hudson, D., & Medeiros, J. (2010). The Soil Moisture Active Passive (SMAP) mission L-Band radar/radiometer instrument. *International Geoscience and Remote Sensing Symposium (IGARSS)*, 3240–3243. https://doi.org/10.1109/IGARSS.2010.5651760

Sruthi, S., & Aslam, M. A. M. (2015). Agricultural Drought Analysis Using the NDVI and Land Surface Temperature Data; a Case Study of Raichur District. *Aquatic Procedia*, *4*(Icwrcoe), 1258–1264. https://doi.org/10.1016/j.aqpro.2015.02.164

Townshend, J. R., Masek, J. G., Huang, C., Vermote, E. F., Gao, F., Channan, S., … Wolfe, R. E. (2012). Global characterization and monitoring of forest cover using Landsat data: Opportunities and challenges. *International Journal of Digital Earth*, *5*(5), 373–397. https://doi.org/10.1080/17538947.2012.713190

Vicente-Serrano, S. M., Beguería, S., Gimeno, L., Eklundh, L., Giuliani, G., Weston, D., … Pegram, G. G. S. (2012). Challenges for drought mitigation in Africa: The potential use of geospatial data and drought information systems. *Applied Geography*, *34*, 471–486. https://doi.org/10.1016/j.apgeog.2012.02.001

Walz, Y., Min, A., Dall, K., Duguru, M., Leon, J. V. De, Graw, V., … Post, J. (2020). Progress in Disaster Science Monitoring progress of the Sendai Framework using a

geospatial model : The example of people affected by agricultural droughts in Eastern Cape , South Africa. *Progress in Disaster Science*, *5*, 100062. https://doi.org/10.1016/j.pdisas.2019.100062

Wessel, M., Brandmeier, M., & Tiede, D. (2018). Evaluation of different machine learning algorithms for scalable classification of tree types and tree species based on Sentinel-2 data. *Remote Sensing*, *10*(9). https://doi.org/10.3390/rs10091419

West, H., Quinn, N., & Horswell, M. (2019). Remote sensing for drought monitoring & impact assessment: Progress, past challenges and future opportunities. *Remote Sensing of Environment*, *232*(November 2018), 111291. https://doi.org/10.1016/j.rse.2019.111291

Wilhelmi, O. V, & Wilhelmi, O. V. (2002). DigitalCommons @ University of Nebraska - Lincoln Assessing Vulnerability to Agricultural Drought : A Nebraska Case Study Assessing Vulnerability to Agricultural Drought : A Nebraska Case Study.

Winkler, K., Gessner, U., & Hochschild, V. (2017). Identifying droughts affecting agriculture in Africa based on remote sensing time series between 2000-2016: Rainfall anomalies and vegetation condition in the context of ENSO. *Remote Sensing*, *9*(8). https://doi.org/10.3390/rs9080831

Wu, B., Ma, Z., & Yan, N. (2020a). Agricultural drought mitigating indices derived from the changes in drought characteristics. *Remote Sensing of Environment*, *244*(May). https://doi.org/10.1016/j.rse.2020.111813

Wu, B., Ma, Z., & Yan, N. (2020b). Agricultural drought mitigating indices derived from the changes in drought characteristics. *Remote Sensing of Environment*, *244*(July). https://doi.org/10.1016/j.rse.2020.111813

Yaa'Cob, N., Abd Rashid, Z. N. A., Tajudin, N., & Kassim, M. (2020). Landslide Possibilities using Remote Sensing and Geographical Information System (GIS). *IOP Conference Series: Earth and Environmental Science*, *540*(1), 0–9. https://doi.org/10.1088/1755-1315/540/1/012084

Zargar, A., Sadiq, R., Naser, B., & Khan, F. I. (2011). A review of drought indices. *Environmental Reviews*, *19*(1), 333–349. https://doi.org/10.1139/a11-013

Zhang, W., Li, A., Jin, H., Bian, J., Zhang, Z., Lei, G., … Huang, C. (2013). An enhanced spatial and temporal data fusion model for fusing landsat and modis surface reflectance to generate high temporal landsat-like data. *Remote Sensing*, *5*(10), 5346–5368. https://doi.org/10.3390/rs5105346

Zhang, X., Yamaguchi, Y., Li, F., He, B., & Chen, Y. (2017). Assessing the Impacts of the

2009/2010 Drought on Vegetation Indices, Normalized Difference Water Index, and Land Surface Temperature in Southwestern China. *Advances in Meteorology, 2017*. https://doi.org/10.1155/2017/6837493

Zhao, Y., Zhang, J., Bai, Y., Zhang, S., Yang, S., Henchiri, M., … Nanzad, L. (2022). Drought Monitoring and Performance Evaluation Based on Machine Learning Fusion of Multi-Source Remote Sensing Drought Factors. *Remote Sensing, 14*(24). https://doi.org/10.3390/rs14246398

Zhu, Q., Luo, Y., Xu, Y. P., Tian, Y., & Yang, T. (2019). Satellite soil moisture for agricultural drought monitoring: Assessment of SMAP-derived soil water deficit index in Xiang River Basin, China. *Remote Sensing, 11*(3). https://doi.org/10.3390/rs11030362

Zhu, X., Helmer, E. H., Gao, F., Liu, D., Chen, J., & Lefsky, M. A. (2016). A flexible spatiotemporal method for fusing satellite images with different resolutions. *Remote Sensing of Environment, 172*, 165–177. https://doi.org/10.1016/j.rse.2015.11.016

Ziervogel, G., New, M., Archer van Garderen, E., Midgley, G., Taylor, A., Hamann, R., … Warburton, M. (2014). Climate change impacts and adaptation in South Africa. *Wiley Interdisciplinary Reviews: Climate Change, 5*(5), 605–620. https://doi.org/10.1002/wcc.295

6. APPENDICES

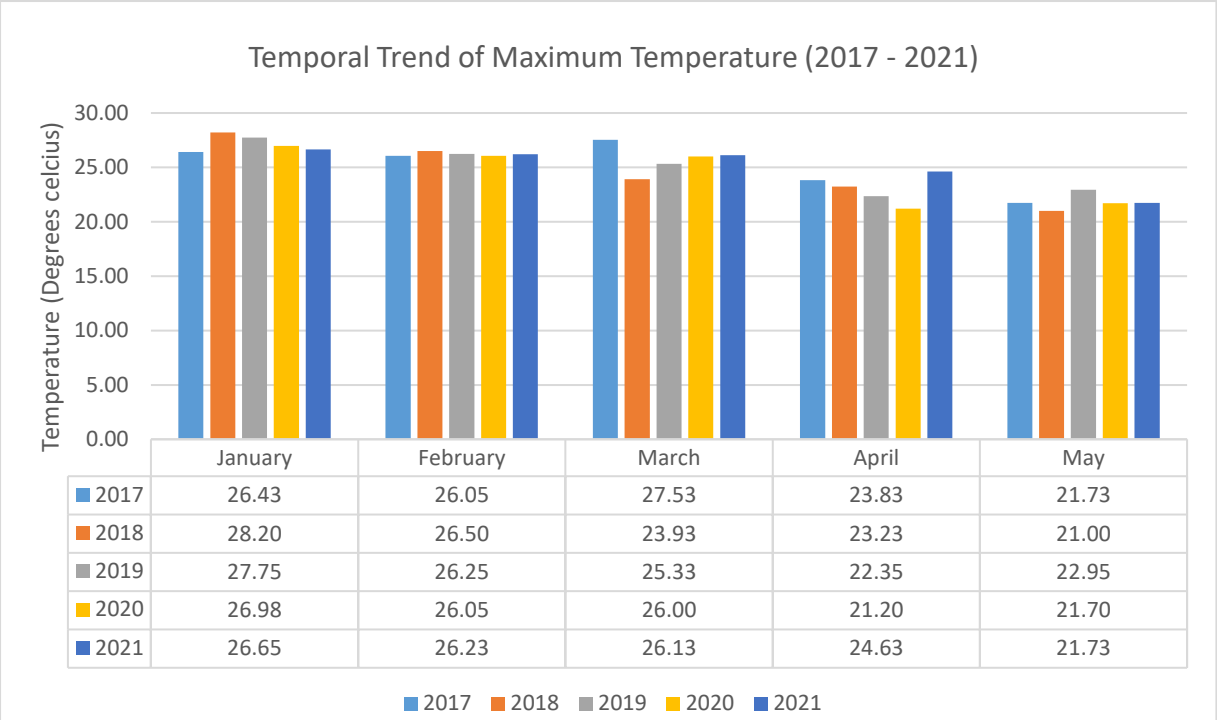

	January	February	March	April	May
2017	26.43	26.05	27.53	23.83	21.73
2018	28.20	26.50	23.93	23.23	21.00
2019	27.75	26.25	25.33	22.35	22.95
2020	26.98	26.05	26.00	21.20	21.70
2021	26.65	26.23	26.13	24.63	21.73

Figure 6.1: Average maximum temperature trend from Umthatha, Queenstown, Elliot and DOHNE – Agr weather stations

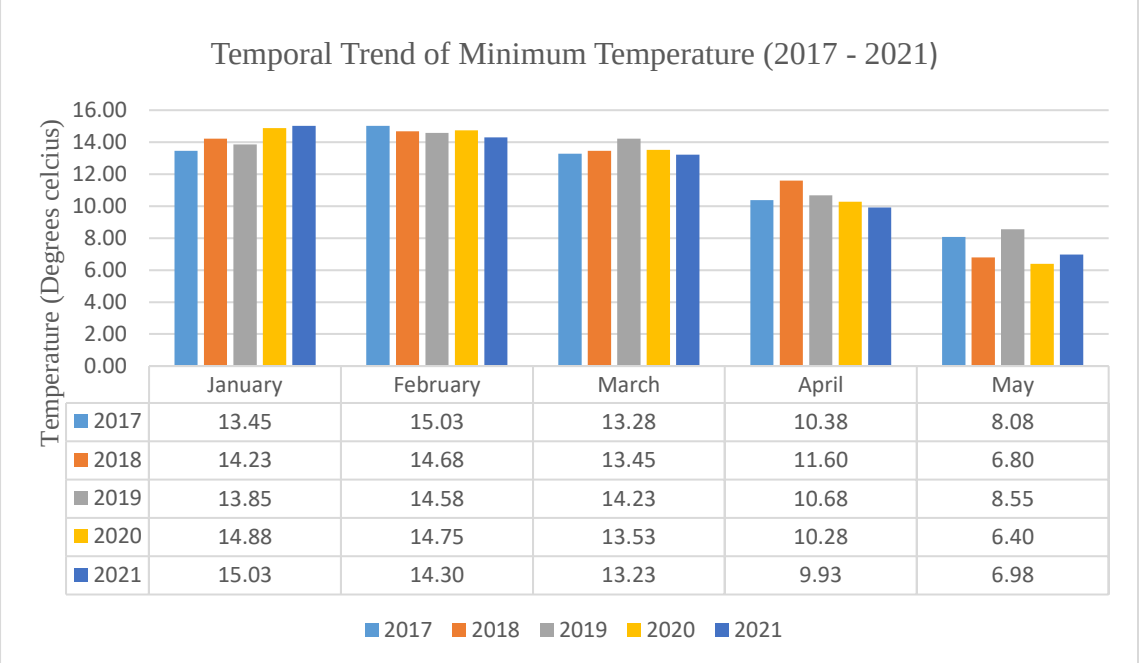

	January	February	March	April	May
2017	13.45	15.03	13.28	10.38	8.08
2018	14.23	14.68	13.45	11.60	6.80
2019	13.85	14.58	14.23	10.68	8.55
2020	14.88	14.75	13.53	10.28	6.40
2021	15.03	14.30	13.23	9.93	6.98

Figure 6.2: Average minimum temperature trend from Umthatha, Queenstown, Elliot and DOHNE – Agr weather stations

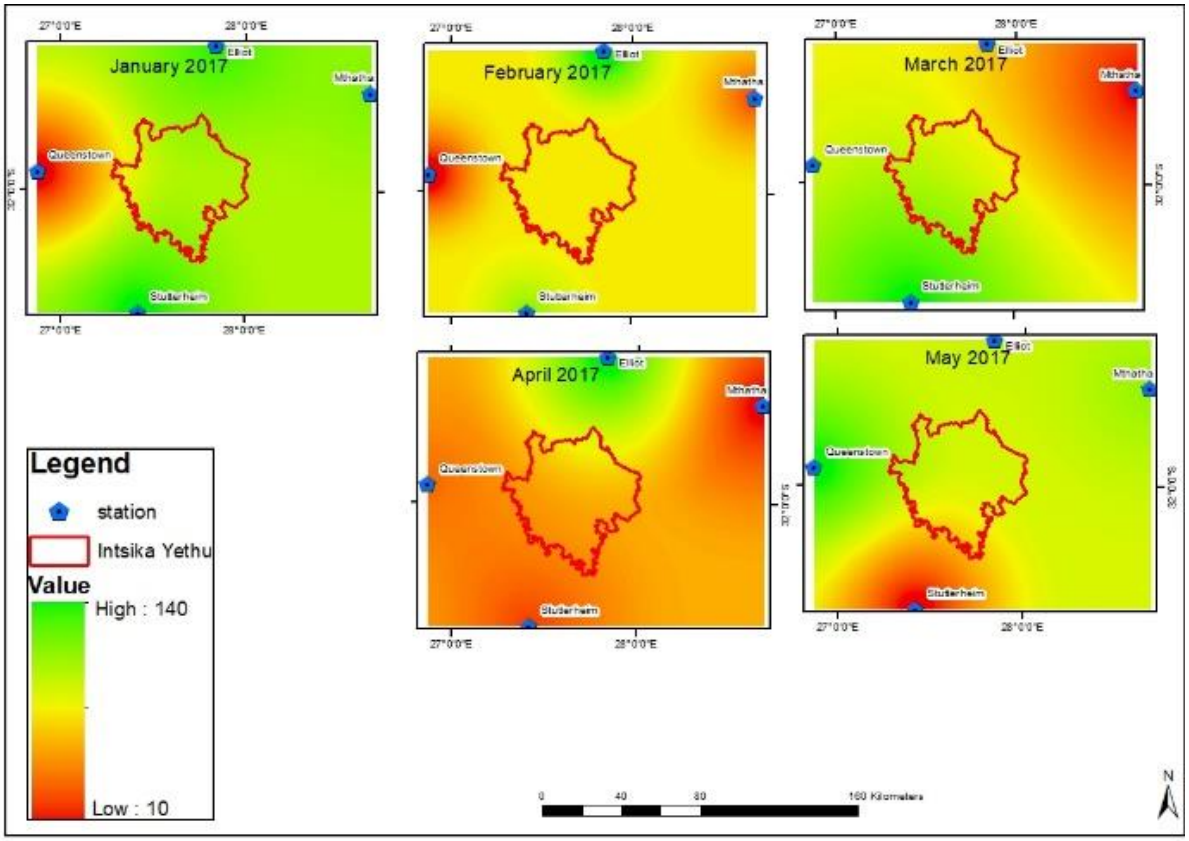

Figure 6.3: Time series, interpolated rainfall data from Umthatha, Queenstown, Elliot and Stutterheim weather stations (January to May of 2017).

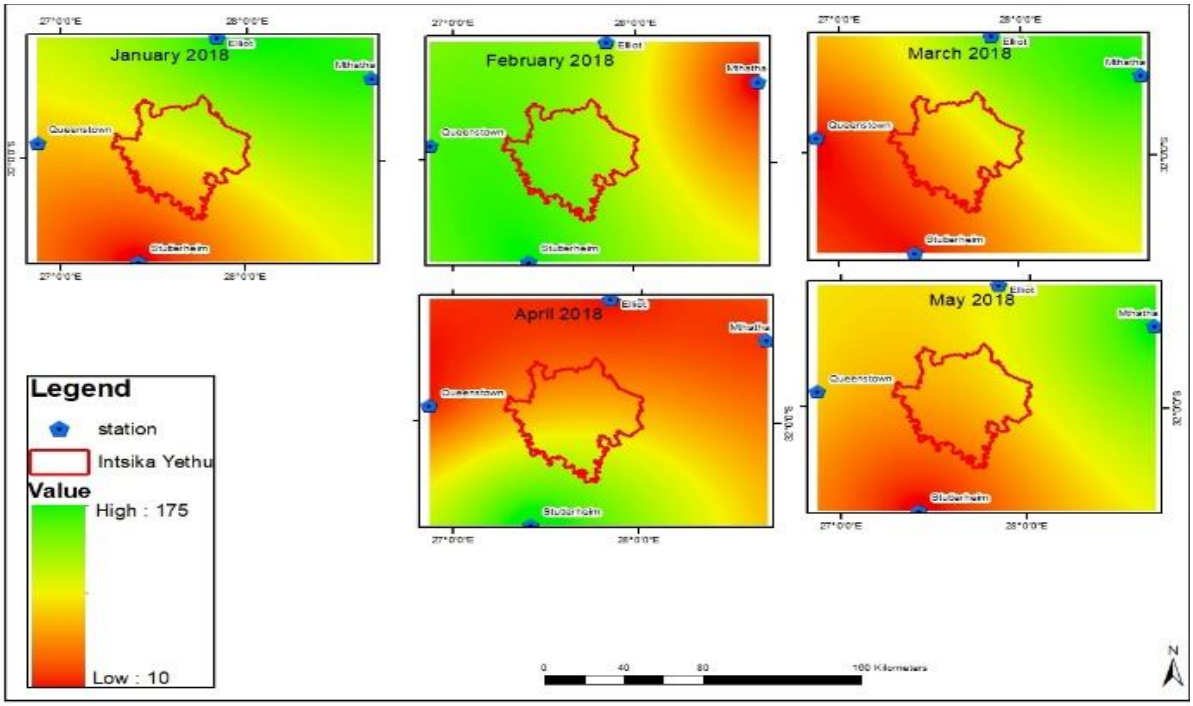

Figure 6.4: Time series, interpolated rainfall data from Umthatha, Queenstown, Elliot and Stutterheim weather stations (January to May of 2018).

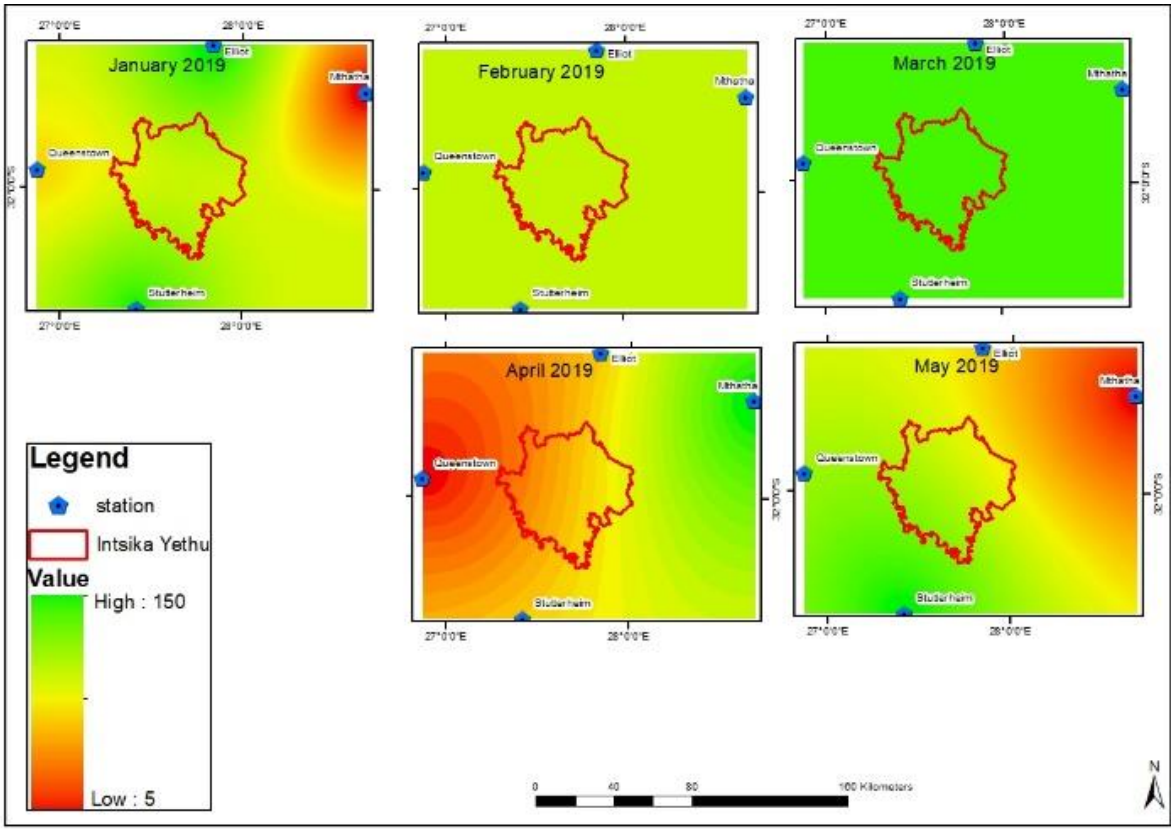

Figure 6.5: Time series, interpolated rainfall data from Umthatha, Queenstown, Elliot and Stutterheim weather stations (January to May of 2019).

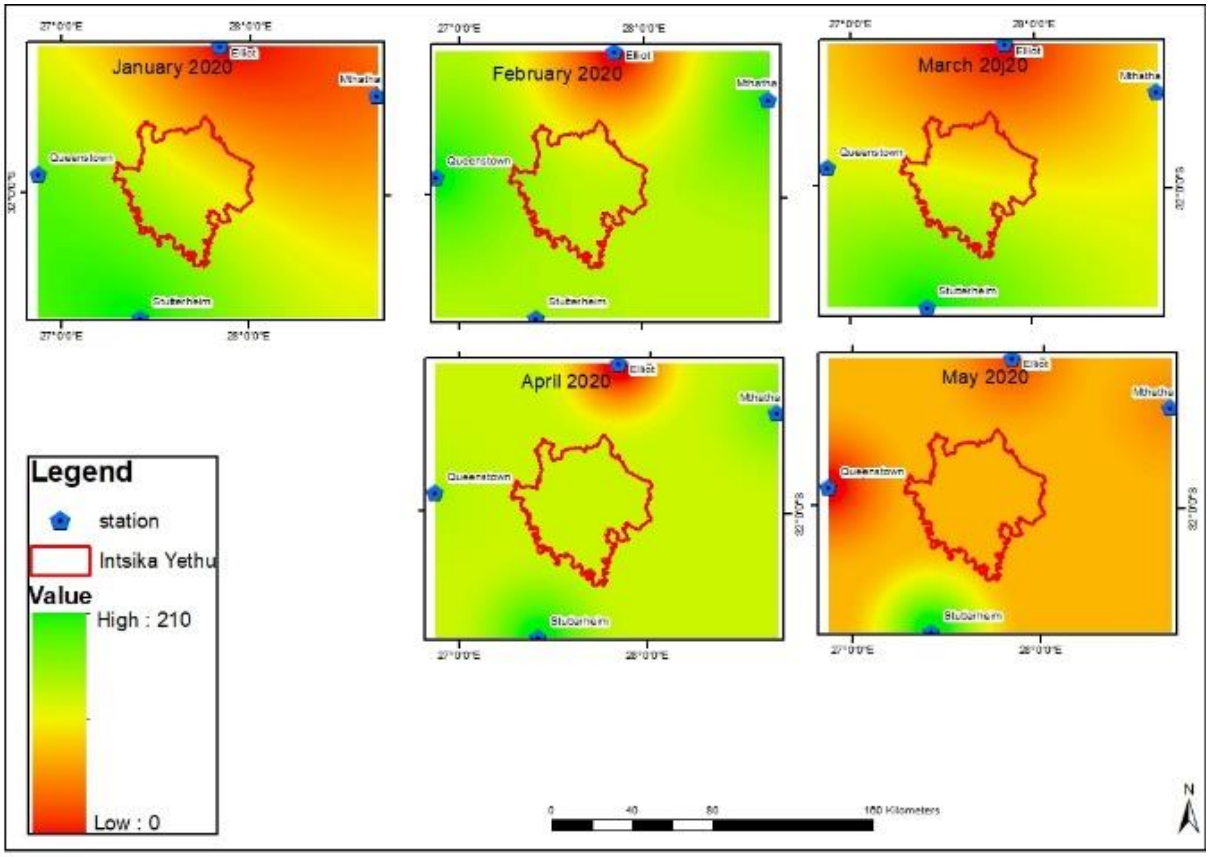

Figure 6.6: Time series, interpolated rainfall data from Umthatha, Queenstown, Elliot and Stutterheim weather stations (January to May of 2020).

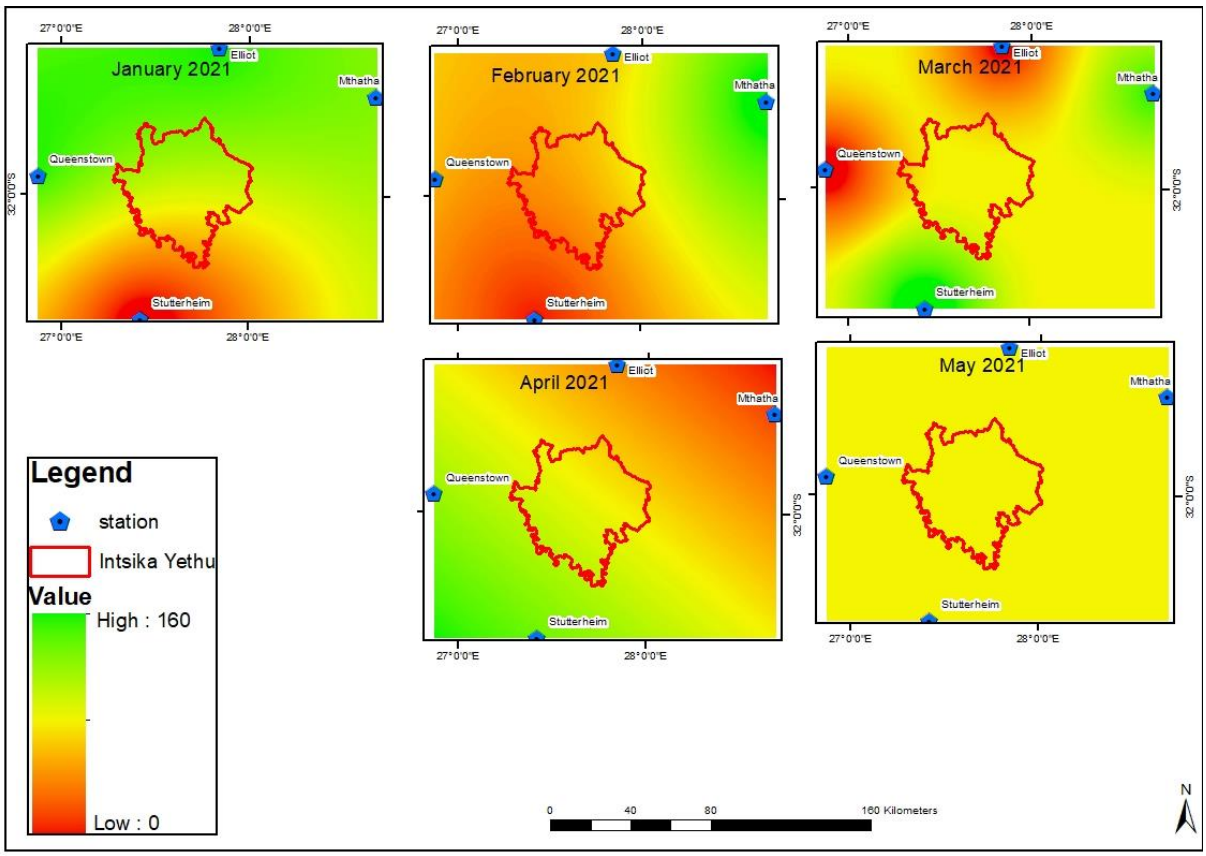

Figure 6.7: Time series, interpolated rainfall data from Umthatha, Queenstown, Elliot and Stutterheim weather stations (January to May of 2021).

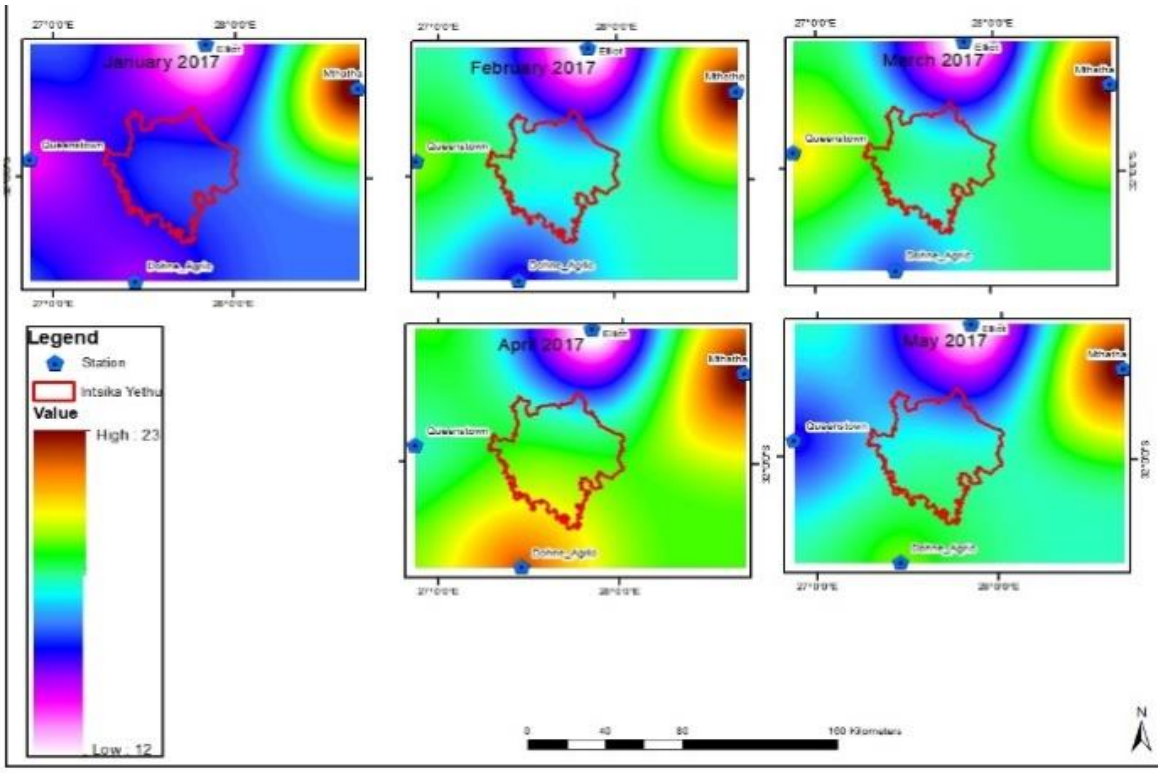

Figure 6.8: Time series, interpolated Average Temperature data from Umthatha, Queenstown, Elliot and Dohne_Agr weather stations (January to May of 2017)

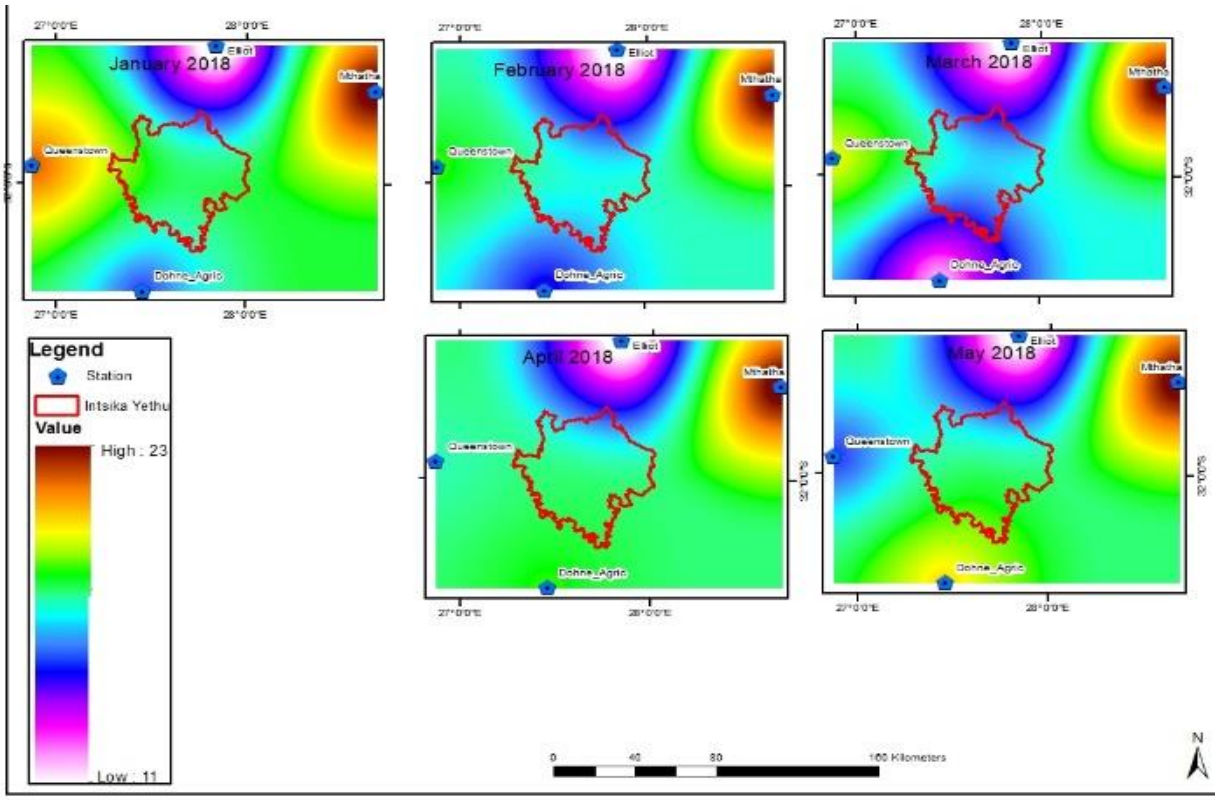

Figure 6.9: Time series, interpolated Average Temperature data from Umthatha, Queenstown, Elliot and Dohne_Agr weather stations (January to May of 2018)

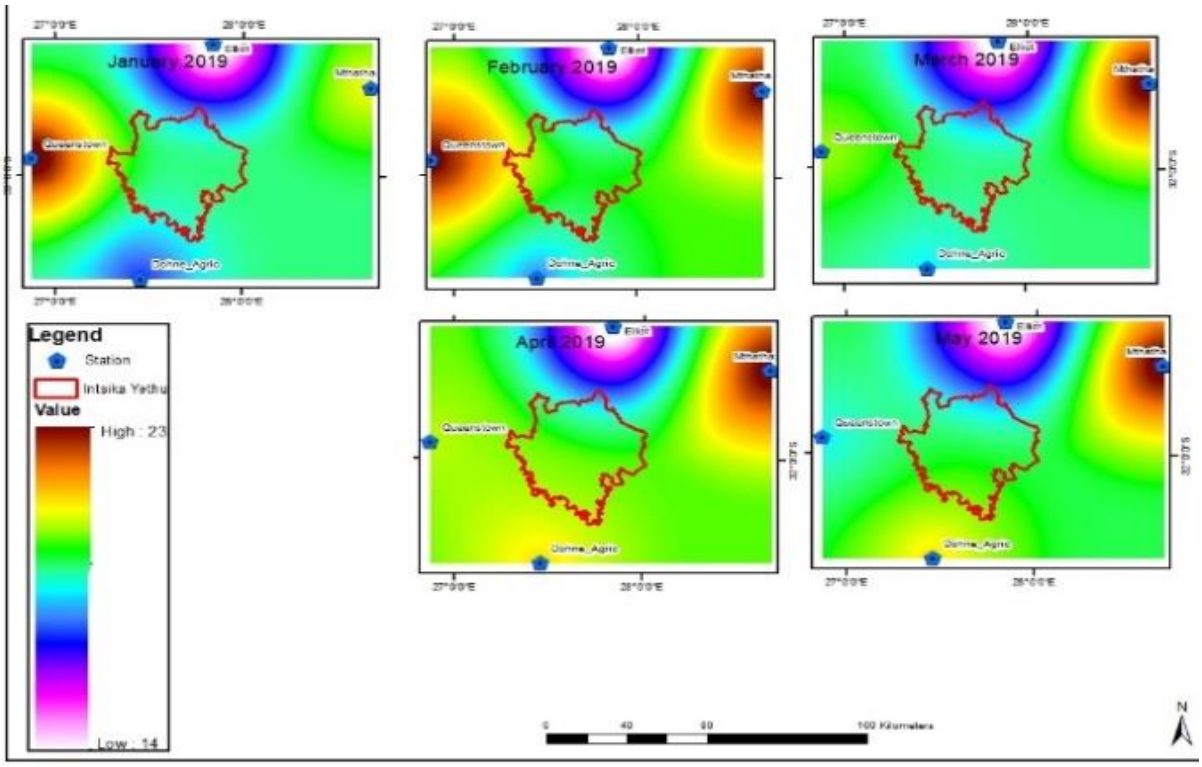

Figure 6.10: Time series, interpolated Average Temperature data from Umthatha, Queenstown, Elliot and Dohne_Agr weather stations (January to May of 2019)

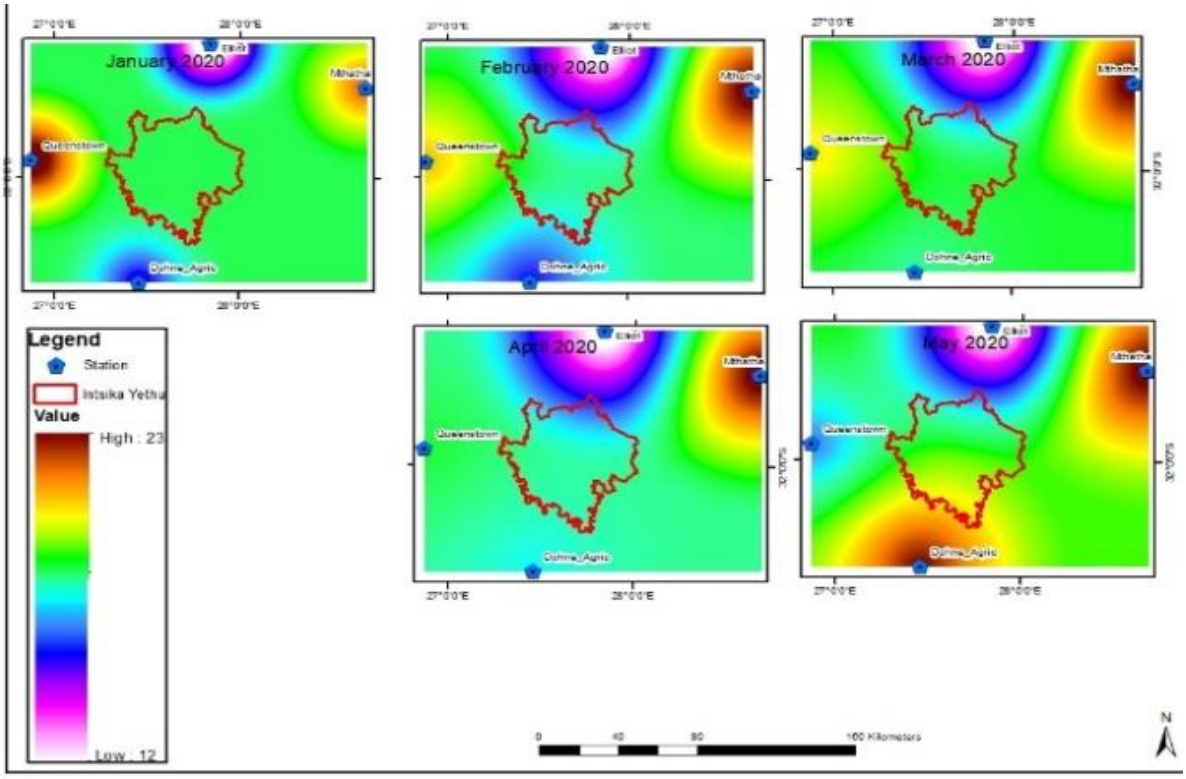

Figure 6.11: Time series, interpolated Average Temperature data from Umthatha, Queenstown, Elliot and Dohne_Agr weather stations (January to May of 2020).

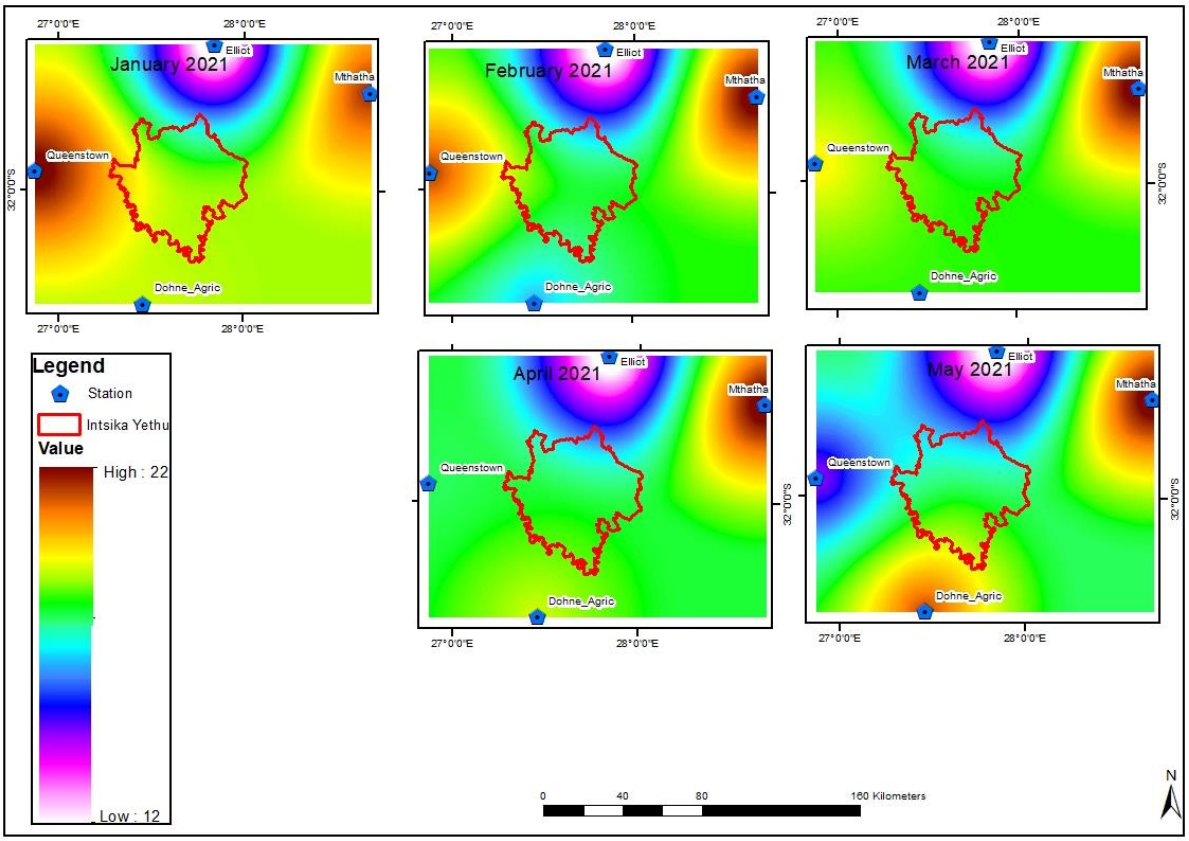

Figure 6.12: Time series, interpolated Average Temperature data from Umthatha, Queenstown, Elliot and Dohne_Agr weather stations (January to May of 2021).